

AD\_\_\_\_\_

AWARD NUMBER DAMD17-94-J-4081

TITLE: Cyclin E, A Potential Prognostic Marker in Breast Cancer

PRINCIPAL INVESTIGATOR: Khandan Keyomarsi, Ph.D.

CONTRACTING ORGANIZATION: Health Research, Incorporated  
Rensselaer, New York 12144-3456

REPORT DATE: October 1998

TYPE OF REPORT: Annual

PREPARED FOR: Commanding General  
U.S. Army Medical Research and Materiel Command  
Fort Detrick, Maryland 21702-5012

DISTRIBUTION STATEMENT: Approved for Public Release;  
Distribution Unlimited

The views, opinions and/or findings contained in this report are those of the author(s) and should not be construed as an official Department of the Army position, policy or decision unless so designated by other documentation.

19990929 056

# REPORT DOCUMENTATION PAGE

Form Approved  
OMB No. 0704-0188

Public reporting burden for this collection of information is estimated to average 1 hour per response, including the time for reviewing instructions, searching existing data sources, gathering and maintaining the data needed, and completing and reviewing the collection of information. Send comments regarding this burden estimate or any other aspect of this collection of information, including suggestions for reducing this burden, to Washington Headquarters Services, Directorate for Information Operations and Reports, 1215 Jefferson Davis Highway, Suite 1204, Arlington, VA 22202-4302, and to the Office of Management and Budget, Paperwork Reduction Project (0704-0188), Washington, DC 20503.

1. AGENCY USE ONLY (Leave blank)		2. REPORT DATE October 1998	3. REPORT TYPE AND DATES COVERED Annual (1 Oct 97 - 30 Sep 98)	
4. TITLE AND SUBTITLE Cyclin E, A Potential Prognostic Marker in Breast Cancer			5. FUNDING NUMBERS DAMD17-94-J-4081	
6. AUTHOR(S) Khandan Keyomarsi, Ph.D.				
7. PERFORMING ORGANIZATION NAME(S) AND ADDRESS(ES) Health Research, Incorporated Rensselaer, New York 12144-3456			8. PERFORMING ORGANIZATION REPORT NUMBER	
9. SPONSORING / MONITORING AGENCY NAME(S) AND ADDRESS(ES) U.S. Army Medical Research and Materiel Command Fort Detrick, Maryland 21702-5012			10. SPONSORING / MONITORING AGENCY REPORT NUMBER	
11. SUPPLEMENTARY NOTES				
12a. DISTRIBUTION / AVAILABILITY STATEMENT Approved for Public Release; Distribution Unlimited			12b. DISTRIBUTION CODE	
13. ABSTRACT (Maximum 200 words) We have established the use of cyclin E as a prognostic marker for breast cancer. Tumor specimens from 400 breast cancer patients were examined; changes of cyclin E expression were compared with seven other established tumor markers to patient outcome. Altered expression of cyclin E was observed in 90% of all breast cancers with poor prognosis where patients either died of breast cancer or were still with cancer at the last contact date. Similarly in 85% of all breast cancer patients where cyclin E was either not altered, or its alteration was minimal, patients had a favorable prognosis. We have also characterized the nature of overexpression and alteration of cyclin E in breast cancer cells in vitro and have found and reported that cyclin E forms an active complex with cdk2 constitutively throughout the tumor cell cycle while this complex is only active in the G1-S transition in normal cells. We have also found that cyclin E, if overexpressed in tumor cells, can bypass the cyclin D-pRb feedback loop and act redundantly and provides tumor cells with yet another mechanism to gain a growth advantage. Lastly, studies using the drug Lovastatin demonstrated that this highly prescribed drug used to lower cholesterol levels is also capable of inducing all four cyclin dependent kinase inhibitors (CKIs) in a cell specific manner via cell cycle independent mechanism. Since the CKIs directly inhibit the activity of cyclin E/cdk2 complexes, future work to elucidate the mechanism of induction in tumor cells could have significant therapeutic implications.				
14. SUBJECT TERMS Breast Cancer, cell cycle, cyclin E, Prognostic marker			15. NUMBER OF PAGES 148	
			16. PRICE CODE	
17. SECURITY CLASSIFICATION OF REPORT Unclassified	18. SECURITY CLASSIFICATION OF THIS PAGE Unclassified	19. SECURITY CLASSIFICATION OF ABSTRACT Unclassified	20. LIMITATION OF ABSTRACT Unlimited	

## FOREWORD

Opinions, interpretations, conclusions and recommendations are those of the author and are not necessarily endorsed by the U.S. Army.

\_\_\_\_ Where copyrighted material is quoted, permission has been obtained to use such material.

\_\_\_\_ Where material from documents designated for limited distribution is quoted, permission has been obtained to use the material.

\_\_\_\_ Citations of commercial organizations and trade names in this report do not constitute an official Department of Army endorsement or approval of the products or services of these organizations.

\_\_\_\_ In conducting research using animals, the investigator(s) adhered to the "Guide for the Care and Use of Laboratory Animals," prepared by the Committee on Care and use of Laboratory Animals of the Institute of Laboratory Resources, national Research Council (NIH Publication No. 86-23, Revised 1985).

☒ For the protection of human subjects, the investigator(s) adhered to policies of applicable Federal Law 45 CFR 46.

☒ In conducting research utilizing recombinant DNA technology, the investigator(s) adhered to current guidelines promulgated by the National Institutes of Health.

☒ In the conduct of research utilizing recombinant DNA, the investigator(s) adhered to the NIH Guidelines for Research Involving Recombinant DNA Molecules.

\_\_\_\_ In the conduct of research involving hazardous organisms, the investigator(s) adhered to the CDC-NIH Guide for Biosafety in Microbiological and Biomedical Laboratories.

K. Keymanur 111 12/23/98  
PI - Signature Date

**TABLE OF CONTENTS**

**Front Cover.....page 1**

**SF 298 Report Documentation Page.....page 2**

**FOREWORD .....page 3**

**Table of Contents.....page 4**

**Introduction.....pages 5-11**

**Body/Results.....pages 11-21**

**Conclusions/Discussion.....page 21**

**References.....pages 22-26**

**Appendix.....page 27**



## 5. Introduction:

The overall purpose of this 5 year study is to use the altered expression of cyclin E as a diagnostic/prognostic marker and to investigate the mechanisms and repercussions of this alteration in breast cancer.

Cyclins are prime cell cycle regulators and central to the control of cell proliferation in eukaryotic cells via their association with and activation of cyclin-dependent protein kinases 1-7 (cdks) (reviewed in (12, 24, 30, 38, 54, 69)). Cyclins were first identified in marine invertebrates as a result of their dramatic cell cycle expression patterns during meiotic and early mitotic divisions (13, 70, 72, 73). Several classes of cyclins have been described and are currently designated as cyclins A-H, some with multiple members. Cyclins can be distinguished on the basis of conserved sequence motifs, patterns of appearance and apparent functional roles during specific phases and regulatory points of the cell cycle in a variety of species. The cdk partners of several of these cyclins have also been identified: Cyclin A forms a complex with cdc2 (cdk1) and cdk2, and is required both at mitosis and DNA replication (6, 49, 56, 75); cyclin B forms a complex solely with cdc2 and is required for entry into mitosis, (reviewed in (54)); cyclin D1, a cyclin active in the G1 phase of the cell cycle, forms complexes primarily with cdk4 and cdk6, while cyclin E, another G1 type cyclin, forms a complex with only cdk2 (1, 39, 40, 48, 54, 69, 79). Lastly, cyclin H has been shown to form a complex with cdk7 and, together, they comprise the cdk-activating kinase (CAK) protein complex which activates the nascent cyclin/cdk complex via phosphorylation (14, 46). Cyclin binding to a cdk enables the kinase to become active, initiating a complex kinase cascade that directs the cell into DNA synthesis and/or mitosis, reviewed in (28, 79).

An additional layer of cell cycle regulation has emerged with the discoveries of low molecular weight cdk inhibitors (CKIs) which represent a novel mode of negative regulation (11, 57, 71). The first class of these inhibitors, p21, was simultaneously characterized in several laboratories as the major p53 inducible gene (WAF1) (8-10), as a CDK inhibitor protein (CIP1,

p21, and p20<sup>CAP1</sup>) (18, 22, 80), as a protein highly expressed in senescent fibroblasts (sdi) (53), and as a melanoma differentiation associated gene (mda6) (31). In normal fibroblasts, this protein has been shown to be associated with and inhibit various cyclin-cdk complexes, including cdk2 associated with cyclins A and E, cdk4 associated with D-type cyclins (22, 23, 80-82), and is also found weakly associated cdc2-cyclin B (82). This protein which represents one of the major p53 inducible genes, is also induced during differentiation. It most likely acts as a general purpose brake used during terminal differentiation and p53 directed DNA damage control (7). The second protein in this family, p27<sup>KIP1</sup>, is both structurally and functionally similar to p21. p27<sup>KIP1</sup> was identified simultaneously as a protein associated with inactive cyclin E-cdk2 complexes in TGF $\beta$  treated and contact inhibited cells (59, 60) and as a protein that interacts with cyclin D1-cdk4 complexes (74). TGF $\beta$  arrests certain cell types in G1 and p27 is thought to be a cellular mediator for this anti-proliferative signal (41). Hence, p21 and p27 may function similarly to inhibit cdk activity and proliferation in response to different environmental stimuli.

A second, structurally and functionally distinct family of CKIs is comprised of p16, p15 and their homologous (5, 19, 21, 27, 82). Structural features of these Ink4 (for inhibitor of cdk4) proteins include 4 ankyrin like repeats which are postulated to be involved in mediating protein-protein interactions (21, 67). Curiously these CKIs share significant homology to the Notch proteins involved in the differentiation and fate determination of cells during embryogenesis (19). Inhibitors of this family bind cdk monomers (cdk4 or cdk6) rather than cyclin-cdk complexes (67, 82). It is believed that binding of ink4 proteins to cdks prevents and/or disrupts cyclin-cdk complex formation thereby negating cdk activity. p16 and p15 proteins, encoded on human chromosome 9, have been the subjects of intense study as this genomic region is frequently mutated in a variety of tumor cell lines and fewer tumor tissue specimens (67, 82). As their alternate names imply (MTS1 and MTS2 for multiple tumor suppressor) p16 and p15 are postulated to function as growth inhibitory tumor suppressor molecules.

The connection between cyclins CKIs and cancer has been substantiated with the D type cyclins (28-30, 70). Cyclin D1 was identified simultaneously by several laboratories using

independent systems: It was identified in mouse macrophages due to its induction by colony stimulating factor 1 during G1 (47). It was also identified in complementation studies using yeast strains deficient in G1 cyclins (44, 79); as the product of the *bcl-1* oncogene (78), and as the PRAD1 proto-oncogene in some parathyroid tumors where its locus is overexpressed as a result of a chromosomal rearrangement that translocates it to the enhancer of the parathyroid hormone gene (47, 50, 51, 62). In centrocytic B cell lymphomas cyclin D1 (PRAD1)/BCL1 is targeted by chromosomal translocations at the BCL1 breakpoint, t(11;14)(q13;q32) (64, 65). Furthermore, the cyclin D1 locus undergoes gene amplification in mouse skin carcinogenesis, as well as in breast, esophageal, colorectal and squamous cell carcinomas (2-4, 32, 33, 42, 43). Several groups have examined the ability of cyclin D1 to transform cells directly in culture with mixed results (25, 26, 33, 45, 52, 62, 63, 70). However, the overexpression of cyclin D1 was recently observed in mammary cells of transgenic mice and results in abnormal proliferation of these cells and the development of mammary adenocarcinomas (77). This observation strengthens the hypothesis that the inappropriate expression of a G1 type cyclin may lead to loss of growth control.

Cyclins D2 and A have also been implicated in oncogenesis. The cyclin D2 gene appears to be the integration site of a murine leukemia provirus in mouse T cell leukemias, resulting in its overexpression (20). Cyclin A was found to be the site of integration of a fragment of the hepatitis B virus genome in a hepatocellular carcinoma (76). Cyclin A is also associated with the adenovirus transforming protein E1A in adenovirus transformed cells (15, 58)

The linkage between oncogenesis and the cell cycle was recently reinforced by correlating the deranged expression of cyclins to the loss of growth control in breast cancer (4, 37). Using proliferating normal versus human tumor breast cell lines in culture as a model system, several changes were seen in all or most of these lines. These include increased cyclin mRNA stability, resulting in overexpression of mitotic cyclins and *cdc2* RNAs and proteins in 9/10 tumor lines, leading to the deranged order of appearance of mitotic cyclins prior to G1 cyclins in synchronized tumor cells. The most striking abnormality in cyclin expression was that of cyclin E. Cyclin E

protein not only was overexpressed in 10/10 breast tumor cell lines but it was also present in lower molecular weight isoforms than that found in normal cells (37). The relevance of cyclin derangement to *in vivo* conditions, was directly examined by measuring the expression of cyclin E protein in tumor samples versus normal adjacent tissue obtained from patients with various malignancies (36). These analyses revealed that breast cancers and other solid tumors, as well as malignant lymphocytes from patients with lymphatic leukemia, show severe quantitative and qualitative alteration in cyclin E protein expression independent of the S-phase fraction of the samples. In addition, the alteration of cyclin E becomes more severe with breast tumor stage and grade and is more consistent than cell proliferation or other tumor markers such as PCNA or c-erb B2. These observations strongly suggested the use of cyclin E as a new prognostic marker. These findings were corroborated by immunocytochemical detection of cyclin E which detects tumor proliferation and deregulated cyclin expression. The mechanism of the cyclin E alteration is in part a result of its deregulation in breast cancer. The alteration of cyclin E in breast cancer have been recently further characterized and reveal that while cyclin E is cell cycle regulated in normal cells it is present constitutively and in an active cdk2 complex in synchronized populations of breast cancer cells. Two novel truncated variant forms of cyclin E mRNA as detected by RT-PCR were also identified which are ubiquitously detected in normal and tumor cells and tissues. These variant forms of cyclin E can give rise to an active cyclin/cdk2 complex *in vitro*, but they do not seem to be translated in normal cells.

During the first four years of this application we have used cyclin E antibody as a prognostic marker for breast cancer by analyzing breast tumor tissue specimens for the alterations in cyclin E protein. During the first two years we collected 550 tumor tissue samples from breast cancer patients diagnosed with different stages of breast cancer ranging from pre-malignant to highly invasive. We extracted RNA, DNA and protein from most of these samples. Due to limited sample size received for each patient (i.e 0.1-0.2 g of tissue), protein was initially extracted from all samples and if there was tumor sample left over, DNA and RNA were also extracted. The protein extracts from all 500 samples were then subjected to Western blot analysis and the

expression of cyclin E was compared and correlated with other known prognostic markers examined in the same samples. The prognostic markers include, cyclin D1, erbB-2, as well as PCNA to determine the proliferative activity of these samples. We also obtained information on the estrogen and progesterone receptor status of each sample as well as ploidy and proliferation rate as measured by Ki-67. In the second year of this study we analyzed the results obtained in the first year by quantitating the levels of cyclin E in each tumor specimen with that of cyclin D1, erbB2 and PCNA. These analysis were done by performing densitometric scanning on each lane of each gel with each antibody for each patient sample using at least two autoradiographs with different exposures. Such laborious analysis were necessary to accurately determine the level of cyclin E protein in every patient and correlate the alteration of cyclin E protein from each patient to the stage of their disease. During the third year of this application we contacted the 20 hospitals where these samples were obtained, and have been successful in collecting the following information on 400 of these patients: final diagnosis, TNM staging, treatment given, and final outcome (i.e quality of survival). Having all this information we have performed correlative analysis on these samples and evaluate the role of cyclin E as a prognosticator for breast cancer. During the third year of this application we have also developed a new antibody to cyclin E which can be used for detection of the alteration of cyclin E in immunohistochemical analysis using tissue slides obtained from frozen tissue samples.

During the fourth year of this application we added several other cell cycle markers to our panel of tumor markers. These include cyclin D3, p21, p27, p16 and pRb. The reason for the inclusion of these markers was that several of these markers are thought to functionally interact with or act on cyclin E and hence their over or altered expression in conjunction with cyclin E could have profound effects of prognosis. During the fourth year of the study we have also initiated the statistical analysis of correlating cyclin E overexpression to outcome and determine whether indeed it is an independent tumor marker for poor prognosis.

In addition to the clinical research outlined above we have also engaged in studies to determine the mode of regulation of cyclin E in normal cells and how this regulation is altered in

cancer cells. During the second and third years of the grant we documented that cyclin E is in fact deregulated in breast cancer and such deregulation gives rise to redundancy in function. We show that under conditions where cyclin E is overexpressed it can act redundantly and replace cyclin D as well as cyclin A in breast cancer cell lines. We also document that such redundancy is also seen in tumor tissue specimen (17). During the third year of the application we have documented that not only are the expression of CKIs including p21<sup>CIP1</sup> in normal versus tumor cells different, but the CKIs can be pharmacologically induced in tumor cells and that such overexpression could lead to induction of the Estrogen Receptor in otherwise Estrogen Receptor negative breast tumor cells (16). During the fourth year of this application we have engaged in several studies aimed at further addressing the mechanisms of deregulation of cyclin E in breast cancer cells. These studies include addressing how cyclin E is altered in breast cancer cells and identifying the altered forms of this cyclin found only in breast cancer cells and tissues. We have also initiated studies on using the altered expression of cyclin E as an example of loss of G1 checkpoint control in tumor cells, and exploiting this phenomenon therapeutically. Lastly, we have further expanded our studies on the pharmacological induction of CKIs in breast cancer cells by addressing the cellular pathways altered by such induction and mechanism by which lovastatin (i.e. the pharmacological agent) is capable of inducing the CKIs in breast cancer cells.

## **6: Body (Results/Discussion)**

During the fourth year of this grant application we finished most of the experimental section and some of the data analysis of all 4 aims. We are currently in the process of writing the manuscripts and expanding on the initial observations made for each aim by addressing the next series of questions our data have raised. Below is a brief description of what we have accomplished in the last year, what new data we have generated and what our goals are for the fifth and final year of this application.

***Use of cyclin E as a prognostic marker for breast cancer:*** For the first study we collected 550 breast cancer specimens, analyzed cyclin E on 500 of these samples, and were able to obtain clinical and outcome data on 385 of these cases. In the first to third years of the study we were able to analyze the expression of Cyclin E, Cyclin D1, and PCNA on Western blot analysis and correlate their expression to prognosis and outcome of patients. In the fourth year of the study we also examined the expressions of cyclin D3, pRb, p21, p27 and p16 in all the patient samples. These new markers are in addition to what we originally planned in our application and the reason for their inclusion is as follows: Cyclin D3: When we examined the overexpression of cyclin D1 in our panel of breast tumor tissues, we found that even though cyclin D1 is overexpressed in 50% of all breast cancers, its overexpression is not correlated to outcome. Cyclin D3 is a member of the same family as cyclin D1, yet its expression is more consistent with cyclin E in our in vitro studies (data not shown). For that purpose, we rationalized that maybe the key member of the cyclin D family whose overexpression could be associated with poor outcome is cyclin D3 and not cyclin D1. However, following our analysis of cyclin D3, we found that the overexpression of cyclin D3 in the breast cancer tissues mirrored that of cyclin D1 and not cyclin E. Hence, even though the cyclin D family of proteins are overexpressed in 50% of all cases of breast cancer we examined, their overexpression is not associated with poor prognosis nor overexpression of cyclin E.

pRb/p16: In a study we published last year on the redundancy of cyclin E in breast cancer (17), we found that in cell lines and tumor tissue samples overexpressing both cyclin E and p16, cyclin E/cdk2 complexes and not cyclin D/cdk4 complexes could phosphorylate pRb. These results strongly suggested that cyclin E can act redundantly for cyclin D to phosphorylate pRb. For that purpose we examined the levels and phosphorylation status of pRb in our breast tumor samples and correlated it with overexpression of cyclin E and p16. Our results indicated that in 60% of all tumors where cyclin E and p16 were overexpressed, pRb was also expressed and present in its hyperphosphorylated state. This is very significant, as it suggests that overexpression of cyclin E has functional significance in giving the tumor cell a growth advantage by constitutively phosphorylating substrates throughout the cell cycle.

P21/p27 These two CKIs can inhibit the



functional activity of cyclin E by binding to the cyclin E/cdk2 complexes and inhibiting their activation. There has been some reports in literature that there is an inverse correlation between the overexpression of cyclin E and under expression of p27, and such inverse correlation has prognostic value (61). We wanted to know if such an inverse correlation held true for our breast tissue samples. Our analysis revealed that indeed there was an inverse correlation between cyclin E overexpressors and p27 underexpressors. However we also found that several of the breast tumors which overexpressed pRb also overexpressed p27. We are currently in the process of performing statistical analysis on our results and we will be summarizing these analysis in 2 manuscripts currently under preparation. The first manuscript primarily deals with cyclin E, cyclin D1, cyclin D3 and patient outcome. The second manuscript covers the data on pRb/p16, p21, p27, and poor prognosis. In order to ensure that our follow up period for every patient is at least 5 years, we will update our patient outcome files in the spring of 1999 and incorporate that into our statistical analysis. It is anticipated that these two manuscripts will be completed during the 5<sup>th</sup> year of our study.

***Utilization of cyclin E deletional mutations to detect early metastatic breast cancer.*** Early on in the study, during the first year, we determined that the cyclin E forms we had referred to as deletional mutations turned out not to be deletional mutations, but rather splicing variants of cyclin E that are present in both normal and tumor cell lines and tissue samples. However, these truncated forms of cyclin E will help us decipher the mechanisms of alteration of cyclin E in breast cancer. Even though this aim was elucidated right away, we chose to examine how these alternative splice variants would give rise to the lower molecular weight isoforms we observe in tumor but not normal cells. As a result we expanded this aim to read "Identification of the lower molecular weight isoforms of cyclin E in tumor cells". Below is a description of our progress on this aim which is near completion.

Examination of a tumor cell or tumor tissue western blot shows that cyclin E is present in a number of low molecular weight forms in addition to the expected 50 kDa form (Fig 1). Just how



these low molecular weight forms are generated whether by proteolysis, alternate translation start sites or alternate splice variants is not known. It is the goal of this expanded second aim to discover the mechanism which generates these low molecular weight forms. The pattern of cyclin E processing in tumor tissue has valuable prognostic power. Five splice variants have been identified using RT-PCR, including the 50 kDa form considered the wild type (Fig 2). A form which is 45 base pairs longer than wild type (55) is termed EL, a form which deletes the cyclin box and is unable to activate cdk2 in vitro is termed ES (68), a 9 base pair elimination in the 5' domain of the message is termed delta 9 and finally a 148 base pair elimination causing a frame shift is found in the 3' domain of the cyclin E message (35) (Fig 2). It is not known whether all these forms are expressed as protein under any circumstances but the ability to activate cdk2 in vitro using histone H1 as a substrate has been examined (35). It is also not known whether the splice variants have an altered specificity toward the natural substrate pRb. The message which gives rise to the predominant 50 Kda form found in western blots could be either the wild type or the EL form. Since cyclin E was discovered by its ability to rescue a yeast triple *cln* mutant the actual protein sequence, especially the amino terminus has not been determined. Northern blot analysis (Fig 3) shows that there is a single major species of mRNA coding for cyclin E. However, Northern blot analysis is not particularly accurate for determining small differences in base length. A more sensitive RNase protection assay was used to fully characterize the amount of cyclin E mRNA in normal and tumor cell lines. An additional advantage of the RNase protection assay is the ability to detect splice variants and small variations in sequence.

RNase protection probes were designed to examine cyclin E mRNA (Fig 4). Four overlapping antisense probes were used to quantitate the coding domain of the message as well as scan for splice variants. The quantitation was accomplished in seven cell lines including two derived from normal tissue and five derived from tumor tissue (Fig 5). The results of the quantitation showed that there are 2-3 copies of cyclin E mRNA per cell in unsynchronized normal breast epithelial cells (76N) and a normal breast cell line (MCF 10A). Breast tumor cell lines exhibited a range of cyclin E mRNA expression from as low as 1 copy per cell (MCF 7 and

ZR75T) to four copies per cell (MDA MB 231) to 8 copies per cell (MDA MB 436) to a whopping 40 copies per cell in MDA MB 157. Human beta actin was quantitated by RPA in each preparation of total RNA as a control. For comparison, beta actin was present consistently at about 3000 copies per cell regardless of cell type (Fig 10).

An unexplained curiosity was discovered when the cyclin E mRNA was quantitated using four overlapping probes scanning the full length of the coding sequence (Fig 4). In the case of the tumor cell line MDA MB 157 the RPA probe specific for bases 190-523 of the coding sequence showed that this segment is over-represented four-fold when compared to the rest of the mRNA (Fig 4). This part of the mRNA codes for the "cyclin box" domain of the cyclin E protein. When a longer probe was used in the RPA (bases -25 to 523) two distinct protected fragments were detected, one representing the full length mRNA and a second at least 100 bases shorter. This qualitative result is consistent with the previous quantitative data indicating that there is an over-represented segment of the cyclin E mRNA. This could represent a new splice variant containing only a short segment of the known coding sequence for cyclin E.

To complement the RPA analysis of cyclin E mRNA found in normal and tumor cells, we devised a method to enumerate the relative abundance of the known forms of cyclin E mRNA. A single restriction enzyme *Sau* IIIA is used to digest the cyclin E cDNA into fragments which upon analysis by Southern blot can distinguish between the various known cyclin E splice variants (Fig 6). Cyclin E cDNA was prepared from normal and tumor cell lines and ligated into the T/A cloning vector to create a plasmid library representative of the various forms of cyclin E mRNA. Southern blot analysis of individual plasmids from these shows the relative abundance of the known splice variants of cyclin E. This library analysis shows that there are no major splice variants in the cell lines which have not already been described except for a combination of the delta-9 and delta-148 forms. The frequency of the known splice variants relative to the wild type form does not differ between normal and tumor cell lines (Fig 6). This analysis allows us to conclude that the major species of cyclin E mRNA is that of the full length (EL) form. For every 100 molecules of cyclin E mRNA 60 are of this species while the remaining forms are equally divided among the delta-9,

delta-148 and EL forms. We conclude from the Northern blot analysis, RNase protection assay and Southern blot assay that there are no detectable forms of cyclin E mRNA which could account for the low molecular weight forms found in tumor cells and tumor tissue (Figs 2-6). We believe that the low molecular weight forms are produced primarily through the action of a protease activity, as described below.

To determine the amino-terminal residues of the various molecular weight forms of cyclin E protein processed in tumor cells, the protein was purified with an antibody affinity column and subjected to mass spectroscopy (MALDI TOF) analysis. The goal of this purification is to eventually purify enough cyclin E protein for automated Edman sequencing. Cyclin E was purified using a polyclonal antibody directed to a carboxy-terminus derived peptide (Fig 7). The polyclonal antibody was covalently attached to protein A-sepharose. Soluble protein was extracted from the tumor cells MDA MB 157 grown in culture as previously described (35). The soluble protein (120 mg) was batch adsorbed to the antibody affinity column at 4° C overnight. The affinity resin was transferred to a column where the resin was washed and the cyclin E was eluted with a low pH buffer. Samples from each step of the purification were boiled in reducing sample buffer and separated by SDS PAGE and western blotted, to detect cyclin E. The cyclin E is quantitatively recovered from the affinity column as shown in Fig 7. The combined, eluted, purified cyclin E was concentrated by centrifugation in a Centricon 10, boiled in reducing sample buffer and the protein separated by SDS PAGE. The gel was then silver stained and bands were cut from the gel (Fig 8). 1 mm of each gel band was removed, dehydrated in acetonitrile, re-hydrated in reducing sample buffer, boiled and run again on a SDS PAGE gel for western blotting. This procedure identifies the precise gel slice which contains cyclin E and the known proteins which associate with cyclin E, for example cdk2. The remaining portion of each gel slice was processed and digested with trypsin overnight at 37°C. The tryptic peptides were then extracted from the gel, first with 30% acetonitrile, followed by a second extraction in 70% acetonitrile. The extracted peptides were analyzed by MALDI TOF mass spectroscopy, and the resulting peptide masses characterized using the internet software package, Protein Prospector (Fig 9). The tryptic peptide analysis of various

bands from the silver stained gel show that in addition to the expected cyclin E and cdk2 there are a number of contaminating bands and some potential unknown proteins which may or may not be specifically binding the cyclin E/cdk2 complexes (Figs 8, 9). This method has clearly identified a single band containing only cdk2. The staining intensity would indicate approximately 5 pmol of protein in this band. Since cdk2 can only be present on the gel through its association with cyclin E, we assume that cyclin E is present in equimolar amounts. The gel slices containing cyclin E contain a significant amount of actin, which is overlaid on the tryptic peptide cyclin E signal. To complement this polyclonal affinity column we are also using a commercially available monoclonal antibody affinity column (HE111) for the purification of cyclin E and associated proteins. We hope that the various methods of purification will resolve between contaminating proteins and proteins which have a functional association with cyclin E.

***Cyclin E truncations and deletions to find the domain processed in vivo.*** An independent approach taken to identify the lower molecular weight isoforms of cyclin E was to ask how these forms are processed in tumor cells. As a method to answer this question, we introduced the different splice variant forms of cyclin E (Fig 2) in tumor and normal cells and examined how these cDNAs get processed into proteins. The 5 different cyclin E mRNA's shown in figure 2 represent the whole population of cyclin E transcripts which could potentially give rise to a protein product. Even if all 5 of the mRNA's are translated into protein, this would still not be sufficient to account for all of the lower molecular weight forms found in MDA-MB-157 (Fig 1). This suggests that there is some form of translational or post-translational processing of the full length cyclin E into the lower molecular weight isoforms, and that this processing is only active in tumor cells which express the isoforms. We have devised a strategy to test this hypothesis which involves the expression of the full length cyclin E cDNA's in normal and tumor cells, and studying the protein products for processing events. The 4 active forms of cyclin E, WT (L1),  $\Delta 9$ ,  $\Delta 148$ , and EL (trunk 1), were cloned into the mammalian expression vector pCDNA3.1, which will allow in vitro expression of cyclin E, constitutive expression of high levels of cyclin E in mammalian

cells, and a neomycin resistance gene for stable selection. The cyclin E forms have also been engineered with a FLAG sequence at the 3' end, which will be used as a tag for monitoring both expression levels, and processing of the full length cyclin E into the lower molecular weight isoforms (Fig 10). The truncated 5' end have all been given identical ribosome binding sites for equal expression levels in vivo. The FLAG tag is a powerful way to study the expression of the cyclin E which is transfected into the cells, separate from that which is endogenously present within the cells. We also constructed 3 FLAG tagged N-terminal truncated cyclin E forms, trunk 4, 6, and 10 (Fig 10). These will be used for size determination of the lower molecular weight forms, along with kinase activity studies of cyclin E. The trunk forms will be discussed in more detail below.

We have determined conditions for achieving high transfection efficiency using our normal, MCF-10A, versus tumor, MDA-MB-157, model system. Transfection conditions by electroporation yields 50-70% efficiency. Positive transfectants were identified by flow cytometric analysis for green fluorescence protein (GFP) emission, and shown in a chart as percentage cells expressing GFP versus cell type (Fig 11). Efficiency of MDA-MB-157 transfection was a maximum of 55%, and MCF-10A was at a maximum of 70%, while the background remained at about 1%. This data holds importance to this study since we will be using transient expression of cyclin E to study the differences in processing between normal and tumor cells, and different efficiencies will lead to different expression levels shown on the gels.

To determine if a single cyclin E mRNA can give rise to lower molecular weight forms in normal and tumor cells, we transfected both MDA-MB-157 and MCF-10A cells with the wild type L1 and trunk 1 cyclin E (Fig 12). Cyclin E L1 seems to migrate at a lower molecular weight than the endogenous full length seen in cells. This suggests that L1 does not represent the endogenous full length cyclin E seen in cells. The longer cyclin E EL which uses an upstream ATG was constructed to represent the full length in the cells, called trunk 1 (Fig 10). In vivo expression of the wild type L1 or trunk 1 cyclin E cDNA in MDA-MB-157 show the appearance of lower molecular weight isoforms predominantly in tumor cells (Fig 12). This suggests that a single

cyclin E transcript has the capacity to give rise to lower molecular weight forms in tumor cells. When normal cells are transfected with the wild type L1 or trunk 1, they exhibit predominantly the expression of the high molecular weight cyclin E. This normal - tumor difference is indicative of what is seen with the endogenous cyclin E. Although normal cells do have the ability to give rise to some of the lower molecular weight forms that MDA-MB-157 express, the proportion of the lower molecular weight isoforms to the full length is significantly higher in the tumor cells than normal cells. This means that whatever mechanism gives rise to the lower molecular weight forms is more predominant, or more active in tumor cells. Moreover, this processing mechanism can give rise to these forms from one single full length message. Since the transfected cyclin E is a cDNA copy, the isoforms it gives rise to cannot be from a splicing event, hence the generation of the forms can only be explained by some type of specific proteolytic processing event, or an alternate translation initiation.

We next wanted to estimate the sizes of the isoforms by examining the amino acid sequences within the suspected region of processing which could harbor alternate ribosome start sites, or protease consensus sequences. To determine more closely where the processing of cyclin E was taking place, a series of N terminal truncations of cyclin E cDNA were constructed (Fig 10). Our lab has already determined that the truncated forms of cyclin E are due to N terminal deletions by using antibodies to scan the length of the protein (data not shown). Figure 10 illustrates the truncated forms of cyclin E we have used in the constitutive expression vector pCDNA3.1. Expression of the truncated forms of cyclin E in vitro is shown in figure 13 by a cyclin E monoclonal antibody, as well as a FLAG monoclonal and polyclonal. The in vitro TnT Westerns of the trunk forms show multiple bands appearing, which are probably due to alternate translation sites. When the trunk forms are transfected into MDA-MB-157 cells, each trunk form is processed into the next set of lower forms (Fig 14A, B). MDA-MB-157 results in more extensive processing of the trunk forms than the TnT in vitro expression system. This provides additional evidence for the ability of 157 cells to process a cyclin E cDNA into smaller forms. When MCF-10A express

the trunk forms, they once again express predominantly the longest form of each trunk (Fig 14C, D) providing additional evidence that the processing mechanism is more active in tumor cells.

To initiate our studies into the biochemistry of the cyclin E lower molecular weight forms, we have used the trunk cyclin E forms as a representation of the endogenous forms found between 50 and 33 kDa in tumor cells. To examine if N terminal deleted cyclin E is able to bind to and activate CDK2, the truncated cyclin E forms were made using an in vitro transcription translation kit. The in vitro synthesized cyclin E forms were mixed with 157 cell extracts, and immunoprecipitated using the anti flag antibody. Western blot analysis with CDK2 antibody confirm binding by all of the trunk forms to CDK2 (Fig 15). This binding affinity is however seen to decrease as the truncation gets shorter, up to the cyclin box. The CDK2 associated catalytic activity was measured using an H1 kinase assay (Fig 15). The kinase activity also decreased along with the shorter truncated forms. This is probably not due to reduced activity due to the trunks, but rather the lower amount of CDK2 which is bound to the shorter trunk forms (Fig 15). Trunk 10 however shows CDK2 binding, but is completely inactive. This suggests an important role of the region of cyclin E between amino acids 65 and 116 in CDK2 activation, which is separate from its binding capacity. A recent study has shown that 2 sets of amino acids, 64-67 and 108-110, are crucial for CDK2 activation by cyclin E (34). These amino acids fall directly within the region which is deleted in trunk 10, but not trunk 6. This region might be involved in CDK2 activation, phosphorylation (66), or substrate recognition, which we are currently examining. This data gives evidence that the endogenous truncated cyclin E forms are catalytically active, since most fall between trunk 1 and trunk 6. The greater overall CDK2 activity would give the tumor cells which express these forms a growth advantage at the G1-S checkpoint, and throughout the rest of the cell cycle.

To determine the kinetics of the generation of the lower molecular weight forms over several time points in vivo, we transfected 157 and 10A cells with the full length Trunk 1 and L1 forms of cyclin E and harvested cells at the indicated time points (Fig 16). The maximum level of expression seems to peak between 12 and 24 hours, and then drops down steadily afterwards.

This is likely due to the transient plasmid being lost over time. There was no change in the levels of the isoforms and the full length with respect to each other, indicating that they are either generated together by translation differences, or that there is a constant level of both production of the full length and the processing into the lower forms. Again, notice the processing difference of cyclin E between the 2 cell lines over the time points, providing evidence for the ability of tumor but not normal cells to process cyclin E.

Based on the above studies the region of cyclin E suspected of containing a proteolytic site was determined by making targeted amino-terminal deletions in the protein sequence (Fig 17). Plasmid vectors were mutated using oligonucleotides containing the amino-terminal deletion to PCR amplify a domain which was then cloned, sequenced and substituted into the wild type cyclin E/Flag expression vector (pcDNA 3.1) using restriction endonuclease sites. The Flag epitope tag was previously added to the carboxy-terminus of cyclin E (Fig 17). These plasmids were transiently expressed in normal cells and tumor cells (Fig 18). The Flag epitope-tagged truncated proteins were examined by western blot where only the transfected forms of Flag-epitope tagged cyclin E is detected with antibody specific for the Flag peptide. Since splicing of the mRNA from the transfected plasmid is not expected, the altered forms of cyclin E detected by western blot would have to be generated by post-translational processing as described above. The region of cyclin E where proteolytic processing occurs was narrowed with a series of truncated versions of cyclin E (Fig 18). These truncated versions of cyclin E show two important things. One, the transfected forms are all expressed and processed in the tumor cell line similarly. Two, a doublet formed when cyclin E is processed in the tumor cells is found very near to the amino-terminus of the Trunk 6 version of cyclin E. We attacked this doublet by making block deletions of six amino acids in the region just 3' of the start codon for the Trunk 6 amino terminus. . The results from these deletions show that the two proteolytically sensitive sites exist within a ten amino-acid stretch of cyclin E (data not shown). To define the exact amino acids involved in the processing, a series of serial alanine substitutions (alanine scan) are currently being prepared in a plasmid expression



vector. The results from these transient transfections will pinpoint the amino acids essential for the proteolytic processing of cyclin E found in tumor cells.

***Role of p21/p27 in G1/S checkpoint control in normal and tumor cells.*** The 3rd and 4th aims of the study deal with the interplay of the negative cell cycle regulators, p21 and p27, on the overexpression of cyclin E which leads to G1/S checkpoint deregulation in tumor cells. We have made significant strides on these two aims which have resulted in three manuscripts, one published, and two submitted. Since I have enclosed copies of these manuscripts in the Appendix I will only summarize the results of these three studies in the following paragraphs.

In the first study entitled "Lovastatin Mediated G1 Arrest in Normal and Tumor Breast Cells is Through Inhibition of CDK2 Activity and Redistribution of p21 and p27, Independent of p53" we have investigated the nature of the CKIs (p21 and p27) alterations resulting in G1 arrest in both normal and tumor breast cell lines by lovastatin. We show that even though lovastatin treatment causes G1 arrest in a wide variety of normal and tumor breast cells irrespective of their p53 or pRb status, the p21 and p27 protein levels are not increased in all cell lines treated suggesting that the increase in p21 and p27 protein expression per se is not necessary for lovastatin mediated G1 arrest. However, the binding of p21 and p27 to CDK2 increases significantly following treatment of cells with lovastatin leading to inhibition of CDK2 activity and a subsequent arrest of cells in G1. The increased CKI binding to CDK2 is achieved by the redistribution of both p21 and p27 from CDK4 to CDK2 complexes subsequent to decreases in CDK4 and cyclin D3 expression following lovastatin treatment. Lastly, we show that lovastatin treatment of 76N-E6 breast cell line with an altered p53 pathway also results in G1 arrest and similar redistribution of CKIs from CDK4 to CDK2 as observed in other breast cell lines examined. These observations suggest that lovastatin induced G1 arrest of breast cell lines is through a p53 independent pathway and is mediated by decreased CDK2 activity through redistribution of CKIs from CDK4 to CDK2.

In the second study entitled "Lovastatin induction of CKIs (p21 and p27) and mevalonate reversal of lactacystin are both through modulation of the proteasome, independent of HMG-CoA

reductase" we show that the mechanism of lovastatin mediated stabilization of p21 and p27 may be due to a previously unknown function of the pro-drug,  $\beta$ -lactone ring form of lovastatin to inhibit the proteasome degradation of these CKIs. We show that lovastatin pro-drug (20% of the lovastatin mixture) inhibits the 20S proteasome but does not inhibit HMG-CoA reductase. In addition, many of the properties of proteasome inhibition by the pro-drug are the same as the specific proteasome inhibitor lactacystin. Lastly, mevalonate (used to rescue cells from lovastatin arrest) unexpectedly reverses the lactacystin inhibition of the proteasome. Mevalonate increases the activity of the proteasome, which could result in degradation of the CKIs causing the release of lovastatin- and lactacystin-arrested cells.

In the third study entitled "UCN-01 Mediated G1 Arrest in Normal But Not Tumor Breast Cells is pRb Dependent and p53 Independent", we pharmacologically assessed how alteration of G1/S checkpoint could lead to reponse to inducers of G1 arrest in tumor cells. In this study we investigated the growth inhibitory affects of UCN-01 in several normal and tumor-derived human breast epithelial cells. We found that while normal mammary epithelial cells were very sensitive to UCN-01 with an IC<sub>50</sub> of 10 nM, tumor cells displayed little to no inhibition of growth with any measurable IC<sub>50</sub> at low UCN-01 concentrations (i.e. 0-80nM). The UCN-01 treated normal cells arrested in G1 phase and displayed decreased expression of most key cell cycle regulators examined, resulting in inhibition of CDK2 activity due to increased binding of p27 to CDK2. Tumor cells on the other hand displayed no change in any cell cycle distribution or expression of cell cycle regulators. Examination of E6 and E7 derived strains of normal cells revealed that pRb and not p53 function is essential for UCN-01 mediated G1 arrest. Lastly, treatment of normal and tumor cells with high doses of UCN-01 (i.e. 300 nM) revealed a necessary role for a functional G1 checkpoint in mediating growth arrest. Normal cells, which have a functional G1 checkpoint, always arrest in G1 even at very high concentrations of UCN-01. Tumor cells on the other hand have a defective G1 checkpoint and only arrest in S phase with high concentrations of UCN-01. The effect of UCN-01 on the cell cycle is thus quite different from staurosporine, a structural analogue of UCN-01, which arrests normal cells in both G1 and G2, while tumor cells arrest only

in the G2 phase of the cell cycle. Our results show the different sensitivity to UCN-01 of normal compared to tumor cells is dependent on a functional pRb and a regulated G1 checkpoint.

## **7: Conclusions:**

As evident we have made significant strides in completing all the proposed aims. In fact not only all the aims are either completed or near completion, we have surpassed most of them. The first aim of our studies, use of cyclin E antibody as a diagnostic prognostic marker for breast cancer is completed and we summarized most of the data in the last annual report. We are currently waiting to complete the 5-year survival statistics from the patients from whom we examined cyclin E expression. Some of these patients were diagnosed with the disease less than 5 years ago, and their 5 years mark will be reached in the spring of 1999, at which point we will update our statistic data. In the original application we intended to examine only 150 patients, however we have surpassed our initial goal of collecting and extracting 150 tissue samples per year by increasing this number to 550 samples. We also have completed our analysis of cyclin E and other tumor markers not stated on the grant application by Western blot analysis and have obtained all the pertinent clinical information on each patient and have correlated cyclin E alteration to patient outcome. We will complete this aim by submitting our final manuscript for publication soon after compiling the final statistical data. We anticipate this task to be done by fall of 1999. The second Aim of the application deals with utilizing the deletional mutations of cyclin E to detect early metastatic breast cancer. We have documented (35) that these truncated forms of cyclin E are not deletional mutations and are in fact splicing variants of cyclin E found in normal and tumor cells and tissue samples. As outlined above, we have made several key observations as to what the lower molecular weight forms are and we anticipate that in the coming year we will have concluded this aim. The last two aims of our proposal are also near completion as we have addressed how induction of the CKIs by lovastatin can lead to growth inhibition in tumor cells, even in the presence of high levels of cyclin E. We anticipate that in the last year of this application we will finalize and publish these studies.

## 8. References

1. **Baldin, V., J. Likas, M. J. Marcote, M. Pagano, J. Barteck, and G. Draetta.** 1993. Cyclin D1 is a nuclear protein required for cell cycle progression in G1. *Genes Dev.* **7**:812-821.
2. **Bianchi, A. B., S. M. Fischer, A. I. Robles, E. M. Rinchik, and C. J. Conti.** 1993. Overexpression of cyclin D1 in mouse skin carcinogenesis. *Oncogene* **8**:1127-1133.
3. **Buckler, A. J., D. D. Chang, S. L. Graw, J. D. Brrok, D. A. Haber, P. A. Sharp, and D. E. Housman.** 1991. Exon amplification: a strategy to isolate mammalian genes based on RNA splicing. *Proc. Natl. Acad. Sci. USA* **88**:4005-4009.
4. **Buckley, M. F., K. J. E. Sweeney, J. A. Hamilton, R. L. Sini, D. L. Manning, R. I. Nicholson, A. deFazio, C. K. W. Watts, E. A. Musgrove, and R. L. Sutherland.** 1993. Expression and amplification of cyclin genes in human breast cancer. *Oncogene* **8**:2127-2133.
5. **Chan, F. K. M., J. Zhang, L. Cheng, D. Shapiro, and A. Winoto.** 1995. Identification of human and mouse p19, a novel cdk4 and cdk6 inhibitor with homology to p16ink4. *Mol. Cell. Biol.* **15**:2682-2688.
6. **Draetta, G.** 1990. Cell cycle control in eukaryotes: molecular mechanisms of cdc2 activation. *Trends Biochem.* **15**:378-383.
7. **Dulic, V., W. K. Kaufman, S. Wilson, T. D. Tlsty, E. Lees, J. W. Harper, S. J. Elledge, and S. I. Reed.** 1994. p53-dependent inhibition of cyclin dependent kinase activities in human fibroblasts during radiation-induced G1 arrest. *Cell* **76**:1013-1023.
8. **El-Deiry, W. S., J. W. Harper, P. M. O'Connor, V. E. Velculescu, C. E. Canman, J. Jackman, J. A. Pietenpol, M. Burrell, D. E. Hill, Y. Wang, K. G. Wiman, W. E. Mercer, M. B. Kastan, K. W. Kohn, S. J. Elledge, K. W. Kinzler, and B. Vogelstein.** 1994. WAF1/CIP1 is induced in p53-mediated G<sub>1</sub> arrest and apoptosis. *Advances in Brief* **1**:1169-1173.
9. **El-Deiry, W. S., T. T., T. Waldman, J. D. Oliner, V. E. Velculescu, M. Burrell, D. E. Hill, E. Healy, J. L. Rees, S. R. Hamilton, K. W. Kinzler, and B. Vogelstein.** 1995. Topological control of p21<sup>WAF1/CIP1</sup> expression in normal and neoplastic tissues. *Cancer Res.* **55**:2910-2919.
10. **El-Deiry, W. S., T. Tokino, V. E. Velculescu, D. B. Levy, R. Parsons, J. M. Trent, D. Lin, W. E. Mercer, K. W. Kinzler, and B. Vogelstein.** 1993. WAF-1, a potential mediator of p53 tumor suppression. *Cell* **75**:817-825.
11. **Elledge, S. J., and J. W. Harper.** 1994. Cdk inhibitors; on the threshold of checkpoints and development. *Curr. Opin Cell Biol.* **6**:847-852.
12. **Elledge, S. J., and M. R. Spottswood.** 1991. A new human p34 protein kinase, CDK2, identified by complementation of a cdc28 mutation in *Saccharomyces cerevisiae*, is a homolog of *Xenopus* *Eg1*. *EMBO J* **10**:2643-2659.
13. **Evans, T., E. Rosenthal, J. Youngblom, D. Kistel, and T. Hunt.** 1983. Cyclin: a protein specified by maternal mRNA in sea urchin eggs that is destroyed at each cleavage division. *Cell* **33**:389-396.
14. **Fisher, P. B., J. Herms, H., W. E. Soloway, M. C. Dietrich, G. M. Edwards, I. B. Weinstein, J. A. Langer, S. Pestka, P. Giacomini, M. Kusama, and S. Ferrone.** 1986. Effect of recombinant human fibroblast interferon and mezerein on growth, differentiation, immune interferon binding and tumor associated antigen expression in human melanoma cells. *Anticancer Res.* **6**:765-774.

15. **Giordano, A., P. Whyte, E. Harlow, B. R. Franza, Jr., D. Beach, and G. Draetta.** 1989. A 60 kd cdc2-associated polypeptide complexes with the E1A protein in adenovirus-infected cells. *Cell* **58**:981-990.
16. **Gray-Bablin, J., S. Rao, and K. Keyomarsi.** 1997. Lovastatin Induction of cyclin-dependent kinase inhibitors in human breast cells occurs in a cell cycle independent fashion. *Cancer Res.* **57**:604-609.
17. **Gray-Bablin, J., J. Zalvide, M. P. Fox, C. J. Knickerbocker, J. A. DeCaprio, and K. Keyomarsi.** 1996. Cyclin E, a redundant cyclin in breast cancer. *Proc. Natl. Acad. Sci.* **93**:15215-15220.
18. **Gu, Y., c. W. Turck, and D. O. Morgan.** 1993. Inhibition of cdk2 activity in vivo by as associated 20K regulatory subunit. *Nature* **366**:707-710.
19. **Guan, K., C. W. Jenkins, Y. Li, M. A. Nichols, X. Wu, C. L. O'Keefe, A. G. Matera, and Y. Xiong.** 1994. Growth suppression by p18, a p16INK4/MTS1- and p14INK4/MTS2- related cdk6 inhibitor correlates with wild-type pRb function. *Genes & Dev.* **8**:2939-2952.
20. **Hanna, Z., M. Jankowski, P. Tremblay, X. Jiang, A. Milatovich, U. Francke, and P. Jolicoeur.** 1993. The vin-1 gene, identified by provirus insertional mutagenesis, is the cyclin D2. *Oncogene* **8**:1661-1666.
21. **Hannon, G. J., and B. D.** 1994. p15INK4B is a potential effector of TGF- $\beta$  induced cell cycle arrest. *Nature* **371**:257-261.
22. **Harper, J. W., G. R. Adami, N. Wei, K. Keyomarsi, and S. J. Elledge.** 1993. The p21 Cdk-interacting protein Cip1 is a potent inhibitor of G1 cyclin-dependent kinases. *Cell* **75**:805-816.
23. **Harper, J. W., S. J. Elledge, K. Keyomarsi, B. Dynlacht, L.-H. Tsai, P. Zhang, S. Dobrowolski, C. Bai, L. Connell-Crowley, E. Swindell, M. P. Fox, and N. Wei.** 1995. Inhibition of cyclin-dependent kinases by p21. *Mol. Biol. Cell* **6**:387-400.
24. **Heichman, K. A., and J. M. Roberts.** 1994. Rules to replicate by. *Cell* **79**:557-562.
25. **Hinds, P. W., S. F. Dowdy, E. N. Eaton, A. Arnold, and R. A. Weinberg.** 1994. Function of a human cyclin gene as an oncogene. *Proc. Natl. Acad. Sci* **91**:709-713.
26. **Hinds, P. W., S. Mittnacht, V. Dulic, A. Arnold, S. I. Reed, and R. A. Weinberg.** 1992. Regulation of retinoblastoma protein functions by ectopic expression of human cyclins. *Cell* **70**:993-1006.
27. **Hirai, H., M. F. Roussel, J.-Y. Kato, R. A. Ashmun, and C. J. Sherr.** 1995. Novel ink4 proteins, p19 and p18, are specific inhibitors of the cyclin D-dependent kinases cdk4 and cdk6. *Mol. Cell. Biol.* **15**:2672-2681.
28. **Hunt, T.** 1991. Cyclins and their partners: from a simple idea to complicated reality. *Seminars in Cell Biology* **2**:213-222.
29. **Hunter, T., and J. Pines.** 1991. Cyclins and Cancer. *Cell* **66**:1071-1074.
30. **Hunter, T., and J. Pines.** 1994. Cyclins and cancer II: cyclin D and cdk inhibitors come of age. *Cell* **79**:573-582.
31. **Jiang, H., and P. B. Fisher.** 1993. Use of a sensitive and efficient subtraction hybridization protocol for the identification of genes differentially regulated during the induction of differentiation in human melanoma cells. *Molec. and Cell. Differen.* **3**:285-299.
32. **Jiang, W., S. M. Kahn, N. Tomita, Y.-J. Zhang, S.-H. Lu, and B. Weinstein.** 1992. Amplification and expression of the human cyclin D gene in esophageal cancer. *Cancer Res.* **52**:2980-2983.
33. **Jiang, W., S. M. Kahn, P. Zhou, Y.-J. Zhang, A. M. Cacace, A. S. Infante, S. Doi, R. M. Santella, and I. B. Weinstein.** 1993. Overexpression of cyclin D1 in rat fibroblasts causes abnormalities in growth control, cell cycle progression and gene expression. *Oncogene* **8**:3447-3457.
34. **Kelly, B. L., K. G. Wolfe, and J. M. Roberts.** 1998. Identification of a substrate-targeting domain in cyclin E necessary for phosphorylation of the retinoblastoma protein. *Proc. Natl. Acad. Sci. USA* **95**:2535-2540.

35. **Keyomarsi, K., D. Conte, W. Toyofuku, and M. P. Fox.** 1995. Deregulation of cyclin E in breast cancer. *Oncogene* **11**:941-950.
36. **Keyomarsi, K., N. O'Leary, G. Molnar, E. Lees, H. J. Fingert, and A. B. Pardee.** 1994. Cyclin E, a Potential Prognostic Marker for Breast Cancer. *Cancer Res.* **54**:380-385.
37. **Keyomarsi, K., and A. B. Pardee.** 1993. Redundant cyclin overexpression and gene amplification in breast cancer cells. *Proc. Natl. Acad. Sci. USA* **90**:1112-1116.
38. **King, R. W., P. K. Jackson, and M. W. Kirschner.** 1994. Mitosis in transition. *Cell* **79**:563-571.
39. **Koff, A., F. Cross, A. Fisher, J. Schumacher, K. Leguellec, M. Philippe, and J. M. Roberts.** 1991. Human cyclin E, a new cyclin that interacts with two members of the CDC2 gene family. *Cell* **66**:1217-1228.
40. **Koff, A., A. Giordano, D. Desia, K. Yamashita, J. W. Harper, S. J. Elledge, T. Nishimoto, D. O. Morgan, R. Franza, and J. M. Roberts.** 1992. Formation and activation of a cyclin E-cdk2 complex during the G1 phase of the human cell cycle. *Science* **257**:1689-1694.
41. **Koff, A., M. Ohtsuki, K. Polyak, J. M. Roberts, and J. Massague.** 1993. Negative regulation of G1 in mammalian cells: inhibition of cyclin E-dependent kinase by TGF- $\beta$ . *Science* **260**:536-539.
42. **Lammie, G. A., V. Fantl, R. Smith, E. Shuuring, S. Brookes, R. Michalides, C. Dickson, A. Arnold, and G. Peters.** 1991. D11S287, a putative oncogene on chromosome 11q13, is amplified and expressed in squamous cell and mammary carcinomas and linked to BCL-1. *Oncogene* **6**:439-444.
43. **Leach, S. F., S. J. Elledge, C. J. Sherr, J. K. V. Willson, S. Markowitz, K. W. Kinzler, and B. Vogelstein.** 1993. Amplification of cyclin genes in colorectal carcinomas. *Cancer Res.* **53**:1986-1989.
44. **Lew, D. J., V. Dulic, and S. I. Reed.** 1991. Isolation of three novel human cyclins by rescue of G1 cyclin (cln) function in yeast. *Cell* **66**:1197-1206.
45. **Lovec, H., A. Sewing, F. C. Lucibello, R. Müller, and T. Möröy.** 1994. Oncogenic activity of cyclin D1 revealed through cooperation with Ha-ras: link between cell cycle control and malignant transformation. *Oncogene* **9**:323-326.
46. **Matsuoka, M., J. Kato, R. P. Fisher, D. O. Morgan, and C. J. Sherr.** 1994. Activation of cyclin-dependent kinase-4 (CDK4) by mouse MO15-associated kinase. *Mol. Cell Biol.* **78**:713-724.
47. **Matsushime, H., M. F. Roussel, and C. J. Sherr.** 1991. Novel Mammalian cyclins (CYL genes) expressed during G1, vol. 56. Cold Spring Harbor Laboratory Press.
48. **Meyerson, M., and E. Harlow.** 1994. Identification of G1 kinase activity for cdk6, a novel cyclin D partner. *Mol. Cell Biol.* **14**:2077-2086.
49. **Minshull, J., R. Golsteyn, C. S. Hill, and T. Hunt.** 1990. The A- and B-type cyclin associated cdc2 kinases in *Xenopus* turn on and off at different times in the cell cycle. *EMBO J* **9**:2865-2875.
50. **Motokura, T., and A. Arnold.** 1993. Cyclin D and oncogenesis. *Curr. Opin. Genet. & Devel.* **3**:5-10.
51. **Motokura, T., T. Bloom, H. G. Kim, H. Jüppner, J. V. Ruderman, H. M. Kronenberg, and A. Arnold.** 1991. A BCL1-linked candidate oncogene which is rearranged in parathyroid tumors encodes a novel cyclin. *Nature* **350**:512-515.
52. **Musgrove, E. A., C. S. L. Lee, M. F. Buckley, and S. R.L.** 1994. Cyclin D1 induction in breast cancer cells shortens G1 and is sufficient for cells arrested in G1 to complete the cell cycle. *Proc. Natl. Acad. Sci.* **91**:8022-8026.
53. **Noda, A. F., Y. Ning, S. Venable, O. M. Pereira-Smith, and J. R. Smith.** 1994. Cloning of senescent cell-derived inhibitors of DNA synthesis using an expression screen. *Exp. Cell. Res.* **211**:90-98.
54. **Nurse, P.** 1994. Ordering S phase and M phase in the cell cycle. *Cell* **79**:547-550.



55. **Ohtsubo, M., A. M. Theodoras, J. Schumacher, J. M. Roberts, and M. Pagano.** 1995. Human cyclin E, a nuclear protein essential for the G1-to-S phase transition. *Mol. Cell. Biol.* **15**:2612-2624.
56. **Pagano, M., R. Pepperkok, F. Verde, W. Ansorge, and G. Draetta.** 1992. Cyclin A is required at two points in the human cell cycle. *EMBO J* **11**:961-971.
57. **Peter, M., and I. Herskowitz.** 1994. Joining the complex: Cyclin-dependent kinase inhibitory proteins and the cell cycle. *Cell* **79**:181-184.
58. **Pines, J., and T. Hunter.** 1990. Human cyclin A is adenovirus E1A-associated protein p60 and behaves differently from cyclin B. *Nature* **346**:760-763.
59. **Polyak, K., J.-y. Kato, M. I. Soloman, C. J. Sherr, J. Massague, J. M. Roberts, and A. Koff.** 1994. p27KIP1, a cyclin-cdk inhibitor, links transforming growth factor $\beta$  and contact inhibition to cell cycle arrest. *Genes & Dev.* **8**:9-22.
60. **Polyak, K., M.-H. Lee, H. Erdjument-bromage, P. Tempst, and J. Massague.** 1994. Cloning of p27KIP1, a cyclin-dependent kinase inhibitor and potential mediator of extracellular antimotogenic signals. *Cell* **78**:59-66.
61. **Porter, P. L., K. E. Malone, P. J. Heagerty, G. M. Alexander, L. A. Gatti, E. J. Firpo, J. R. Daling, and J. M. Roberts.** 1997. Expression of cell-cycle regulators p27 and cyclin E, alone and in combination, correlate with survival in young breast cancer patients. *Nat. Med.* **3**:222-225.
62. **Quelle, D. E., R. A. Ashmun, S. A. Shurleff, J.-y. Kato, D. Bar-Sagi, M. F. Roussel, and C. J. Sherr.** 1993. Overexpression of mouse D-type cyclins accelerates G1 phase in rodent fibroblasts. *Genes & Dev.* **7**:1559-1571.
63. **Resnitzky, D., G. M., H. Bujard, and S. I. Reed.** 1994. Acceleration of the G1/S phase transition by expression of cyclins D1 and e with an inducible system. *Mol. Cell Biol.* **14**:1669-1679.
64. **Rosenberg, C. L., H. G. Kim, T. B. Shows, H. M. Kronenberg, and A. Arnold.** 1991. Rearrangement and overexpression of D11S287E, a candidate oncogene on chromosome 11q13 in benign parathyroid tumors. *Oncogene* **6**:449-453.
65. **Rosenberg, C. L., E. Wong, E. M. Pety, A. E. Bale, Y. Tsujimoto, N. L. Harris, and A. Arnold.** 1991. PRAD1, a candidate BCL1 oncogene: mapping and expression in centrocytic lymphoma. *Proc. Natl. Acad. Sci USA* **88**:9638-9642.
66. **Scalfani, R. A.** 1998. Cyclin dependent kinase activating kinases. *Curr. Opin. Cell Biol.* **8**:788-794.
67. **Serrano, M., G. J. Hannon, and D. Beach.** 1994. A new regulatory motif in cell-cycle control causing specific inhibition of cyclin D/CDK4. *Nature* **366**:704-707.
68. **Sewing, A., V. Ronicke, C. Burger, M. Funk, and R. Muller.** 1994. Alternative splicing of human cyclin E. *J. Cell Science* **107**:581-588.
69. **Sherr, C. J.** 1994. G1 phase progression: cycling on cue. *Cell* **79**:551-555.
70. **Sherr, C. J.** 1993. Mammalian G1 cyclins. *Cell* **73**:1059-1065.
71. **Sherr, C. J., and J. M. Roberts.** 1995. Inhibitors of mammalian G1 cyclin-dependent kinases. *Genes & Dev.* **9**:1149-1163.
72. **Standart, N., J. Minshull, J. Pines, and T. Hunt.** 1987. Cyclin synthesis, modification and destruction during meiotic maturation of the starfish oocyte. *Dev. Biol.* **124**:248-254.
73. **Swenson, K. I., K. M. Farrell, and J. V. Ruderman.** 1986. The clam embryo protein cyclin A induces entry into M phase and the resumption of meiosis in *Xenopus* oocytes. *Cell* **47**:861-870.
74. **Toyoshima, H., and T. Hunter.** 1994. p27, a novel inhibitor of G1 cyclin-cdk protein kinase activity is related to p21. *Cell* **78**:67-74.
75. **Tsai, L.-H., E. Harlow, and M. Meyerson.** 1991. Isolation of the human *cdk 2* gene that encodes the cyclin A- and adenovirus E1A-associated p33 kinase. *Nature* **353**:174-177.
76. **Wang, J., X. Chenivresse, B. Henglein, and C. Br  chot.** 1990. Hepatitis B virus integration in a cyclin A gene in a hepatocellular carcinoma. *Nature* **343**:555-557.

77. **Wang, T. C., R. D. Cardiff, L. Zukerberg, E. Lees, A. Arnold, and E. V. Schmidt.** 1994. Mammary hyperplasia and carcinoma in MMTV-cyclin D1 transgenic mice. *Nature* **369**:669-671.
78. **Withers, D., R. Harvey, J. Faust, O. Melnyk, K. Carey, and T. Meeker.** 1991. Characterization of a candidate bcl-1 gene. *Mol. Cell Biol.* **11**:4846-4853.
79. **Xiong, Y., T. Connolly, B. Futcher, and D. Beach.** 1991. Human D-type cyclin. *Cell* **65**:691-699.
80. **Xiong, Y., G. J. Hannon, G. J. Zhang, D. Gasso, R. Kobayashi, and D. Beach.** 1993. p21, a universal inhibitor of cyclin kinases. *Nature* **366**:710-704.
81. **Xiong, Y., H. Zhang, and D. Beach.** 1993. D type cyclins associate with multiple protein kinases and the DNA replication and repair factor, PCNA. *Cell* **71**:505-514.
82. **Xiong, Y., H. Zhang, and D. Beach.** 1992. Subunit rearrangement of the cyclin dependent kinases is associated with cellular transformation. *Genes & Dev.* **7**:1572-1583.



## Appendix

We are including 19 figures, and their figure legends. We are also including reprints and copies of 3 manuscripts which are a result of the last two aims of our grant

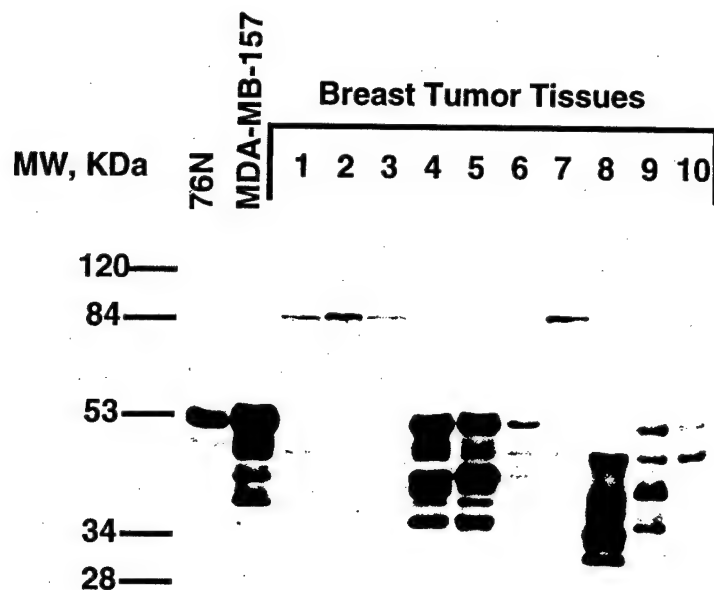


**Figure 1.** Western blot analysis showing an altered cyclin E expression in tumor cells. Whole cell lysates were extracted from 10 breast cancer tissues as well as 76N normal and MDA-MB-157 tumor cell lines. Breast cancer types and tumor stages are: lane 1, ductal carcinoma in situ (DCIS); lane 2, stage 1 DCIS; lane 3, stage 1 DCIS; lane 4, stage 4 invasive ductal carcinoma (metastasis to Omentum); lane 5, stage 4 invasive ductal carcinoma (metastasis to Omentum); lane 6, stage 2 DCIS; lane 7, stage 1 DCIS; lane 8, stage 4 invasive ductal carcinoma (metastasis to ovaries); lane 9, stage 3 invasive ductal carcinoma (no metastasis); lane 10, stage 2 DCIS. Protein extracts were loaded 50 ug per lane and probed with affinity purified anti-cyclin E monoclonal antibody.

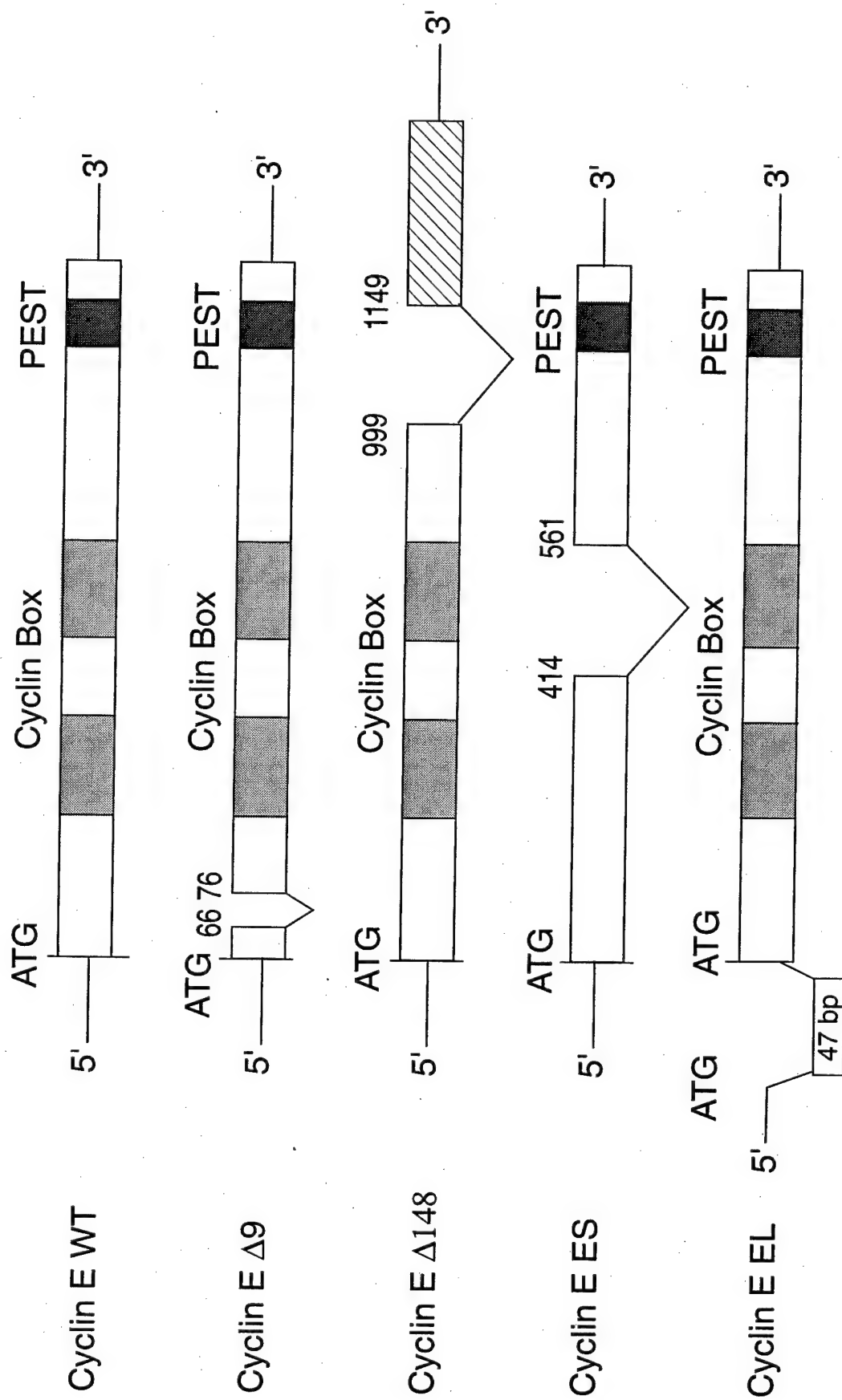


Figure 2. Alternatively spliced forms of cyclin E. Cyclin E WT is the wild type form of cyclin E mRNA. Cyclin E  $\Delta 9$  and  $\Delta 148$  are alternatively spliced mRNA's isolated by RT-PCR from the tumor cell line MDA-MB-157. The cyclin box is the region where cyclin E binds to CDK2 (55). The PEST sequence is necessary for the cell cycle regulated destruction of cyclin E.

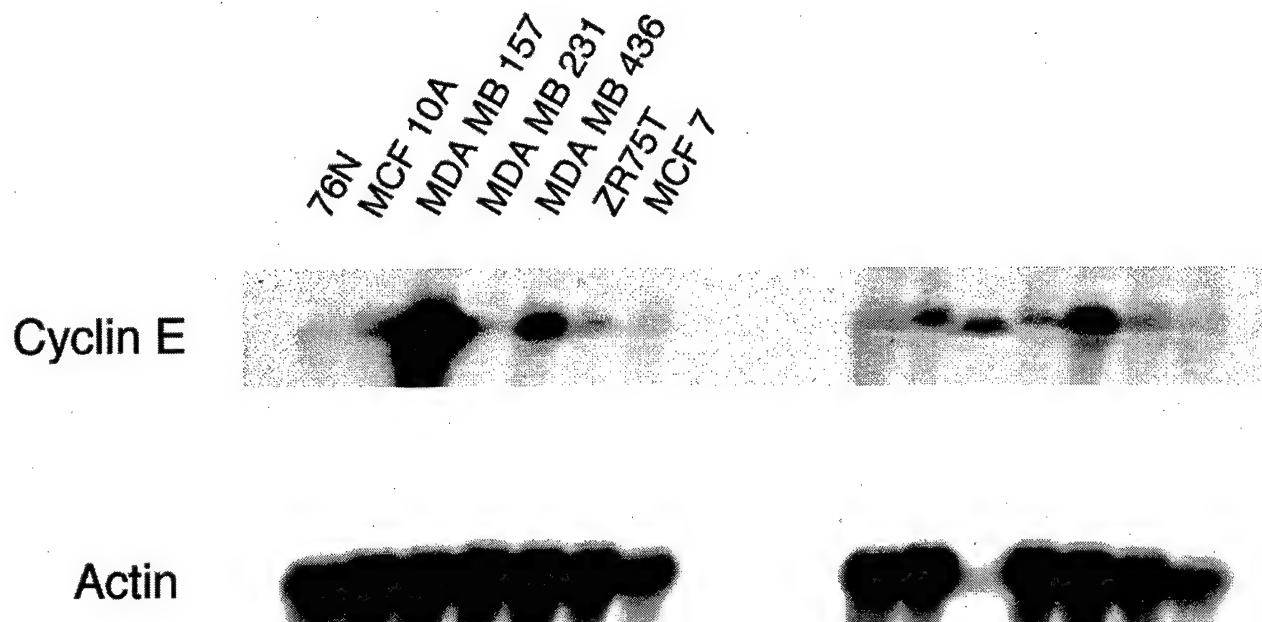
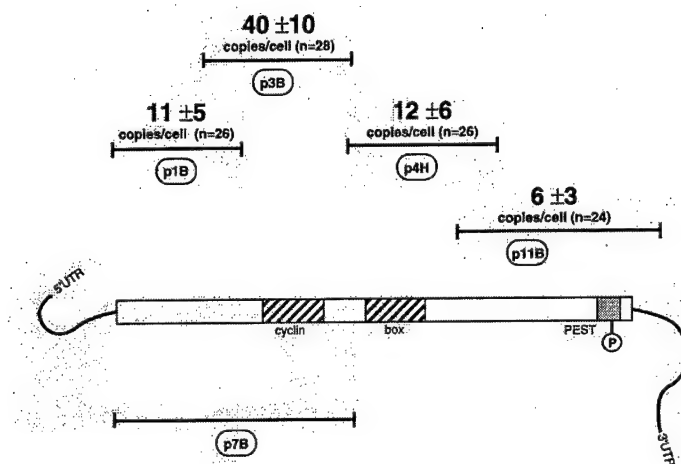


Figure 3.

Northern blot of total RNA extracted from various human breast cell lines. The normal cell strain is 76N and normal immortal cell line is MCF 10A. Other cell lines shown are tumor derived. Left panel: 10  $\mu$ g of total RNA was electrophoresed, transferred to nylon membrane, probed with a  $^{32}$ P-labeled cDNA probe and exposed to X-ray film. The tumor cell line MDA MB 157 overexpresses cyclin E mRNA and was loaded at 1  $\mu$ g in the panels on the right. As labeled, the Northern blots were probed with either cyclin E or actin.



**Figure 4.**  
Quantitation of cyclin E mRNA in MDA MB 157 human breast tumor cell line with the RNase protection assay.  $^{32}\text{P}$ -labeled antisense RNA probes from the regions shown above were hybridized to 5 and 10  $\mu\text{g}$  total RNA isolated from tissue culture cells. After digestion with RNase, the protected double stranded RNA was electrophoresed on 5% TBE acrylamide gels. The gel was dried on 3MM paper, exposed to X-ray film and the labeled bands excised and the Cerenkov counts determined. A standard curve using full length cyclin E mRNA synthesized in vitro was used to calculate the pmol per cell which was converted into copies per cell as shown.

Cell Lines	Probe 3B	Actin
	Copies per cell	Copies per cell
76N	$3.1 \pm 0.4$	$3400 \pm 10$
MCF-10A	$2.2 \pm 1.1$	$4200 \pm 300$
MDA-MB-157	$43.5 \pm 2.1$	$2400 \pm 10$
MDA-MB-231	$3.6 \pm 1.3$	$4100 \pm 300$
MDA-MB-436	$8.3 \pm 1.4$	$6300 \pm 60$
ZR75T	$0.9 \pm 0.5$	$3100 \pm 200$
MCF-7	$1.0 \pm 0.6$	$2200 \pm 200$

**Figure 5: RPA quantitation of cyclin E mRNA in normal and tumor breast cell lines.**

The total RNA from various human breast normal and tumor cell lines was analyzed by the RNase protection assay. The probe 3B was used to quantitate the amount of cyclin E mRNA present in the various cell lines. Actin is used as a control and for comparison. Cyclin E message is at very low copy number per cell.

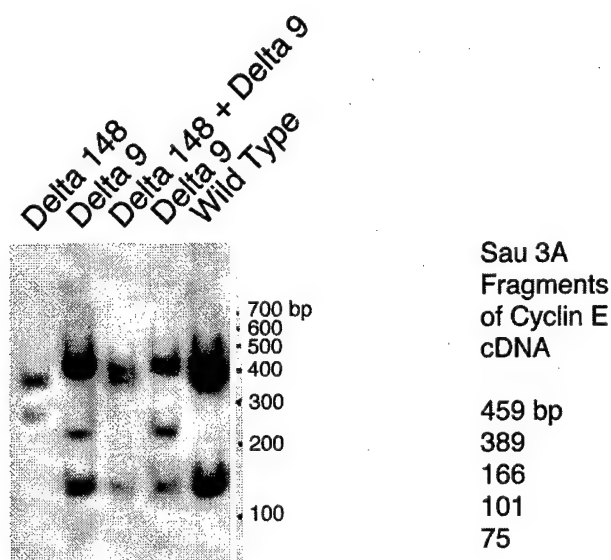


**Figure 6.**

Southern blot analysis to detect cyclin E cDNA variants in an RT-PCR plasmid library. RT-PCR was performed on normal and tumor total RNA using 3' and 5' flanking oligonucleotides to the known cyclin E cDNA sequence. The resulting PCR products which represent the cyclin E mRNA species present in the total RNA were ligated into the plasmid pCR II and electroporated into the *E. coli* strain DH10B. The transformants were plated at single colony density and filter lifts were probed with a <sup>32</sup>P-labeled cDNA probe to cyclin E. Plasmid preps to positive colonies were prepared, digested with *Sau* 3A, electrophoresed on 5% TBE acrylamide gels, transferred to nylon membrane and probed with a <sup>32</sup>P-labeled cDNA. The Southern blots were exposed to X-ray film. The new cDNA containing the delta 9 and delta 148 splice variations was sequenced to confirm its identity.

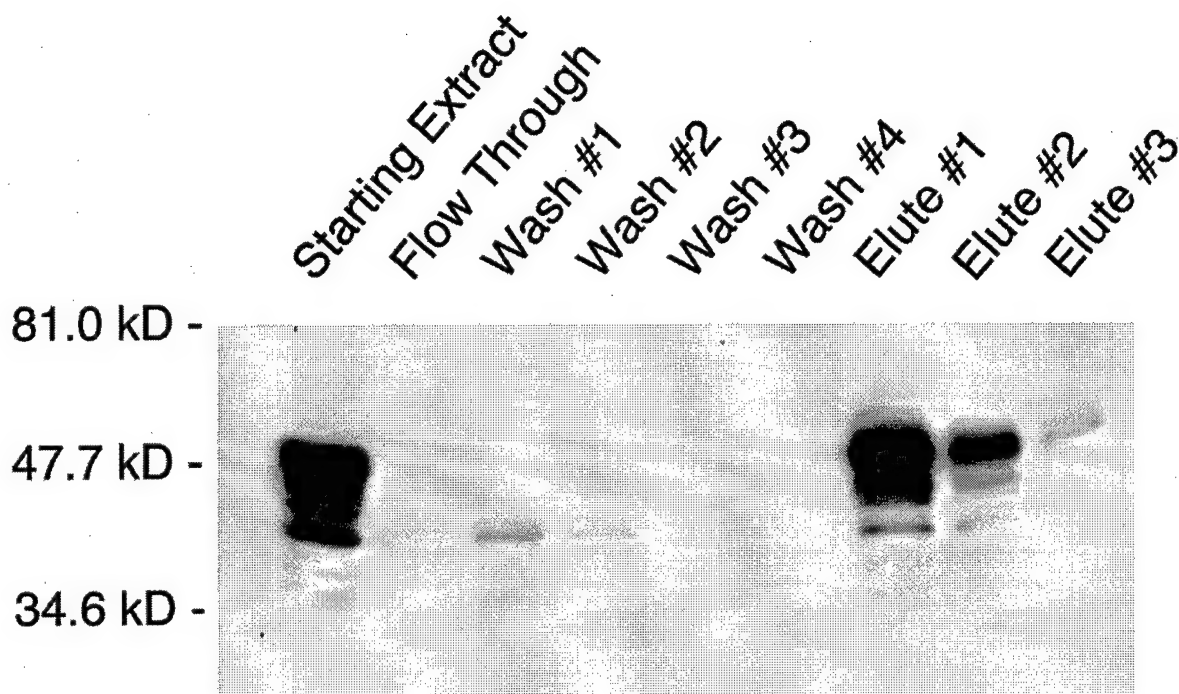
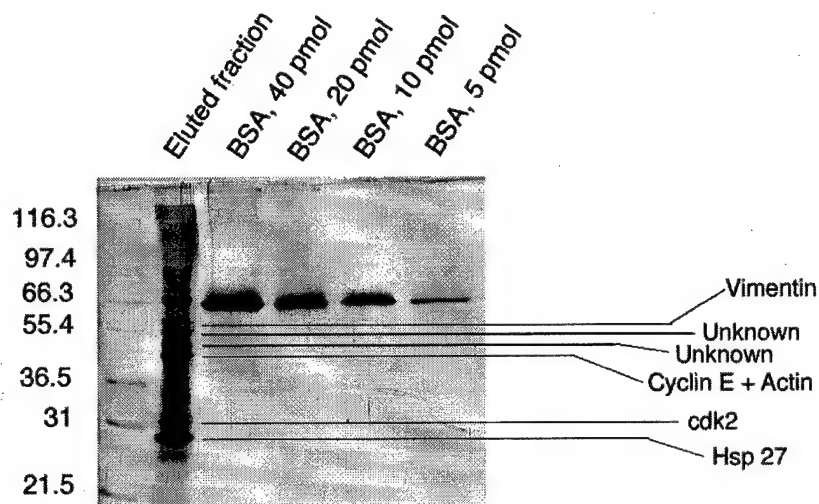


Figure 7.

Immuno-affinity purification of cyclin E from the human breast tumor cell line MDA-MB-157. The affinity column was prepared by cross-linking a polyclonal antibody (reactive to a carboxy-terminal peptide) to protein A sepharose. Cell extracts were prepared from tissue culture cells by sonication and ultracentrifugation as described. 8 mg of extract was incubated with the affinity resin overnight at 4o C. The flow through was collected and the column washed with a series of buffers (1-4) and then eluted with 0.1 M glycine pH 4.0. A representative volume from each fraction was boiled in reducing sample buffer and analyzed by SDS PAGE and cyclin E Western blot. The Western blot was visualized on X-ray film with ECL chemiluminescence.





**Figure 8.**

Silver stained SDS PAGE gel showing cyclin E and associated proteins purified on an polyclonal antibody affinity column. Cyclin E eluted from the anti-cyclin E affinity column was concentrated by centrifugation on a Centricon 10 concentrator boiled in reducing sample buffer, separated by SDS PAGE and silver stained. The bands labeled in the figure were identified by MALDI TOF mass spectrometry. Cyclin E and cdk2 were confirmed by western blot of a small portion of the band cut from the silver stained gel. Bovine serum albumin (BSA) was electrophoresed at the shown concentrations for comparison.

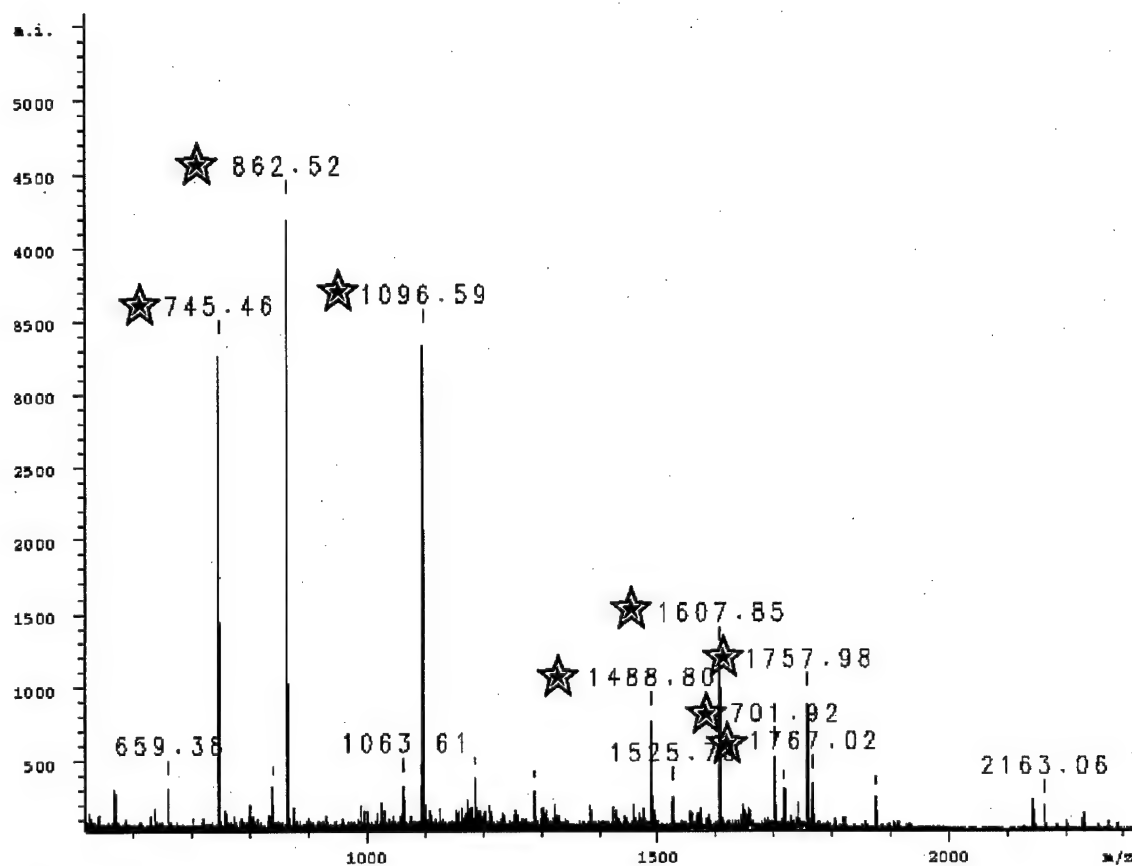


Figure 9.

Mass spectrometry analysis of the cdk2 band from a silver stained gel. After purification of cyclin E from MDA MB 157 cell extracts as described in Fig 7, the band identified as cdk2 by Western blotting was prepared for in gel trypsin digestion. The tryptic peptides were extracted with acetonitrile and prepared for MALDI TOF analysis. The major peaks identified all correspond to cdk2 when compared to the available databases through Protein Prospector via the internet. Cdk2 peaks are identified with a star. Unlabeled peaks correspond to trypsin self-digestion products.

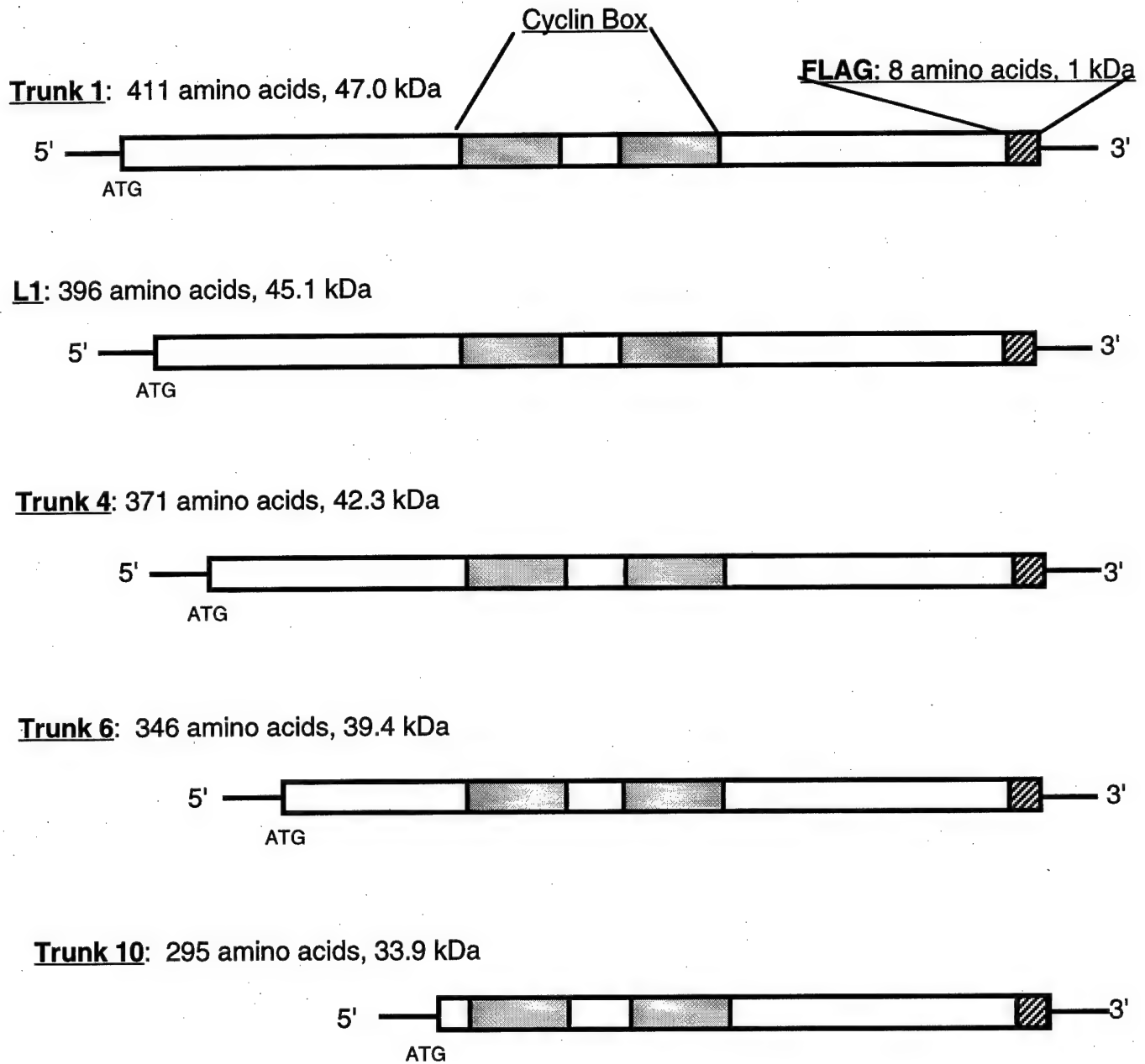
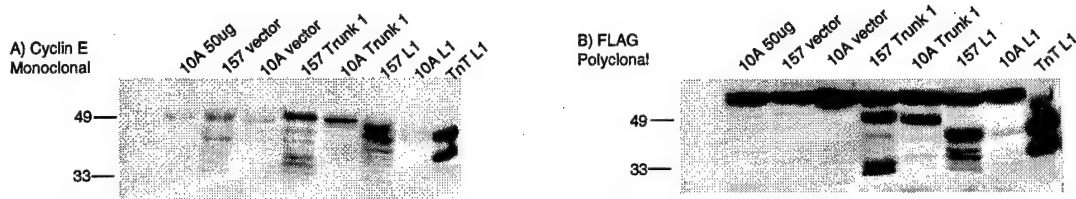


Figure 10. The wild type and truncated cyclin E forms to be used for transfection. L1 represents the published full length cyclin E form found in the cells. The other trunks were constructed by creating N terminal deletions of the wild type cyclin E protein. Trunk1 contains a portion of the 5' untranslated region up to an upstream ATG. The cyclin box is the portion of cyclin E which binds to CDK2. FLAG is a C terminal immunogenic peptide sequence to the FLAG antibody. All of these genes have been cloned into the expression vector pCDNA3.1 under the control of a CMV promoter.

Cell line	No DNA	GFP vector
MDA-MB-157	0.8%	55%
MCF-10A	1.6%	68%

**Figure 11: Flow cytometric analysis of green fluorescent protein expression of transfected cells.** MDA-MB-157 cells were transfected at 0.3 mV with either no DNA or 40  $\mu$ g of plasmid. MCF-10A cells were transfected at 0.33 mV with either no DNA or 40  $\mu$ g of plasmid. All cells were electrophoresed in a 0.4 cm gap cuvette at a 960  $\mu$ F capacitance with  $1 \times 10^7$  cells in a volume of 500  $\mu$ l of media. The percentages represent percentage of cells expressing green fluorescent protein.



**Figure 12. Normal vs Tumor expression of FLAG cyclin E.** MDA-MB-157 cells were transfected with both Trunk 1 and L1 cyclin E at 0.3 kV with 40  $\mu$ g of DNA at 960  $\mu$ F capacitance with  $1 \times 10^7$  cells in 0.5 mls of media. MCF-10A cells were transfected with both Trunk1 and L1 cyclin E at 0.33 kV with 40  $\mu$ g of DNA at 960  $\mu$ F capacitance with  $1 \times 10^7$  cells in 0.5 mls of media. Cells were harvested 48 hours post transfection, lysed, and 50  $\mu$ g of protein were run on a 10% SDS acrylamide gel. Blots were blocked 24 hours, washed with TBST, probed with primary (A) cyclin E monoclonal and (B) FLAG polyclonal antibodies for 2 hours, washed with TBST, probed with secondary antibody for 1 hour, washed with TBST, and developed using the Pierce chemiluminescence kit.

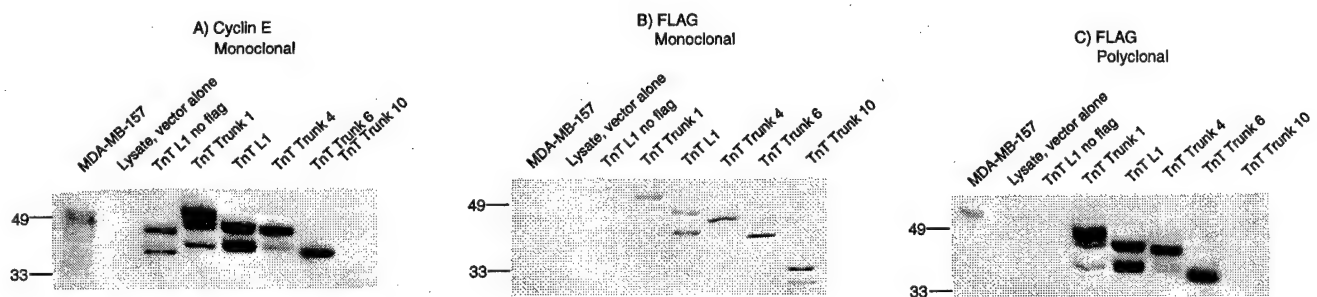
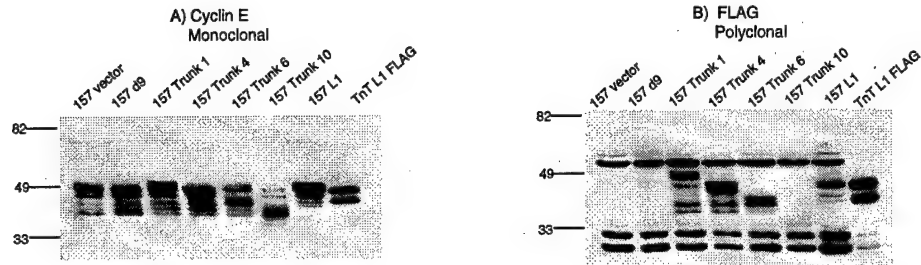


**Figure 13. In vitro expression of FLAG tagged truncated cyclin E forms.** Protein was made using the Promega in vitro TnT reticulocyte lysate kit. 1  $\mu$ l of TnT reaction was loaded on a 10% SDS acrylamide gel. Blots were blocked 24 hours, washed with TBST, probed with primary (A) cyclin E monoclonal, (B) FLAG monoclonal, or (C) FLAG polyclonal antibodies for 2 hours, washed with TBST, probed with secondary antibody for 1 hour, washed with TBST, and developed using the Pierce chemiluminescence kit.

### MDA-MB-157



### MCF-10A

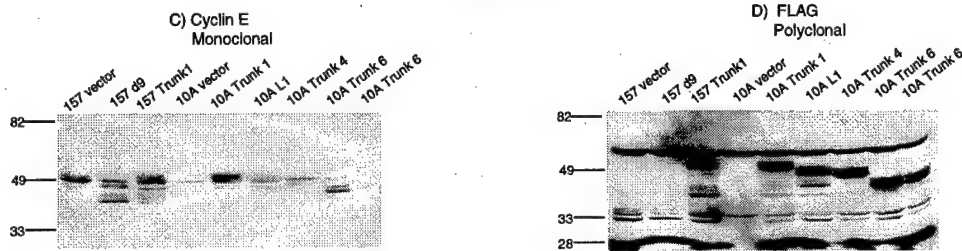
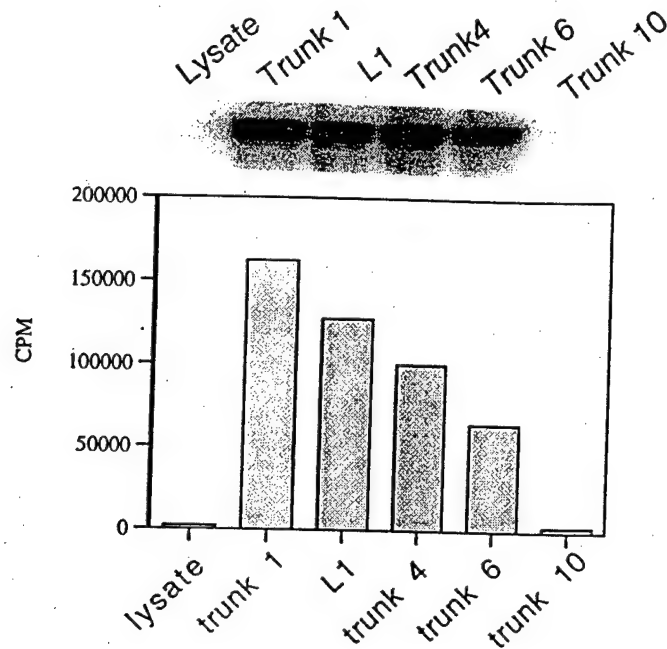


Figure 14. Expression of FLAG tagged truncated cyclin E forms in normal vs tumor cells. MDA-MB-157 cells were transfected with truncated forms of cyclin E at 0.3 kV with 40 ug of DNA at 960 uF capacitance with  $1 \times 10^7$  cells in 0.5 mls of media. MCF-10A cells were transfected with truncated forms of cyclin E at 0.33 kV with 40 ug of DNA at 960 uF capacitance with  $1 \times 10^7$  cells in 0.5 mls of media. Cells were harvested 48 hours post transfection, lysed, and 50 ug of protein were run on a 10% SDS acrylamide gel. Blots were blocked 24 hours, washed with TBST, probed with primary (A, C) cyclin E monoclonal and (B, D) FLAG polyclonal antibodies for 2 hours, washed with TBST, probed with secondary antibody for 1 hour, washed with TBST, and developed using the Pierce chemiluminescence kit.

### A) H1 KINASE ACTIVITY



### B) CDK2 DENSITOMETRY

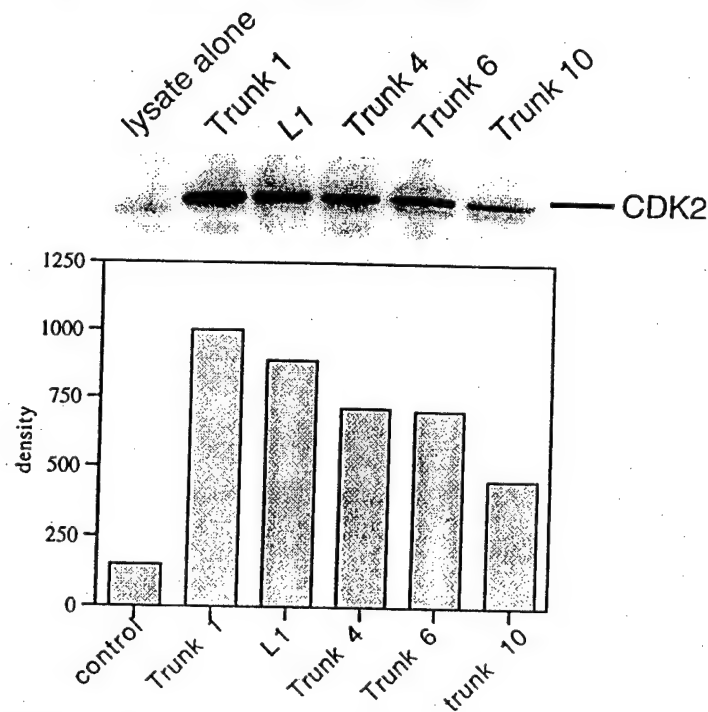
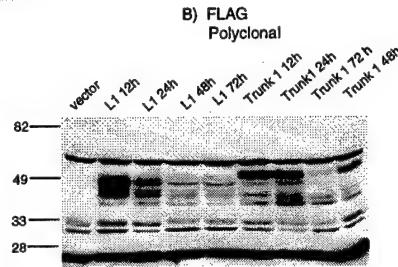
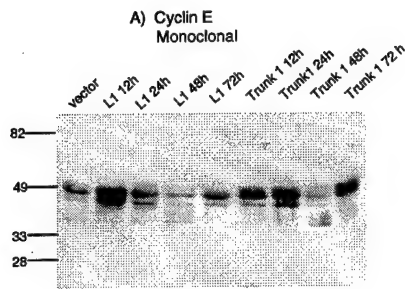


Figure 15 In vitro synthesized cyclin E trunk forms mixed with MDA-MB-157 cell extracts overnight. Immunoprecipitations were performed on samples using the anti-FLAG antibody. (A) H1 kinase assays were performed on samples, and then run on a 12% SDS page gel, and exposed on film. (B) Samples were run on a 12% SDS page gel and probed using the anti-CDK2 antibody. Densitometry was obtained using the Kodak Biomax 1D system.

# MDA-MB-157



# MCF-10A

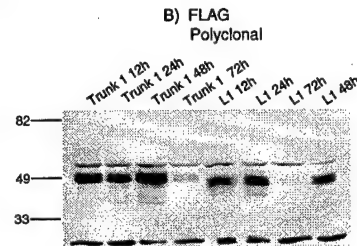
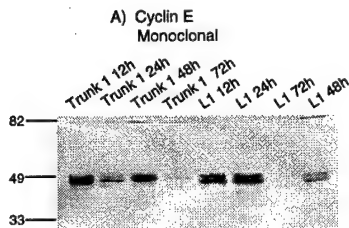


Figure 16. Time course of expression of FLAG tagged cyclin E in normal and tumor cells. MDA-MB-157 cells were transfected with both Trunk 1 and L1 cyclin E at 0.3 kV with 40 ug of DNA at 960 uF capacitance with  $1 \times 10^7$  cells in 0.5 mls of media. MCF-10A cells were transfected with both Trunk1 and L1 cyclin E at 0.33 kV with 40 ug of DNA at 960 uF capacitance with  $1 \times 10^7$  cells in 0.5 mls of media. Cells were harvested at 12, 24, 48, and 72 hours post transfection, lysed, and 50 ug of protein were run on a 10% SDS acrylamide gel. Blots were blocked 24 hours, washed with TBST, probed with primary (A, C) cyclin E monoclonal and (B, D) FLAG polyclonal antibodies for 2 hours, washed with TBST, probed with secondary antibody for 1 hour, washed with TBST, and developed using the Pierce chemiluminescence kit.

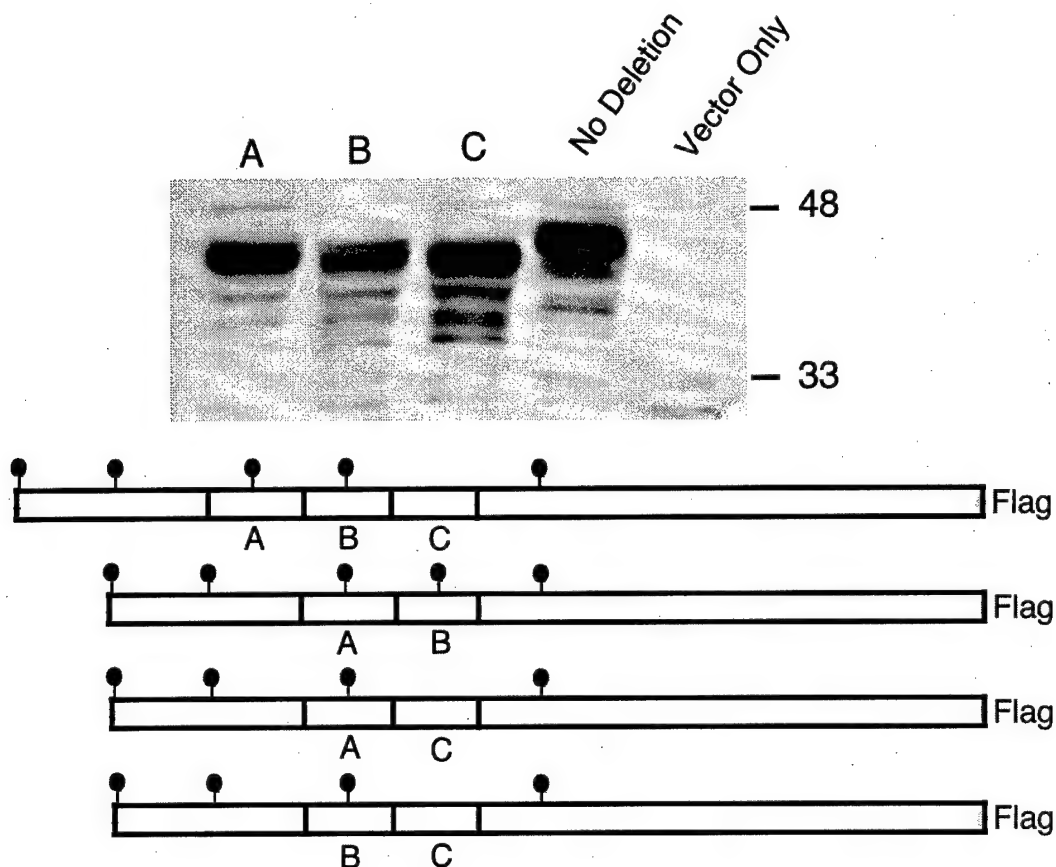
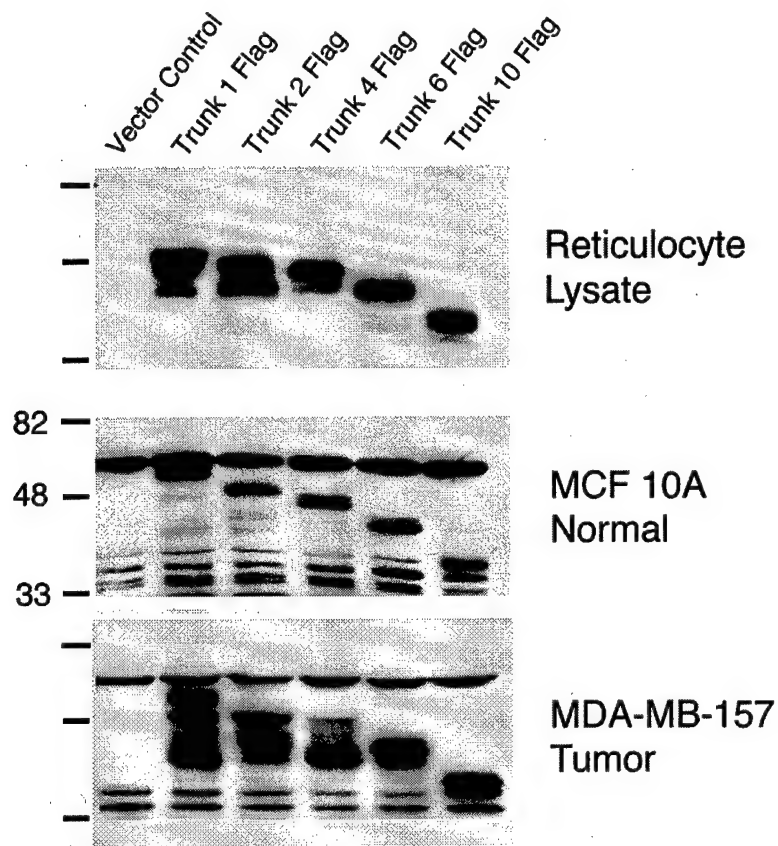


Figure 17.

Deletion analysis is used to locate the region of cyclin E proteolytic processing. Processing of cyclin E occurs in every truncated version of cyclin E except the smallest, Trunk 10. The processing of cyclin E into a doublet occurs very near to the amino terminus of Trunk 6. Three block deletions of 6 amino acids each were made in the cyclin E cDNA sequence just downstream of the amino terminus of the Trunk 6 version of cyclin E (see Fig 19). These block deletions are designated A, B and C. These deletions were mutated into the cyclin E/Trunk 1/Flag eucaryotic expression vector and transiently transfected into the tumor cell line MDA MB 157. Protein was extracted and analyzed by SDS PAGE and the transfected proteins detected by Western blot using an anti-Flag antibody. The deletions of blocks A and B resulted in the loss of a single band of the processed cyclin E which indicates the deletion of a proteolytic domain. The gel pattern is consistent with the loss of two potential proteolytic sites, one in block A and one in block B. The deletion of block C only reduces the size of the protein and indicates the C block deletion is downstream of the proteolytic processing which occurs in the tumor cells.





**Figure 18.**

Expression of amino-terminal truncated forms of cyclin E. Amino-terminal deletions of cyclin E were prepared by site directed mutagenesis using oligonucleotides and PCR. The mutated forms of cyclin E were ligated into the eucaryotic expression vector pCDNA 3.1 and expressed in reticulocyte lysate (top panel), transiently transfected into the normal cell line MCF 10A (center panel) and transiently transfected into the tumor cell line MDA MB 157. After transfection the cells were lifted, sonicated and ultracentrifuged to obtain total soluble protein extract. Two microliters of in vitro transcribed/translated cyclin E in reticulocyte lysate was boiled in reducing sample buffer and electrophoresed. 50  $\mu$ g of cell protein extract was boiled in reducing sample buffer and electrophoresed. The electrophoresed protein was western blotted and detected using an anti-FLAG polyclonal antibody and ECL chemiluminescence.



# Lovastatin mediated G1 arrest in normal and tumor breast cells is through inhibition of CDK2 activity and redistribution of p21 and p27, independent of p53

Sharmila Rao<sup>1</sup>, Michael Lowe<sup>1</sup>, Thaddeus W Herliczek<sup>1</sup> and Khandan Keyomarsi<sup>1,2</sup>

<sup>1</sup>Laboratory of Diagnostic Oncology, Division of Molecular Medicine, Wadsworth Center, Albany, New York 12201-0509;

<sup>2</sup>Department of Biomedical Sciences, State University of New York, Albany, New York 12222, USA

Previously, we reported that lovastatin, a potent inhibitor of the enzyme HMG CoA reductase also acts as an antimitogenic agent by arresting cells in the G1 phase of the cell cycle resulting in cell cycle-independent alteration of cyclin dependent kinase inhibitors (CKIs). In the present study we have investigated the nature of the CKIs (p21 and p27) alterations resulting in G1 arrest in both normal and tumor breast cell lines by lovastatin. We show that even though lovastatin treatment causes G1 arrest in a wide variety of normal and tumor breast cells irrespective of their p53 or pRb status, the p21 and p27 protein levels are not increased in all cell lines treated suggesting that the increase in p21 and p27 protein expression per se is not necessary for lovastatin mediated G1 arrest. However, the binding of p21 and p27 to CDK2 increases significantly following treatment of cells with lovastatin leading to inhibition of CDK2 activity and a subsequent arrest of cells in G1. The increased CKI binding to CDK2 is achieved by the redistribution of both p21 and p27 from CDK4 to CDK2 complexes subsequent to decreases in CDK4 and cyclin D3 expression following lovastatin treatment. Lastly, we show that lovastatin treatment of 76N-E6 breast cell line with an altered p53 pathway also results in G1 arrest and similar redistribution of CKIs from CDK4 to CDK2 as observed in other breast cell lines examined. These observations suggest that lovastatin induced G1 arrest of breast cell lines is through a p53 independent pathway and is mediated by decreased CDK2 activity through redistribution of CKIs from CDK4 to CDK2.

**Keywords:** lovastatin; cell cycle; cyclins; CKIs; CDKs; adaptor molecule

## Introduction

The mammalian cell cycle, defined as a sequence of events between two cell divisions, is positively regulated by cyclins and cyclin dependent kinases (CDKs) which associate to form heterodimeric complexes (Sherr, 1994, 1996; Elledge *et al.*, 1996; Nasmyth, 1996). Mitogenic stimuli results in the phosphorylation and thereby activation of cyclin-CDK complexes by CDK activating kinase, CAK (Fisher and Morgan, 1994; Makela *et al.*, 1994; Harper and Elledge, 1998). The activated

cyclin/CDK complexes in turn sequentially phosphorylate substrates such as the retinoblastoma protein (pRb) throughout the cell cycle (Ewen *et al.*, 1993a; Matsushime *et al.*, 1994; Sherr, 1996). Phosphorylation of pRb which is necessary for the progression through G1 is regulated primarily by cyclin D/CDK4/CDK6 complexes while the cyclin E/CDK2 complex regulates the passage of cells from late G1 to S phase and further contribute to pRb hyper-phosphorylation (Sherr, 1994, 1996; Bartek *et al.*, 1997). The hypo-phosphorylated pRb serves as a tumor suppressor by interacting with and inhibiting cellular proteins such as E2F-DP heterodimeric transcription factors which activate many genes required for DNA replication pivotal for G1/S transition (Weinberg, 1995; Bartek *et al.*, 1996, 1997; Ikeda *et al.*, 1996). The complete hyper-phosphorylation of pRb by cyclin E/CDK2 complexes and consequent activation of E2F-DP transcription complex are thought to play a major role in overcoming of the restriction point (Pardee, 1989; Planas-Silva and Weinberg, 1997b).

Progression through the cell cycle and the restriction point is also negatively regulated through the association with CDK inhibitors, CKIs (Elledge and Harper, 1994; Sherr and Roberts, 1995; Harper and Elledge, 1996; Harper, 1997). There are two families of structurally distinct CKIs, the CIP/KIP family which inhibit a broad range of CDKs by selectively binding and inhibiting the fully associated cyclin/CDK complexes and the INK family which bind specifically to CDK4 and/or CDK6 and inhibit complex formation with cyclin D (Elledge *et al.*, 1996; Sherr, 1996; Harper, 1997). The CKI p21 (CIP1/WAF1), the first mammalian CKI to be identified was simultaneously characterized by several laboratories as the major p53 inducible gene (WAF1) (El-Deiry *et al.*, 1993) as a CDK inhibitor protein (CIP1, p21 and p20CAP1) (Gu *et al.*, 1993; Harper *et al.*, 1993; Xiong *et al.*, 1993) as a protein highly expressed in senescent fibroblasts (SDI) (Noda *et al.*, 1994), and as a melanoma differentiation associated gene (mda 6) (Jiang and Fisher, 1993). p27 (KIP1), similar in amino acid sequence and inhibitory specificity to p21, was identified as a protein associated with inactive cyclin E/CDK2 complexes in TGF- $\beta$ 1 treated and contact inhibited cells (Polyak *et al.*, 1994a,b), as a protein that interacts with cyclin D1/CDK4 complexes (Toyoshima and Hunter, 1994), and in cells arrested in G1 (Hengst *et al.*, 1994). Although p21 is induced by p53 in response to DNA damage resulting in CDK inhibition and G1 growth arrest (Dulic *et al.*, 1994), it can also be induced by p53

independent mechanisms; by serum, PDGF and EGF in embryonic fibroblasts from p53 knockout mice (Michieli *et al.*, 1994), by serum starvation in p53 mutant human breast carcinoma cells (Sheikh *et al.*, 1994), by EGF in squamous carcinoma cells (Jakus and Yeudall, 1996), by TGF- $\beta$ 1 in p53 mutant cells (Elbendary *et al.*, 1994; Datto *et al.*, 1995; Reynisdottir *et al.*, 1995) and by lovastatin in breast cancer cells (Gray-Bablin *et al.*, 1997). p27 is similarly induced by lovastatin (Hengst *et al.*, 1994; Hengst and Reed, 1996; Gray-Bablin *et al.*, 1997), by TGF- $\beta$ 1 (Polyak *et al.*, 1994a), following cell to cell contact inhibition, by rapamycin and by agents that induce cAMP mediated growth arrest (Kato *et al.*, 1994; Nourse *et al.*, 1994; Polyak *et al.*, 1994b; Toyoshima and Hunter, 1994). Hence, p21 and p27 may function similarly to inhibit CDK activity and proliferation in response to different environmental stimuli. Furthermore, removal by degradation/inactivation of p27 may be necessary for proliferation (Pagano *et al.*, 1995).

We and others have previously reported that treatment of mammary epithelial cells or HeLa cells by lovastatin results in the induction of p21 and p27 in mammary cells (Gray-Bablin *et al.*, 1997) and p27 in HeLa cells (Hengst *et al.*, 1994; Hengst and Reed, 1996). Lovastatin is an inhibitor of HMG CoA reductase which is the rate limiting enzyme of the cholesterol biosynthesis pathway (Alberts *et al.*, 1980). Though lovastatin has been primarily prescribed for patients with high cholesterol levels (Rettersol *et al.*, 1996) it has also been used as an effective agent in cell synchronization for both tumor and normal cells (Keyomarsi *et al.*, 1991; Keyomarsi, 1996). The inhibition of the cholesterol biosynthesis pathway by lovastatin not only blocks mevalonate synthesis (the product of HMG CoA reductase) but also prevents the farnesylation and geranylgeranylation (intermediate products of the cholesterol pathway) of several signal transduction proteins such as Ras, Rap and many G proteins, thereby preventing their proper intracellular localization and function (Goldstein and Brown, 1990; Maltese, 1990). The induction of p21 and p27 by lovastatin in breast cancer cells seems to be independent of the Ras pathway (Keyomarsi *et al.*, 1991). Furthermore, the lovastatin mediated CKI induction is also through cell cycle independent mechanisms, distinct from other G1 arresting agents/conditions such as serum starvation or double thymidine block (Gray-Bablin *et al.*, 1997).

In this study, we have investigated the nature of induction of p21 and p27 by lovastatin in both normal and tumor-derived mammary epithelial cells. We show that lovastatin is capable of inducing G1 arrest in both normal and tumor breast cells. Furthermore, we provide evidence that it is not the increase in protein levels of the p21 and p27 *per se*, but the increase in the binding of both p21 and p27 to CDK2 complexes and the resulting decrease in activity of cyclin/CDK2 complexes that is essential for lovastatin mediated G1 arrest of normal and tumor cells. We also show that the increased binding of CKIs to CDK2 correlates with decreased CDK4 and cyclin D3 levels and the subsequent release of p21 and p27 from the cyclin D/CDK4 complex, providing evidence for the redistribution of both p21 and p27 under physiological conditions *in vivo*. Lastly, we show that binding of

CKIs to CDK2 or the switching of partners from CDK4 to CDK2 following lovastatin treatment is through a p53 independent pathway.

## Results

### *Lovastatin synchronizes a broad range of tumor and normal breast cancer cells*

In order to determine whether lovastatin would have a differential affect of G1 mediated arrest of normal versus tumor breast cells, three normal and six tumor cell lines were treated with lovastatin at the same dose of duration (i.e. 40  $\mu$ M for 36 h) (Table 1). The normal cells examined were 76N and 70N (both mortal) and MCF-10A (immortalized). The tumor cells used were classified on their ability to express tumor suppressor genes p53, pRb and estrogen receptor (ER). The ER positive tumor cells are MCF-7, ZR75T, and T47D and the ER negative tumor cells are MDA-MB-157, MDA-MB-231 and Hs578T. In the ER positive group all 3 tumor cell lines are also wild type for pRb and p53, except for T47D, which has a p53 mutant phenotype. In the ER negative group all three tumor cell lines are negative for p53 and pRb except for MDA-MB-157 which has a wild type pRb. However, the pRb in these cells is expressed at very low levels (see Figure 1) and is inactive because of high levels of p16 and overexpression of cyclin E (Keyomarsi *et al.*, 1995). p16 has been shown to transcriptionally down regulate pRb expression (Fang *et al.*, 1998) while the overexpression of cyclin E results in constitutive hyperphosphorylation of pRb rendering it inactive as a tumor-suppressor (Gray-Bablin *et al.*, 1996). In the case of Hs578T, it too is pRb negative as published

**Table 1** Cell cycle profiles of lovastatin treated normal and tumor (RB and p53 positive and negative) breast cells

Cell lines	Lovastatin, 40 $\mu$ M h	ER	p53	pRb	%G1	%S	%G2
76N	0	—	+	+	56.6	12.1	31.3
	36				72	1.2	27
MCF-10A	0	—	+	+	65	12	23
	36				90	1.6	8.4
70N	0	—	+	+	60	13	27
	36				78	1.2	21
MCF-7	0	+	+	+	77	11	12
	36				82	4	14
ZR75T	0	+	+	+	67	19	14
	36				85	6	9
T47D	0	+	—	+	73	13	14
	36				86	4	10
Hs578T	0	—	—	—	62	16	20
	36				83	5	12
MDA-MB-157	0	—	—	±	55	12	32
	36				60	4.3	36
MDA-MB-231	0	—	—	—	54	22	24
	36				80	7	13

Estrogen Receptor (ER), p53 and pRb status of cell lines were determined previously (Gray-Bablin *et al.*, 1996, and references within). + indicates wild-type, — indicates mutant or deleted, ± indicates wild-type but functionally inactive (see text). Percentages of cells in different phases of the cell cycle for each cell line following lovastatin treatment were obtained from flow cytometric measurements of DNA contents from three separate experiments and the average of the values are indicated

previously (Gray-Bablin *et al.*, 1996). In this cell line the pRb protein, although expressed at very low levels (Figure 1), is highly susceptible to degradation (data not shown). Therefore, Hs578T, MDA-MB-231 and MDA-MB-157 cell lines are considered functionally pRb negative as we previously described (Gray-Bablin *et al.*, 1996).

These studies revealed that lovastatin treatment for 36 h resulted in G1 arrest in both tumor and normal cell lines irrespective of their p53, pRb, or ER status (Table 1). However, the percent S phase decrease may be dependent on the expression of the aforementioned proteins. For example, treatment of normal breast epithelial cells with lovastatin resulted in the largest S phase decrease (89% drop from untreated cells) while the S phase in p53/pRb/ER positive or negative cells dropped by 68% from the untreated controls. Furthermore, no changes in cell cycle distribution were observed after 36 h in untreated control cultures (data not shown). These observations suggest that although lovastatin is capable of arresting both normal and tumor cells in G1, the degree of synchronization is more profound in normal cells. Next, we examined the pattern of expression of key cell cycle regulators in these three classes of cell lines following treatment of cells with lovastatin (Figure 1).

#### Lovastatin treatment causes a decrease in the levels of CDK4 and cyclin D3 in both normal and tumor cells

To determine which key cell cycle regulators were required for lovastatin mediated G1 arrest, we examined the expression of several positive and negative cell cycle proteins in both normal and tumor cells. A subset of the cell lines from Table 1 consisting of two normal cell lines, 76N and MCF-10A, two tumor cell lines which are p53, pRb and ER positive, MCF-7, ZR75T and two tumor cell lines which are p53, pRb and ER negative, Hs578T and MDA-MB-157 cell lines were analysed. The 76N and MCF-10A cells were chosen as they represented normal cells obtained from two different lineages, 76N cell lines are normal mortal cells obtained from reduction mammo-plasty while MCF-10A cell lines were immortalized from normal breast epithelial cell strain, MCF-10, after cultivation in medium containing low calcium concentrations (Soule *et al.*, 1990).

All cells within each category were treated with 40  $\mu$ M lovastatin for 36 h and at the indicated times following treatment, cells were harvested and subjected to Western blot analysis with antibodies to p27, p21, p16, pRb, p53, CDK2, CDK4, cyclin D1 and cyclin D3 (Figure 1). These analyses revealed that the total protein levels of p21 and p27 were induced significantly only in the cells with pRb/p53/ER negative status suggesting that lovastatin causes an induction of these CKI's through a p53 independent mechanism. In p53 and pRb positive cells (MCF-7 and ZR75T) the basal levels of p21 and p27 were very high and no subsequent increase in these CKI's were seen when examining total protein levels. Normal cells on the other hand show an increase in p27 but a decrease in p21 following lovastatin treatment. The p27 levels accumulate by sixfold in MCF-10A cells and 2.5-fold in 76N cells reproducibly. INK CKI, p16 was expressed only in MDA-MB-

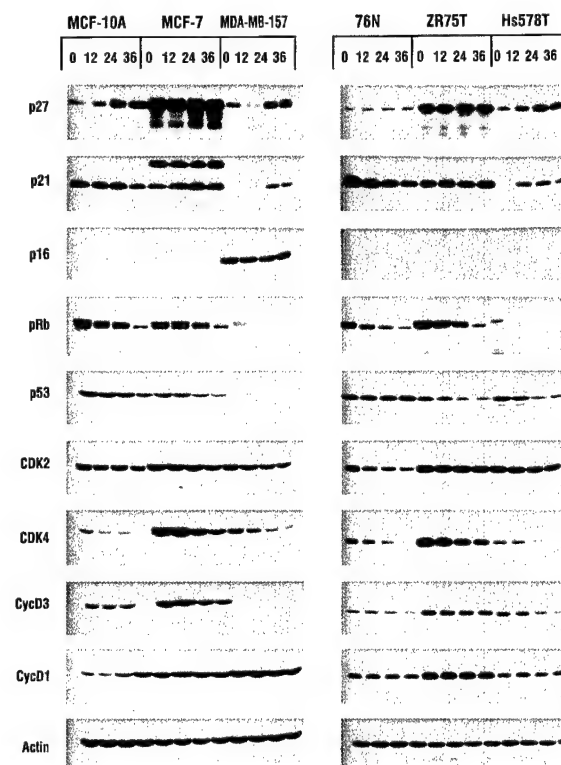


**Figure 1** Expression of positive and negative cell cycle regulators in normal and tumor breast cells following lovastatin treatment. All cells were cultured in medium containing 40  $\mu$ M lovastatin. At the indicated times following treatment cells were harvested, cell lysates prepared and subjected to Western blot analysis: 50  $\mu$ g of protein extract from each condition was analysed by Western blot analysis with the indicated antibodies or actin used for equal loading. The blots were developed by chemiluminescence reagents. The same blots were sequentially hybridized with different antibodies (see Materials and methods). The blots were stripped between the antibodies in 100 mM 2-mercaptoethanol, 62.5 mM Tris-HCl (pH 6.8), and 2% SDS for 10 min at 55°C

157 cells and its levels did not change following lovastatin treatment.

The levels of p53 and pRb tumor suppressor protein decreased in both normal and ER/p53/pRb positive tumor cell lines. The simultaneous decrease in p53 and p21 in normal cells suggest that in normal cells p21 expression may be strongly influenced by p53. A similar decrease in p21 is not noticed in p53 positive tumor cell lines (MCF-7 and ZR75T) even though p53 levels decreased, suggesting that the p53-p21 pathway in these tumor cell lines is not as tightly controlled as seen in normal. Analysis of cyclins and CDKs revealed that following lovastatin treatment CDK4 and cyclin D3 protein levels decreased in all cell lines while cyclin D1 and CDK2 levels remained relatively unchanged. Collectively these results reveal that the only cell cycle regulators which consistently decrease in response to lovastatin are CDK4 and cyclin D3. Furthermore, the increases of p21 and p27 at the protein levels were only apparent in ER/p53/pRb negative cell tumor cell lines and were not universally observed in lovastatin induced G1 arrest which occurred in all cells regardless of their p53 or pRb status (Table 1). Lastly, the arrest of MDA-MB 157 and Hs578T cells which are p53 and pRb negative implies that the activity of the tumor

suppressors is not required for lovastatin mediated G1 arrest. This analysis raised the question if and how p21 and p27 could play a role in lovastatin mediated G1 arrest and how the decrease in the CDK4 and cyclin D3 in response to lovastatin could contribute to this arrest?

*Inactive cyclin CDK2 complexes in lovastatin treated cells are due to increased p21 and p27 binding*

A likely explanation for lovastatin mediated G1 arrest in the different cell types is that lovastatin treatment of cells results in the inhibition of CDK2 activity which is necessary for cells to overcome the restriction point in the G1 phase of the cell cycle. In order to examine the kinase activity associated with CDK2 in normal and tumor cells, we measured the phosphorylation of histone H1 in immunoprecipitates prepared from lovastatin treated cells using an antibody to CDK2 (Figure 2a). This analysis revealed that treatment of all cells by lovastatin resulted in a rapid decrease of CDK2 activity and by 36 h, the time when G1 arrest fully manifests itself in cells, the level of CDK2 activity reaches its nadir in all cells examined. These data suggest that lovastatin mediated G1 arrest results in lowered CDK2 activity in all cells regardless their p53, pRb, normal or tumor status.

To determine if the decreased activity of the CDK2 is due to its association with CKIs, a two step experiment consisting of an immunoprecipitation with anti-CDK2 antibody followed by Western blot analysis with p21 or p27 was performed (Figure 2b). These analyses revealed that the decreased CDK2 activity observed (Figure 2a) was concomitant with increased binding of p27 to CDK2 in all normal and tumor cell lines treated with lovastatin. Furthermore, all tumor cell lines treated with lovastatin exhibited increased binding of p21 to CDK2 as well. In normal cells however, not only were the p21 total protein levels decreased by lovastatin treatment (Figure 1), but the binding of p21 to CDK2 also decreased (Figure 2b), despite complete inhibition of the CDK2 activity (Figure 2a). Collectively these results suggest that the G1 arrest induced by lovastatin is concomitant with decreased activity of CDK2 mediated by increased binding of p27 (in all cells) and p21 (only in tumor cells) to CDK2. Interestingly, MCF-7 and ZR75T which exhibited no increases in p21 or p27 expression (Figure 1) revealed a clear increase in binding of both these CKIs to CDK2 (Figure 2b). These observations raise the question that if the total levels of p21 and p27 are not induced by lovastatin (Figure 1) what accounts for the increased binding of these inhibitors to CDK2 in MCF-7 and ZR75T cells (Figure 2b)?

*Lovastatin treatment causes the CKIs to switch from binding to CDK4 to CDK2*

It has been proposed that cyclin D/CDK4 complexes play a critical role in titrating p21 and p27 by binding to them, resulting in decreased amounts of p21 and p27 which would otherwise bind to and inhibit cyclin/CDK2 complex activity (LaBaer et al., 1997). At low concentrations, the binding of p21 and p27 to CDK4 will not inhibit cyclin D/CDK4 activity but rather promote efficient binding of cyclin D with CDK4, and

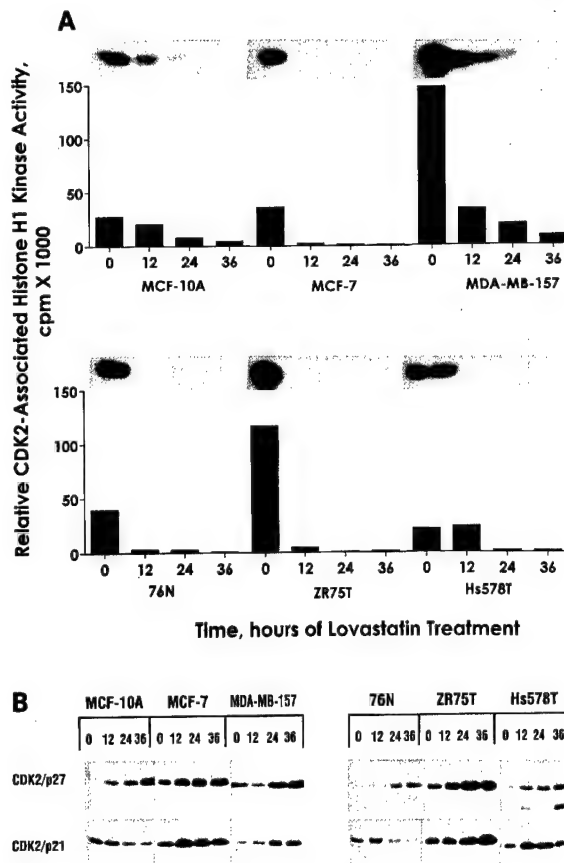


**Figure 2** Lovastatin treatment reduces CDK2 activity by increased p21 and p27 binding. All cells were cultured in medium containing 40  $\mu$ M lovastatin. At the indicated times following treatment cells were harvested, cell lysates prepared and subjected to (a) Histone H1 kinase analysis or (b) Immune-complex formation. For kinase activity, equal amounts of protein (300  $\mu$ g) from cell lysates were prepared from each cell line at the indicated times following lovastatin treatment and immunoprecipitated with anti-CDK2 antibody (polyclonal) coupled to protein A beads using histone H1 as substrate. For each cell line we show the resulting autoradiogram of the histone H1 SDS-PAGE and the quantitation of the histone H1 associated kinase activities by scintillation counting. For immunoprecipitation followed by Western blot analysis, equal amounts of protein (300  $\mu$ g) from cell lysate prepared from each cell lines were immunoprecipitated with anti-CDK2 (polyclonal) coupled to protein A beads and the immunoprecipitates were subjected to Western blot analysis with the indicated antibodies

as such function as adaptor molecules (LaBaer et al., 1997). Since lovastatin causes the synchronization of cells apparently by increasing binding of p21 (tumor cells) and p27 (normal and tumor cells) to CDK2 complexes, it can be hypothesized that this increased binding of CKI's to CDK2 may be due to the switching of the CKI's from CDK4 to CDK2, mediated by lovastatin. To test this hypothesis and to examine this adaptor molecule theory we examined the association of p21 and p27 to CDK4 following lovastatin treatment (Figure 3). Our results clearly demonstrate that in untreated normal and ER/p53/pRb positive tumor cells, p21 and p27 bind to CDK4, and upon treatment with lovastatin, both p21 and p27 are released from CDK4 in a time dependent fashion (Figure 3) which corresponds to their binding (i.e.



switching partners) to CDK2 (Figure 2b). The apparent increase in p27 levels observed in 76N cells following lovastatin treatment seems to be the primary event leading to CDK2 inactivation; primary to redistribution of p27 from CDK4 to CDK2. However, in MCF-7 and ZR75T cells, where no detectable increase in the levels of p21 and p27 following lovastatin treatment is observed, the switching of these CKIs from CDK4 to CDK2 occurs concomitantly with decrease in CDK2 activity, suggesting that in these ER/p53/pRb positive tumor cells the p21 and p27 switch from CDK4 to CDK2 is the primary event leading to CDK2 inactivation. In both sets of cell lines we show that lovastatin creates a signal for these CKIs to switch partners from CDK4 to CDK2 and such switching of partners is concurrent with G1 arrest. The signal that initiates the switching may be the decrease in CDK4 and cyclin D3 protein levels observed in all cells examined following treatment with lovastatin (Figure 1).

The p53/pRb/ER negative tumor cell lines reveal a different pattern of CKI/CDK4 binding than either the normal cells or the p53/pRb/ER positive tumor cell lines (Figure 3). MDA-MB-157 cells which have very low levels of p21 and p27 show no binding of these proteins to CDK4. In fact CDK4 is bound to p16 which is expressed in high quantities in this cell line and can titrate and thus prevent any CDK4 complex formation with p21 or p27. In the Hs578T cell line which do not express detectable p16 levels, CDK4 is not titrated and binds only to p27 in untreated cells and treatment of cells with lovastatin decreases the binding of p27 to CDK4. Collectively, these observations support the validity of the adaptor molecule theory where p21 and p27 switch partners from CDK4 to CDK2 specifically for ER/p53/pRb positive cells which have endogenously high levels of p21 and p27. Furthermore, the decreased binding of the CKIs to CDK4 also suggest that lovastatin affects the cellular pathways that provide the switching signal for CKIs to redistribute from cyclin/CDK4 complex to cyclin/CDK2 complexes.

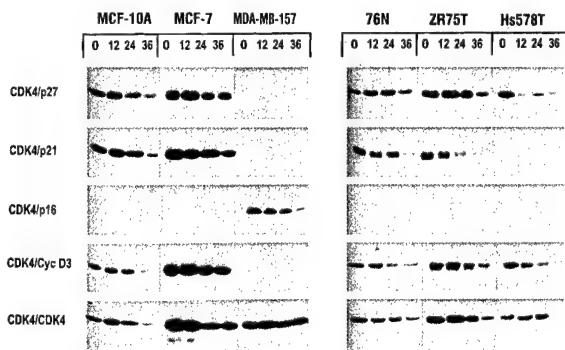


**Figure 3** Redistribution of p21 and p27 from CDK4 to CDK2 following lovastatin treatment. All cells were cultured in medium containing 40  $\mu$ M lovastatin. At the indicated times following treatment cells were harvested, cell lysates prepared and subjected to Immune-complex formation. Equal amounts of protein (300  $\mu$ g) from cell lysate prepared from each cell line was immunoprecipitated with anti-CDK4 (polyclonal) coupled to protein A beads and the immunoprecipitates were subjected to Western blot analysis with the indicated antibodies

#### CDK2 is completely sequestered by p21 and p27 following lovastatin treatment

To determine whether the increased binding of p21 and p27 to CDK2 is sufficient to inactivate CDK2, we examined the proportion of CDK2 bound to p21 and p27 following lovastatin treatment. For these experiments MCF-7 and ZR75T cell lines were chosen as the basal levels p21 and p27 are very high in these cell lines (Figure 1) and treatment with lovastatin results in increased binding of both CKIs to CDK2 (Figure 2). To evaluate the proportion of CDK2 in complex with p21 and p27 we immunodepleted cell extracts with anti-p21 and anti-p27 antibodies. These extracts were prepared from both cell lines before and after lovastatin treatment. Following immunodepletion, the final supernatant was subjected to Western blot analysis with antibodies to p21, p27, CDK2, CDK4 and actin (Figure 4). These results revealed that upon immunodepletion of cells of p21 and p27, there is little or no CDK2 present following lovastatin treatment. CDK4 levels were also not detectable following p21 and p27 immunodepletion in lovastatin treated cells (Figure 4) partly due to the decrease in total CDK4

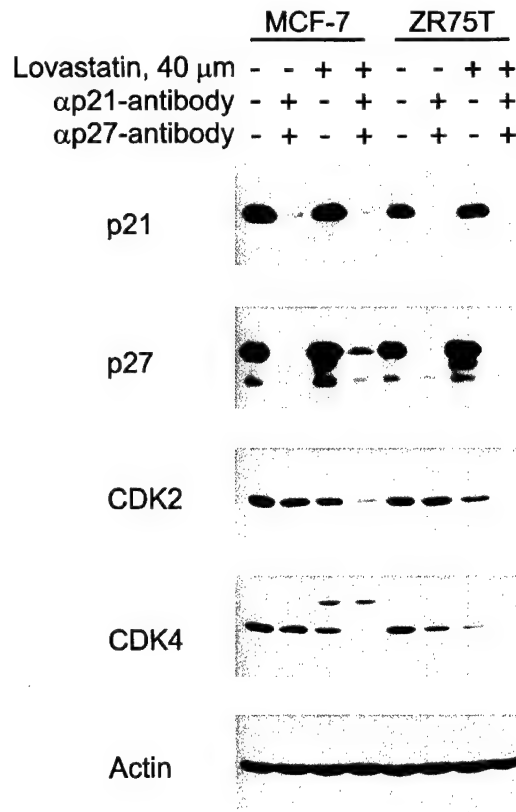


**Figure 4** Immunodepletion of p21 and p27 in lovastatin treated cells also depletes the cells of CDK2. Cells were cultured in medium 40  $\mu$ M lovastatin for 0 and 36 h. Following treatment cells were harvested, cell extracts prepared and immunodepleted with antibodies against p21 and p27. Following three rounds of immunodepletion with anti-p21 and anti-p27 coupled to protein A beads, or protein A beads alone, the remaining supernatant (50  $\mu$ g/lane) were subjected to Western blot analysis with the indicated antibodies

levels following treatment (Figure 1). Hence, upon lovastatin treatment, CDK4 levels decrease, p21 and p27 levels do not change yet their binding to CDK2 increase, and CDK2 activity greatly declines. Furthermore lovastatin results in sequestering of CDK2 by these CKIs suggesting that p21 and p27 alone will inhibit CDK2 activity. These observations also suggest that the amounts of p21 and p27 released from CDK4 complexes in lovastatin treated cells is sufficient to block the CDK2 activity in these cells.

#### Lovastatin mediated G1 arrest is through a p53 independent pathway

To directly examine the role of p53 in the G1 arrest induced by lovastatin in breast epithelial cells, we investigated perturbation of the cell cycle by lovastatin in 76N cells transformed by the human papilloma virus E6 (76N-E6) (Band *et al.*, 1991). Initially, we examined the expression of key cell cycle regulatory proteins in 76N-E6 as compared to 76N parental cell line (Figure 5b, right panel). This analysis showed that aside from lack of expression of p53 and p21 in 76N-E6 cell line, the other cell cycle regulatory proteins are similarly expressed between 76N-E6 and the parental 76N cells. Next, to examine the effects of lovastatin on 76N-E6 cells we treated them with 40  $\mu$ M lovastatin for 36 h. Such treatment resulted in a G1 arrest of 76N-E6 cells despite the absence of p53 (Figure 5a). At the indicated times following treatment, cells were harvested and subjected to Western blot analysis with antibodies to key cell cycle regulators (Figure 5b). These analyses reveal that as expected the cells did not express any p53 due to its rapid degradation by the transfected E6 oncogene. However, both p27 and p21 levels were induced following lovastatin treatment (Figure 5b) which is unlike what was observed in the 76N parental p53 wild-type cells (Figure 1) or HeLa cells where only p27 was shown to be induced by lovastatin (Hengst *et al.*, 1994; Hengst and Reed, 1996). These results suggest that the elimination of p53 in 76N-E6 cells results in induction of p21 by lovastatin through a p53 independent mechanism and that p53 expression is not critical for lovastatin mediated G1 arrest.

All the other cell cycle regulatory proteins examined in 76N-E6 cells revealed a similar pattern of alteration following lovastatin treatment as observed in normal 76N cells (Figure 1); i.e. the expression of hyperphosphorylated pRb, CDK4 and cyclin D3 decreased rapidly and significantly in response to lovastatin while the levels of CDK2 and cyclin D1 remain relatively unchanged (Figure 5b). Similarly, CDK2 activity also decreased profoundly in 76N-E6 cells following lovastatin treatment and G1 arrest (Figure 5c). We also examined the association of p21 and p27 with CDK2 following lovastatin treatment and found that the binding of both p21 and p27 to CDK2 increased significantly during the course of lovastatin treatment, suggesting that p21 and p27 are indeed acting as inhibitors of CDK2 leading to G1 arrest in 76N-E6 cells independent of p53 (Figure 5d). Lastly, we examined the association of p21 and p27 with CDK4 following lovastatin treatment and found that in untreated 76N-E6 cells both p21 and p27 bind to CDK4 only to redistribute from CDK4 to CDK2 upon treatment with lovastatin (Figure 5e). These results

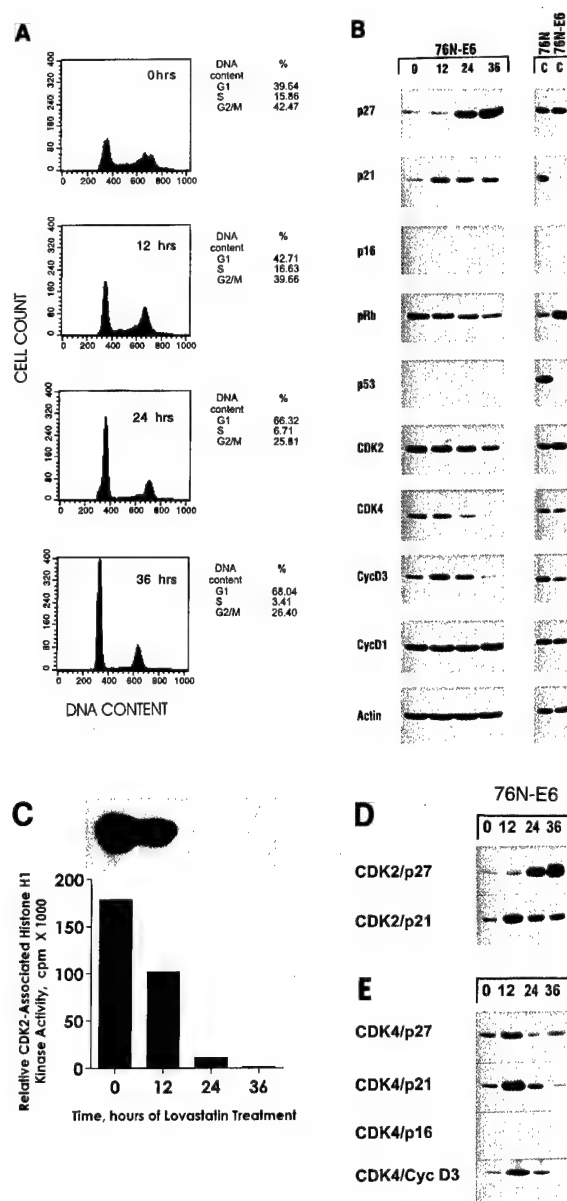


**Figure 5** Induction of CKIs in 76N-E6 cells following lovastatin mediated G1 arrest. 76N-E6 cells treated with 40  $\mu$ M lovastatin. At the indicated times following treatment cells were harvested and subjected to (a) Flow cytometry. Percentages of cells in different phases of the cell cycle for 76N-E6 were determined from flow cytometric measurements of DNA content. (b) Western blot analysis. Fifty  $\mu$ g of protein extracts from each condition was analysed by Western blot analysis with the indicated antibodies or actin used for equal loading and the blots were developed using the chemiluminescence reagents. The right panel shows Western blot analysis using cell extracts from untreated 76N parental and 76N-E6 cell lines on the same blot with identical exposure times. (c) Histone H1 kinase analysis. Equal amounts of protein (300  $\mu$ g) from cell lysates were prepared at the indicated times following lovastatin treatment and immunoprecipitated with anti-CDK2 antibody (polyclonal) coupled to protein A beads using histone H1 as substrate. The autoradiogram of the histone H1 SDS-PAGE and the quantitation of the histone H1 associated kinase activities by scintillation counting are presented. (d) CDK2 Immune-complex formation and (e) CDK4 Immune-complex formation. For immunoprecipitation followed by Western blot analysis, equal amounts of protein (300  $\mu$ g) from cell lysates prepared from lovastatin treated cells were immunoprecipitated with anti-CDK2 (polyclonal) (d) or anti-CDK4 (polyclonal) (e) coupled to protein A beads and the immunoprecipitates were subjected to Western blot analysis with the indicated antibodies.

suggest that the lovastatin mediated G1 arrest in 76N-E6 cells, the concomitant decrease in CDK2 activity, the increased expression of p21 and p27, the increased association of these CKIs to CDK2, and lastly the redistribution of CKIs from CDK4 to CDK2 are all independent of p53.

## Discussion

The outcome of CKI induction in most cells is the cessation of cell proliferation, differentiation or even cell death. In tumor cells the regulation of the CKIs is altered leading to either lack of function, or expression. Hence, if the CKIs could be induced consistently in tumor cells, and their induction lead to G1 arrest the goal of controlling the proliferation of cancer cells could be achieved. As shown in this study we observe that lovastatin can cease cell proliferation in a wide variety of normal and tumor breast cells, independent of their p53, pRb or ER status. We also provide evidence that it is not the increase in the levels of the CKIs per se but the increased binding of p21 and p27 to CDK2 and the consequent reduction of CDK2 activity that is actually responsible for the G1 arrest caused by lovastatin in both normal and tumor breast cell lines. The increased binding of CKIs to CDK2 is through a p53 independent pathway. Our results also reveal that lovastatin like other growth arresting agents such as TGF- $\beta$  (Reynisdottir and Massague, 1997) use the switching of CKI from CDK4 complex to CDK2 as a method to initiate growth arrest.

### *Redistribution of both p21 and p27 from CDK4 complexes to CDK2 complexes following lovastatin treatment*

Recently a new functional role has been assigned to p21 and p27, that of facilitating cyclin D/CDK4 assembly *in vitro* or acting as adaptor molecules (Poon *et al.*, 1995; LaBaer *et al.*, 1997; Planas-Silva and Weinberg, 1997a; Prall *et al.*, 1997). Adaptor molecules facilitate the association or complex formation between proteins without hindering in the function of the complex. Both *in vitro* studies using purified p21, p27 or p57 (KIP2) and *in vivo* studies using cells transiently transfected with p21, CDK4 and cyclin D1, showed an abundance of assembled CDK4/cyclin D1 complex which increased directly with increasing inhibitor levels. In fact, the addition of p21, p27 and p57 were able to promote assembly of the cyclin CDK4 complexes by 35–80-fold without inhibiting the activity of the complex (LaBaer *et al.*, 1997). Hence, at low concentrations p21 and p27 can act as adaptor molecules, facilitate the binding of cyclin D/CDK4 complexes, promote the phosphorylation of pRb and progression through G1, while at higher concentrations, the CKIs can switch partners bind to CDK2 and inhibit cell cycle progression. Similarly, other studies examining the effect of estrogen on the cell cycle of ER positive MCF-7 cells revealed that the addition of  $\beta$ -estradiol or estrogen were able to rescue synchronized cells and induce progression through the cell cycle by increasing the level of cyclin D and increased binding of p21 and p27 to the cyclin D/CDK4 complexes from the cyclin E/CDK2 complexes (Planas-Silva and Weinberg, 1997a;

Prall *et al.*, 1997). This redistribution of p21 caused a marked induction of the cyclin E/CDK2 kinase activity. Similarly, studies with the growth inhibitor TGF- $\beta$  also showed redistribution of the cyclin kinase inhibitors, i.e. CKIs switch from CDK4 to CDK2 in response to growth inhibitory activity of TGF- $\beta$ . In addition TGF- $\beta$  resulted in the reduced synthesis of CDK4 and cyclin D leading to the subsequent dissociation of cyclin D/CDK4 complexes and redistribution of p27 from cyclin D/CDK4 complex to cyclin E/CDK2 leading to a G1 arrest (Ewen *et al.*, 1993b). Subsequent studies have suggested that the redistribution of p27 following TGF- $\beta$  treatment was due to the increased binding of p15 to cyclin D/CDK4 complexes in Mink Lung cells (Reynisdottir *et al.*, 1995; Reynisdottir and Massague, 1997). It therefore has been proposed that cyclin D/CDK4 complexes apart from phosphorylating pRb, titrate the p21 and p27 in the cells and hence prevent the binding of the CKIs to cyclin/CDK2 complexes.

In the present study we also observe that treatment of cells with lovastatin induce a cascade of events leading to cessation of cell proliferation through the redistribution of the CKIs from cyclin D/CDK4 complexes to cyclin E/CDK2 complexes. We observed that lovastatin treatment of all cells examined, normal or tumor caused a reduced synthesis of both cyclin D3 and CDK4 but not cyclin D1. A similar decrease in CDK4 and cyclin D3 but not D1 was seen in retinoic acid arrested MCF-7 cell (Zhu *et al.*, 1997) and glucocorticoids arrested U2OS and SAOS2 cells (Rogatsky *et al.*, 1997) suggesting that the rapid reduction in cyclin D3 or CDK4 levels may be the key signal for redistribution of the CKIs. In the present study we observed that the CKI binding to CDK4 complexes reduced rapidly and significantly following lovastatin treatment (Figure 4). This reduction was seen in both normal and ER/p53/pRb positive tumor cell lines. Hence, the redistribution of both p21 and p27 from CDK4 complexes to CDK2 complexes, apparently signaled by a decrease in the expression of CDK4 and cyclin D3, leads to G1 arrest caused by lovastatin treatment. This switching also explains the increased binding of the CKI's to CDK2 complexes that is observed in ER/p53/pRb positive cells (Figure 2) without the corresponding increase in CKI levels, as these cell lines have a high basal levels of these CKIs (Figure 1). The high levels of both CKIs could be attributed to increase cyclin D/CDK4 activity required to phosphorylate pRb in these cells and thereby giving these tumor cells a growth advantage. We also show that when cell extracts prepared from lovastatin treated cultures of ER/p53/pRb positive tumor cell lines (i.e. MCF-7 and ZR75T) are immunodepleted of both p21 and p27, there is little to no CDK2 or CDK4 left in the final supernatant. These results suggest that CDK2 is completely sequestered by p21 and p27 following lovastatin treatment in the absence of any CKI accumulation. Furthermore, the amounts of p21 and p27 released from CDK4 complexes which then associate with CDK2 complexes in lovastatin treated cells are sufficient to block the CDK2 activity in these cells.

### *Lovastatin mediated G1 arrest is p53 independent*

In this study we analysed the effect of lovastatin on a broad range of breast cells, normal and tumor with



different p53 status. We found that whether a cell is p53 wild-type or mutant the effect of lovastatin was the same in all cells and resulted in G1 arrest suggesting that the p53 pathway is not involved in the G1 arrest induced by lovastatin. We observed this p53 independence under three different conditions. First, the protein levels and CDK2 binding of p21 and p27 in p53/Rb negative cells, (MDA-MB 157 and Hs578T) increased dramatically following lovastatin treatment, resulting in the G1 arrest of these cells. MDA-MB-157 is null for p53 while Hs578T harbors a mutant p53. Hence, the increase in p21 levels following lovastatin treatment in these cells is independent of p53. Secondly, MCF-7 and ZR75T cells which are p53 and pRb positive tumor cells showed a decrease in p53 levels following treatment with lovastatin (Figure 1) even though the binding of p21 and p27 to CDK2 increased resulting in inhibition of CDK2 activity and subsequent G1 arrest (Figure 2). In these cells the increased binding of p21 to CDK2 was independent of p53, due to decrease in p53 levels in response to lovastatin (Figure 1). Finally, and most directly, we show that 76N-E6 cells, stably transformed by the human papilloma virus E6 which renders p53 inactive (Band et al., 1990; 1991), not only were G1 arrested by lovastatin treatment but also revealed an induction of p21 and p27 expression followed by increased binding of p21 (and p27) to CDK2. The above results using three different cell types which are either p53/pRb wild-type, or p53/pRb mutant, or harbor an inactive p53 (i.e. 76N-E6) clearly reveal that the p21 induction and subsequent G1 arrest mediated by lovastatin is p53 independent.

Lovastatin is a widely used drug for patients suffering from hypercholesterolemia (Rettersol et al., 1996). Investigators attempted to use lovastatin as an agent for treatment of cancer because it inhibits the cholesterol biosynthesis pathway and tumor cells have an increased level of cholesterol synthesis (Bernstein and Ross, 1993). However, these studies and recent clinical trials were inconclusive in providing a role for lovastatin as an anti-cancer agent (Thibault et al., 1996). On the other hand, it is reasonable to evaluate the chemo-preventative effect of this drug since data from a large clinical trial of lovastatin for reducing serum cholesterol produced the unexpected finding of a 33% decrease in cancer incidence (Stein et al., 1993). Furthermore, lovastatin has also been shown to inhibit metastasis of highly metastatic B16F10 mouse melanoma in nude mice (Jani et al., 1993). Lastly, in the present study we show that lovastatin treatment of cells leading to G1 arrest is through the induction of p21 and p27 and subsequent inhibition of CDK2 activity. Collectively the above studies suggest that lovastatin may have chemo-preventative properties by inducing the inhibitory activity of the negative regulators of the cell cycle. It therefore is quite pertinent to investigate the direct mechanism by which lovastatin activates the CKIs in the cells, whether by inducing their expression in otherwise CKI negative cells, or mediating their redistribution to cyclin/CDK complexes which inhibit progression through the cell cycle. The universality and the p53 independent action of lovastatin in cessation of cell proliferation, also make it a very attractive agent for use as a potential chemo-preventative agent.

## Materials and methods

### Materials, cell lines and culture conditions

Lovastatin was kindly provided by William Henkler (Merck, Sharp and Dohme Research Pharmaceuticals, Rahway, NJ, USA). Serum was purchased from Hyclone Laboratories (Logan, Utah, USA) and cell culture medium from Life Technologies, Inc. (Grand Island, NY, USA). All other chemicals used were reagent grade. Before addition to cultures, lovastatin was converted from its inactive lactone prodrug form to its active dihydroxy-open acid as described previously (Keyomarsi et al., 1991; Keyomarsi, 1996). The culture conditions for 76N, 70N normal cell strains, MCF-10A immortalized cell line, and MCF-7, ZR75T, MDA-MB-157, Hs578T, T47D, and MDA-MB-231 breast cancer cell lines were described previously (Keyomarsi and Pardee, 1993; Keyomarsi et al., 1995). 76N-E6 cell line (a gift from Dr V Band, Tufts Medical Institute, Boston, MA, USA) were immortalized and cultured as described previously (Band et al., 1990, 1991). All cells were cultured and treated at 37°C in a humidified incubator containing 6.5% CO<sub>2</sub> and maintained free of mycoplasma as determined by Hoechst staining (Hessling et al., 1980).

### Synchronization and flow cytometry

Synchronization by lovastatin treatment was performed as described previously (Keyomarsi et al., 1991). Briefly medium was removed 24–36 h after the initial plating, replaced with fresh medium plus 40 µM lovastatin for 0–36 h. Cells were harvested at the indicated times and flow cytometry analysis was performed. For Fluorescence-Activated Cell Sorter (FACS) analysis 10<sup>6</sup> cells were centrifuged at 1000 g for 5 min, fixed by the gradual addition of ice cold 70% ethanol (30 min at 4°C) and washed with phosphate buffered saline. Cells were then treated with RNase (10 µg/ml) for 30 min at 37°C, washed once with phosphate buffered saline and resuspended and stained in 1 ml of 69 µM propidium iodide in 38 mM sodium citrate for 30 min at room temperature. The cell cycle phase distribution was determined by analytical DNA Flow cytometry as described previously (Keyomarsi et al., 1995).

### Western blot and immune complex kinase analysis

Cell lysates were prepared and subjected to Western blot analysis as previously described (Keyomarsi et al., 1995). Briefly, 50 µg of protein from each condition was electrophoresed in each lane of either a 7% sodium dodecyl sulfate-polyacrylamide gel (SDS-PAGE) (pRb), 10% SDS-PAGE (p53, cyclin A, cyclin D1, cyclin D3), 13% SDS-PAGE (p21, p27, CDK2, CDK4), or a 15% SDS-PAGE (p16), and transferred to Immobilon P overnight at 4°C at 35 mV constant volts. The blots were blocked overnight at 4°C in Blotto (5% nonfat dry milk in 20 mM Tris, 137 mM NaCl, 0.25% Tween, pH 7.6). After six, 10 min washes in TBST (20 mM Tris, 137 mM NaCl, 0.05% Tween, pH 7.6), the blots were incubated in primary antibodies for 3 h. Primary antibodies used were pRb monoclonal antibody (PharMingen, San Diego, CA, USA), at a dilution of 1:100, monoclonal antibody to p16 (a gift from Jim DeCaprio, Dana Farber Cancer Institute) at a dilution of 1:20, CDK2, CDK4 and p27, monoclonal antibodies (Transduction Laboratories, Lexington, KY, USA) each at a dilution of 1:100, p21 and p53 monoclonal antibodies (Oncogene Research Products/Calbiochem, San Diego, CA, USA) at a dilution of 1:100 cyclin D1 monoclonal antibody (Santa Cruz Biochemicals, Santa Cruz, CA, USA) at a dilution of 1:100, and actin

monoclonal antibody (Boehringer-Mannheim, Indianapolis, IN, USA) at 0.63  $\mu\text{g}/\text{ml}$  in Blotto. Following primary antibody incubation, the blots were washed and incubated with goat anti-mouse horseradish peroxidase conjugate at a dilution of 1:5000 in Blotto for 1 h and finally washed and developed with the Renaissance chemiluminescence system as directed by the manufacturers (NEN Life Sciences Products, Boston, MA, USA).

For immunoprecipitations followed by Western blot analysis 300  $\mu\text{g}$  of cell extracts were used per immunoprecipitation with polyclonal antibody to CDK2 [CDK2 antibody was generated by immunizing rabbits with multiple antigenic peptide (MAP peptides) (Posnett *et al.*, 1988) consisting of the 30 amino acids of the N terminal region of the CDK2 protein. MAP peptides consist of branched lysines, with each lysine directly attached to the peptide. Rabbits were primed and boosted subcutaneously, with 2 mg of MAP peptide without a carrier protein and emulsified in complete or incomplete (four boosts) adjuvant, respectively. The rabbits were boosted in 3 week intervals and the titer and the specificity of the serum was monitored by ELISA (Enzyme-linked immunosorbent assay) following each boost.] or CDK4 (a gift from Dr M Pagano, New York University Medical Center, NY, New York) (Tam *et al.*, 1994) in lysis buffer containing 50 mM Tris buffer pH 7.5, 250 mM NaCl, 0.1% NP-40, 25  $\mu\text{g}/\text{ml}$  leupeptin, 25  $\mu\text{g}/\text{ml}$  aprotinin, 10  $\mu\text{g}/\text{ml}$  pepstatin, 1 mM benzamide, 10  $\mu\text{g}/\text{ml}$  soybean trypsin inhibitor, 0.5 mM PMSF, 50 mM NaF, 0.5 mM Sodium Ortho-Vanadate. The protein/antibody mixture was incubated with protein A Sepharose for 1 h and the immunoprecipitates were then washed twice with lysis buffer and four times with kinase buffer (50 mM Tris HCl pH 7.5, 250 mM NaCl, 10 mM  $\text{MgCl}_2$ , 1 mM DTT and 0.1 mg/ml BSA). The immunoprecipitates were then electrophoresed on 10%

(cyclin D3) 13% (p21, p27, CDK4 and CDK2) and 15% gels (p16) transferred to Immobolin P, blocked and incubated with the indicated antibodies at dilutions described above. For Histone H1 kinase assay the immunoprecipitates were incubated with kinase assay buffer containing 60  $\mu\text{M}$  cold ATP and 5  $\mu\text{Ci}$  of [ $^{32}\text{P}$ ]ATP in a final volume of 50  $\mu\text{l}$  at 37°C for 30 min. The products of the reaction were then analysed on a 13% SDS-PAGE gel. The gel was then stained, destained, dried and exposed to X-ray film. For quantitation, the protein bands corresponding to histone H1 were excised and radioactivity was measured by scintillation counting.

For immunodepletion, three sequential immunodepletions were carried out with 500  $\mu\text{g}$  of each cell extract using either anti-p21 and anti-p27 polyclonal antibodies (Santa Cruz Biochemicals, Santa Cruz, CA, USA) bound to protein A beads or protein A beads alone. Fifty  $\mu\text{g}$  aliquots of the remaining supernatant were subjected to Western blot analysis as described above to analyse the presence of remaining proteins.

#### Acknowledgements

We thank Dr M Pagano for polyclonal antibody to CDK4, Dr J DeCaprio for monoclonal antibody to p16 and Dr V Band for providing the 76N-E6 cell line. We also gratefully acknowledge the use of Wadsworth Center's Immunology, Biochemistry, Tissue Culture, Photography/Graphics, and Animal core facilities. SR is a fellow of the Cancer Research Foundation of America. This research was supported in part by Grant DAMD-17-94-J-4081 from the US Army Medical Research Acquisition Activity and by Grant No. R29-CA666062 from the National Cancer Institute (both to KK).

#### References

- Alberts AW, Chen J, Kuron G, Hunt V, Hoffman C, Rothrock J, Lopez M, Joshua H, Harris E, Patchett A, Monaghan R, Currie S, Stapley E, Albers-Schonberg G, Hensens O, Hirshfield G, Hoogsteen K, Liesch J and Springer J. (1980). *Proc. Natl. Acad. Sci. USA*, **77**, 3957–3961.
- Band V, DeCaprio JA, Delmolino L, Kulesa V and Sager R. (1991). *J. Virol.*, **65**, 6671–6676.
- Band V, Zajchowski D, Kulesa V and Sager R. (1990). *Proc. Natl. Acad. Sci. USA*, **87**, 463–467.
- Bartek J, Bartkova J and Lukas J. (1996). *Curr. Opin. Cell Biol.*, **8**, 805–814.
- Bartek J, Bartkova J and Lukas J. (1997). *Exp. Cell Res.*, **237**, 1–6.
- Bernstein L and Ross RK. (1993). *Epidemiology Rev.*, **15**, 48–65.
- Datto MB, Li Y, Panus JF, Howe DJ, Xiong Y and Wang X-F. (1995). *Proc. Natl. Acad. Sci. USA*, **92**, 5545–5549.
- Dulic V, Kaufman WK, Wilson S, Tlsty TD, Lees E, Harper JW, Elledge SJ and Reed SI. (1994). *Cell*, **76**, 1013–1023.
- El-Deiry WS, Tokino T, Velculescu VE, Levy DB, Parsons R, Trent JM, Lin D, Mercer WE, Kinzler KW and Vogelstein B. (1993). *Cell*, **75**, 817–825.
- Elbendary A, Berchuck A, Davis P, Havrilesky L, Bast J, Iglehart RCJ and Marks JR. (1994). *Cell Growth & Diff.*, **5**, 1301–1307.
- Elledge SJ and Harper JW. (1994). *Curr. Opin. Cell Biol.*, **6**, 847–852.
- Elledge SJ, Winston J and Harper JW. (1996). *Trend Cell Biol.*, **6**, 388–392.
- Ewen ME, Sluss HK, Sherr CJ, Natsushime H, Kato J-Y and Livingston DM. (1993a). *Cell*, **73**, 487–497.
- Ewen ME, Sluss HK, Whitehouse LL and Livingston DM. (1993b). *Cell*, **74**, 1009–1020.
- Fang X, Jin X, Xu H-J, Liu L, Peng H-Q, Hogg D, Roth JA, Yu Y, Xu F, Blast RC and Mills GB. (1998). *Oncogene*, **16**, 1–8.
- Fisher RP and Morgan DO. (1994). *Cell*, **78**, 713–724.
- Goldstein JL and Brown MS. (1990). *Nature*, **343**, 425–430.
- Gray-Bablin J, Rao S and Keyomarsi K. (1997). *Cancer Res.*, **57**, 604–609.
- Gray-Bablin J, Zalvide J, Fox MP, Knickerbocker CJ, DeCaprio JA and Keyomarsi K. (1996). *Proc. Natl. Acad. Sci.*, **93**, 15215–15220.
- Gu Y, Turck CW and Morgan DO. (1993). *Nature*, **366**, 707–710.
- Harper JW. (1997). *Cancer Surv.*, **29**, 91–108.
- Harper JW, Adami GR, Wei N, Keyomarsi K and Elledge SJ. (1993). *Cell*, **75**, 805–816.
- Harper JW and Elledge SJ. (1996). *Curr. Opin. Gene & Dev.*, **6**, 56–64.
- Harper JW and Elledge SJ. (1998). *Genes & Dev.*, **12**, 285–289.
- Hengst L, Dulic V, Slingerland JM, Lees E and Reed SI. (1994). *Proc. Natl. Acad. Sci.*, **91**, 5291–5295.
- Hengst L and Reed SI. (1996). *Science*, **271**, 1861–1864.
- Hessling JJ, Miller SE and Levy NL. (1980). *J. Immunol. Meth.*, **38**, 315–324.
- Ikedo MA, Jakoi L and Nevins JR. (1996). *Proc. Natl. Acad. Sci. USA*, **93**, 3215–3220.
- Jakus J and Yeudall WA. (1996). *Oncogene*, **12**, 2369–2376.
- Jani JP, Specht S, Stemmler N, Blanock K, Singh SV, Gupta V and Katoh A. (1993). *Inv. Metas.*, **13**, 314–324.
- Jiang H, Fisher PB. (1993). *Molec. and Cell. Differen.*, **3**, 285–299.
- Kato J, Matsuoka M, Polyak K, Massague J and Sherr CJ. (1994). *Cell*, **79**, 487–496.

- Keyomarsi K. (1996). *Methods in Cell Science*, **118**, 109–114.
- Keyomarsi K, Conte D, Toyofuku W and Fox MP. (1995). *Oncogene*, **11**, 941–950.
- Keyomarsi K and Pardee AB. (1993). *Proc. Natl. Acad. Sci. USA*, **90**, 1112–1116.
- Keyomarsi K, Sandoval L, Band V and Pardee AB. (1991). *Cancer Res.*, **51**, 3602–3609.
- LaBaer J, Garrett MD, Stevenson LF, Slingerland J, Sandhu C, Chou HS, Fattaey A and Harlow E. (1997). *Genes & Dev.*, **11**, 847–862.
- Makela TP, Tassan JP, Nigg EA, Frutiger S, Hughes GJ, Weinberg RA. (1994). *Nature*, **371**, 254–257.
- Maltese WA. (1990). *FASEB J.*, **4**, 3319–3328.
- Matsushime H, Quelle DE, Shurtleff SA, Shibuya M, Sherr CJ, Kato J-Y. (1994). *Mol. Cell. Biol.*, **14**, 2066–2076.
- Michieli P, Chedid M, Lin D, Pierce JH, Mercer WE and Givol D. (1994). *Cancer Res.*, **54**, 3391–3395.
- Nasmyth K. (1996). *Science*, **274**, 1643–1651.
- Noda AF, Ning Y, Venable S, Pereira-Smith OM and Smith JR. (1994). *Exp. Cell. Res.*, **211**, 90–98.
- Nourse J, Firpo E, Flanagan M, Coats S, Polyak C, Lee M, Massague J, Crabtree G and Roberts J. (1994). *Nature*, **372**, 570–573.
- Pagano M, Tam SW, Theodoras AM, Beer-Romero P, Del Sal G, Chau V, Yew RP, Draetta GF and Rolfe M. (1995). *Science*, **269**, 682–685.
- Pardee AB. (1989). *Science*, **246**, 603–608.
- Planas-Silva MD and Weinberg RA. (1997a). *Mol. Cell. Biol.*, **17**, 4059–4069.
- Planas-Silva MD and Weinberg RA. (1997b). *Curr. Opin. Cell Biol.*, **9**, 768–772.
- Polyak K, Kato J-Y, Solomon MI, Sherr CJ, Massague J, Roberts JM and Koff A. (1994a). *Genes & Dev.*, **8**, 9–22.
- Polyak K, Lee M-H, Erdjument-bromage H, Tempst P and Massague J. (1994b). *Cell*, **78**, 59–66.
- Poon RYC, Toyoshima H and Hunter T. (1995). *Mol. Biol. Cell*, **6**, 1197–1213.
- Posnett DN, McGrath H and Tam JP. (1988). *J. Biol. Chem.*, **263**, 1719–1725.
- Prall OWJ, Sarcevic B, Musgrove EA, Watts CKW and Sutherland RL. (1997). *J. Biol. Chem.*, **272**, 10882–10894.
- Rettersol K, Staggard M, Gorbitz C and Ose L. (1996). *Am. J. Card.*, **78**, 1369–1374.
- Reynisdottir I and Massague J. (1997). *Genes & Dev.*, **11**, 492–503.
- Reynisdottir I, Polyak K, Iavarone A and Massague J. (1995). *Genes & Dev.*, **9**, 1831–1845.
- Rogatsky I, Trowbridge JM and Garabedian MJ. (1997). *Mol. Cell. Biol.*, **17**, 3181–3193.
- Sheikh MS, Li X, Chen J, Shao Z, Ordonez JV and Fontana JA. (1994). *Oncogene*, **9**, 3407–3415.
- Sherr CJ. (1994). *Cell*, **79**, 551–555.
- Sherr CJ. (1996). *Science*, **274**, 1672–1677.
- Sherr CJ and Roberts J. M. (1995). *Genes & Dev.*, **9**, 1149–1163.
- Soule HD, Maloney TM, Wolman SR, Peterson SR, Jr, Brenz R, McGrath CM, Russo J, Pauley RJ, Jones, RF and Brooks SC. (1990). *Cancer Res.*, **50**, 6075–6086.
- Stein EA, Lazkarszewski P, Steiner P and Lovastatin Study Groups I through IV. (1993). *Arch. Intern. Med.*, **153**, 1079–1087.
- Tam SW, Theodoras AM, Shay JW, Draetta G and Pagano M. (1994). *Oncogene*, **9**, 2663–2674.
- Thibault A, Samid D, Tompkins AC, Figg WD, Cooper M., Hohl RJ, Trepel J, Liang B, Patronas N, Venzon DJ, Reed E and Myers CE. (1996). *Clin. Can. Res.*, **2**, 483–491.
- Toyoshima H and Hunter T. (1994). *Cell*, **78**, 67–74.
- Weinberg RA. (1995). *Cell*, **81**, 323–330.
- Xiong Y, Hannon GJ, Zhang GJ, Gasso D, Kobayashi R and Beach D. (1993). *Nature*, **366**, 710–714.
- Zhu W-Y, Jones CS, Kiss A, Matsukuma K, Amin S and De Luca LM. (1997). *Exp. Cell Res.*, **234**: 293–299.

**Lovastatin induction of CKIs (p21 and p27)  
and mevalonate reversal of lactacystin are  
both through modulation of the proteasome,  
independent of HMG-CoA reductase.**

Sharmila Rao<sup>1</sup>, Donald C. Porter<sup>1</sup>, Thaddeus Herlizcek<sup>1</sup>,  
Michael Lowe<sup>1</sup> and Khandan Keyomarsi<sup>\*1,2</sup>

<sup>1</sup> Laboratory of Diagnostic Oncology, Division of Molecular Medicine,  
Wadsworth Center, Albany, NY 12201-0509

<sup>2</sup> Department of Biomedical Sciences, State University of New York,  
Albany, NY 12222.

\* To whom correspondence should be addressed:

Wadsworth Center  
Room C-400  
Empire State Plaza  
P.O. Box 509  
Albany, NY 12201-0509

Phone: (518) 486-5799  
FAX: (518) 486-5798  
email: keyomars@wadsworth.org

Running title: Lovastatin inhibits the proteasome

Key Words: Lovastatin, proteasome, cell cycle, p21, p27, HMG-CoA  
Reductase

## Summary

Lovastatin is an inhibitor of HMG-CoA reductase, the rate-limiting enzyme in cholesterol synthesis. Previously, we reported that lovastatin can be used to arrest cultured cells in the G1 phase of the cell cycle, resulting in the stabilization of the cyclin dependent kinase inhibitors (CKIs) p21 and p27. In this report we show that this stabilization of p21 and p27 may be due to a previously unknown function of the pro-drug,  $\beta$ -lactone ring form of lovastatin to inhibit the proteasome degradation of these CKIs. We show that lovastatin pro-drug (20% of the lovastatin mixture) inhibits the 20S proteasome but does not inhibit HMG-CoA reductase. In addition, many of the properties of proteasome inhibition by the pro-drug are the same as the specific proteasome inhibitor lactacystin. Lastly, mevalonate (used to rescue cells from lovastatin arrest) unexpectedly reverses the lactacystin inhibition of the proteasome. Mevalonate increases the activity of the proteasome, which could result in degradation of the CKIs causing the release of lovastatin- and lactacystin-arrested cells.

## Introduction

Metabolic and cellular processes that require exquisite temporal precision, like the cell cycle, often involve selective proteolytic degradation of regulated proteins (Hershko and Ciechanover, 1992). One major degradative pathway capable of such activity is the proteasome pathway (Ciechanover, 1994; Hochstrasser, 1992; Hochstrasser, 1995; Hochstrasser, 1996). This pathway is involved in the regulation of diverse processes including embryogenesis, signal transduction (Jentsch, 1992), and cell cycle progression (Pagano, 1997). For example, degradation of several cell cycle proteins including Clns, Clbs (Lanker et al., 1996), cyclins A, B (Glutzer et al., 1991; Mahaffey et al., 1995; Murray, 1995), D (Diehl et al., 1997), and E (Clurman et al., 1996; Won and Reed, 1996), as well as tumor suppressor genes such as p53 and pRb (Haupt et al., 1997; Kubbatat et al., 1997) is via ubiquitin-mediated proteolysis. The ubiquitin pathway also regulates the levels of cyclin dependent kinase inhibitors Sic1p, Far1p, p27 and more recently p21 (Blagosklonny et al., 1996; Feldman et al., 1997; Henchoz et al., 1997; Maki and Howley, 1997; Pagano et al., 1995; Skowyra et al., 1997). Differences in ubiquitination activity observed in proliferating and quiescent cells contribute to the observed differences in p27 half-life (Pagano, 1997; Pagano et al., 1995).

The 26S proteasome, the central protease of the ubiquitin dependent pathway of protein degradation, consists of the two asymmetrical 19S cap complexes attached to the ends of a barrel shaped 20S particle which recognize and unfold ubiquitinated proteins (Peters et al., 1993). The 20 S particle is generally referred to as the multi-

catalytic unit, or the 20S proteasome (Tanahashi et al., 1993). The 20 S proteasome consists of four seven-membered rings that contain fourteen related subunits that fall into two families, the  $\alpha$ -subunits, which form the outer rings, and the  $\beta$ -subunits, which form the inner rings, of the 20S complex (Lupas et al., 1993).

Proteins targeted for degradation by the proteasome pathway are modified by the covalent attachment of multiple ubiquitin polypeptides. The poly-ubiquitinated substrate is then degraded by the 26S proteasome multi-enzyme complex (Varshavsky, 1997). This pathway is a multi-step process that involves several enzymes and intermediary products. The first energy-dependent step is catalyzed by ubiquitin-activating enzyme E1. The product is an E1-bound ubiquitinyl adenylate which is then transferred to one of the several ubiquitin (Ub) conjugating enzymes E2. This complex, often with an additional factor E3, catalyzes the isopeptide bond formation between ubiquitin and the targeted substrate (Hochstrasser, 1996). Additional Ub molecules are added to substrates to be degraded by this same enzyme cascade. Ultimately, a chain of Ub molecules in isopeptide linkage to the substrate is formed which is recognized and degraded by the 26S-proteasome complexes (Ichihara and Tanaka, 1995). The overall specificity of the pathway is regulated by both substrate recognition in the ligation step and conjugate partitioning by the isopeptidase (Haas and Siepmann, 1997).

Proteasome activity is inhibited by several peptide aldehydes (e.g. LLnL) and compounds like 3,4-dichloroisocoumarin and lactacystin (Fenteany et al., 1995; Rock

et al., 1994). Lactacystin, a *Streptomyces* metabolite containing a  $\beta$ -lactone ring, selectively inhibits proteolytic activities of the proteasome (Dick et al., 1997; Fenteany et al., 1995). The moiety crucial for inhibition of the proteasome activity is the  $\beta$ -lactone electrophilic carbonyl. This moiety targets enzymes containing a catalytic nucleophile such as a protease. In contrast, the dihydroxy acid form of lactacystin is essentially inert to nucleophilic attack and is incapable of inhibiting the proteasome (Fenteany et al., 1995; Fenteany et al., 1994). These findings suggest that the pro-drug form of another  $\beta$ -lactone, lovastatin, similar in structure to lactacystin, may inhibit the ubiquitin mediated proteolysis of key regulatory proteins such as the cyclins and CKIs.

Lovastatin is widely used for the treatment of hypercholesterolemia (Rettersol et al., 1996). Lovastatin inhibits hydroxymethyl-glutaryl coenzyme A (HMG-CoA) reductase, and HMG-CoA is not converted into mevalonic acid (Corsini et al., 1995; Endo et al., 1976). When mevalonate levels decrease, isoprenylation of key signal transduction proteins (e.g., Ras, Rap, etc) is prevented, their subcellular localization is disrupted, and they are inactivated as signal transducers (Casey et al., 1989; Maltese, 1990; Maltese and Sheridan, 1987; Wedje et al., 1993). Perhaps by reducing cholesterol and its intermediary metabolites, administration of lovastatin to cells in culture impacts cell cycle progression. Previously we reported that lovastatin can be used as an effective agent in cell synchronization for both tumor and normal cells (Keyomarsi, 1996; Keyomarsi et al., 1991), arresting cells in G1. Mevalonate releases arrested cells from G1 block, suggesting that mevalonate or one of its downstream products is essential for cell division. The effects of inhibitors to squalene synthase (SS) define



the boundary of this "mevalonate effect", the first committed step to sterol synthesis downstream of HMG-CoA reductase. Inhibitors of SS (e.g., Zaragozic A and Squalestatin) do not inhibit cell growth. Smooth muscle cells can grow in the presence of SS inhibitors, but not in the presence of HMG-CoA reductase inhibitors (Raiteri et al., 1997). Also, cell lines with defective SS can grow in medium minimally supplemented with lipids (Bradford et al., 1992). It appears that the critical intermediates of the cholesterol synthesis pathway required for cell division are between mevalonate and squalene.

The studies presented here suggest that alternative pathways may be targeted by lovastatin; these pathways may mediate the lovastatin effects on cell proliferation. Substantial evidence suggests that the mechanism of lovastatin-mediated inhibition of cell proliferation is through the accumulation of p21 and p27 and subsequent inhibition of CDK2 activity (Gray-Bablin et al., 1997; Hengst and Reed, 1996; Rao et al., 1998). While investigating the mechanism of lovastatin arrest, we found that lovastatin in its pro-drug form ( $\beta$ -lactone) is entirely responsible for the effects on p21 and p27 leading to G1 arrest. The open-ring form, which is active against HMG-CoA reductase, and a similar active drug, pravastatin, do not affect p21 or p27 or cause arrest. Because the pro-drug form of lovastatin does not inhibit HMG-CoA reductase, we addressed the question whether the pro-drug arrest of cell growth was via a mechanism unrelated to the HMG-CoA reductase pathway. As an alternative, the ubiquitin-proteasome pathway was identified based on the structural similarities between the pro-drug form of lovastatin and the specific proteasome inhibitor

lactacystin. Our studies also show that mevalonate, the product of the reaction catalyzed by HMG-CoA reductase, reverses the pro-drug form of lovastatin mediated G1 arrest. Surprisingly mevalonate has a second role, reversing lactacystin-mediated apoptosis in breast cancer cells. Our data suggest the pro-drug form of lovastatin is acting as a proteasome inhibitor, which leads to cell arrest in ways that closely mimic the effects of lactacystin. An entirely new role for mevalonate is to reverse the effects of both lactacystin and the pro-drug form of lovastatin by increasing the activity of the proteasome.

## Results

**Lovastatin mediated induction of p21 and p27 is independent of the HMG-CoA reductase block.** Lovastatin is an inactive lactone pro-drug that must be chemically or enzymatically converted to its dihydroxy open-acid form to inhibit HMG-CoA reductase. For the studies presented here, we chemically modified lovastatin to its open lactone, hydroxy acid form to inhibit the cholesterol biosynthetic pathway. In its closed  $\beta$ -lactone (i.e. pro-drug) form lovastatin is entirely inactive as an HMG-CoA inhibitor (see below).

Based on the recent lactacystin reports (see Introduction) and our own studies (Rao et al., 1998) with lovastatin, we hypothesized that the induction of CKIs by lovastatin would not be solely through inhibition of the HMG-CoA reductase pathway, but also through the inhibition of the proteasome pathway. The chemical form of lovastatin likely to inhibit the proteasome pathway is the closed  $\beta$ -lactone ring (i.e. pro-drug) form. To determine the efficiency of pro-drug conversion we used reversed phase HPLC to separate the different forms of lovastatin and found that the chemical conversion of lovastatin was 80% efficient; 20% of the lovastatin mixture is the unmodified pro-drug, closed  $\beta$ -lactone ring (Fig 1A). HPLC analysis of the chemically unmodified form of lovastatin (i.e. the closed ring) revealed only one peak which occurred at the exact HPLC retention time as the second peak of the lovastatin mixture, suggesting that the lovastatin we used in our studies contained both forms. This observation was further corroborated through molecular weight determination by electrospray ionization mass spectrometry analysis using eluted HPLC peaks for

analysis (Fig 1B). These analyses revealed the first peak of the lovastatin mixture was indeed the open ring form, with a molecular weight of 423 (and was 80% of the mixture), while the 2nd peak of the lovastatin mixture and the only peak of the  $\beta$ -lactone HPLC profiles had identical molecular weights (i.e., 405), suggesting that they were the same compound (Fig 1B). To examine the hypothesis that the pro-drug inhibits the proteasome, cells were treated with a) the chemically modified form of lovastatin (i.e. mixture), b) the pro-drug form of lovastatin ( $\beta$ -lactone) and c) an analogue of lovastatin, called pravastatin, present only in its open ring form as a sodium salt. Pravastatin is similar in structure and potency to the open ring form of lovastatin and it does not require modification for activity.

MDA-MB-157 cells were treated with the indicated concentrations of the lovastatin mixture, lovastatin closed ring form, or pravastatin for 36 hours. Cell cycle perturbations induced by these agents were monitored by flow cytometry and analyzed on Western blots with antisera to p21, p27, or actin (Fig 1C). As expected, treatment of cells with the lovastatin mixture induced both p21 and p27 in a dose dependent fashion; the increase in the CKI expression inhibited cell proliferation, detected as a decrease in S phase. Treatment of cells with the  $\beta$ -lactone form of lovastatin, i.e. the pro-drug, also resulted in inhibition of cell proliferation and a more pronounced CKI induction in a dose dependent manner (Fig 1C). Densitometric analysis revealed that the CKIs were induced twice as much in cells treated with the pro-drug form versus the lovastatin mixture (data not shown). The highest concentrations of the pro-drug, i.e. 160  $\mu$ M, resulted in apoptosis of most of the cells. Pravastatin, which exists only in

the open ring form, on the other hand, was incapable of inducing the CKIs at any concentration examined (Fig 1C) and did not arrest the cells. Collectively these studies corroborate our hypothesis that: a) the induction of CKIs by lovastatin is sufficient to arrest cells; and b) the mechanism of CKI induction by lovastatin may not be through the inhibition of the HMG-CoA reductase enzyme. Pravastatin, which exists solely in its open hydroxy ring form, targets only the HMG-CoA reductase pathway, and is incapable of inducing the CKIs. In contrast, the pro-drug form of lovastatin (inactive against HMG-CoA reductase) is capable of inducing the CKIs and causing a G1 arrest.

To directly determine the abilities of the lovastatin mixture, lovastatin pro-drug form, and pravastatin to inhibit HMG-CoA reductase we prepared cell extracts from MDA-MB-157 cells and assayed in vitro for HMG-CoA reductase as described (Halpin et al., 1993; Larsson et al., 1989). The results of this assay revealed that while both pravastatin and lovastatin active drug form inhibited the HMG-CoA reductase in a dose dependent manner (Fig 2), the pro-drug form of lovastatin was incapable of inhibiting the activity of HMG-CoA reductase over the concentration range examined. The data strongly suggest that the mechanism by which the closed ring pro-drug form of lovastatin induces the CKIs through a pathway independent of HMG-CoA reductase and that inhibition of this enzyme is not essential for G1 arrest and CKI induction. Next, we examined the ability of the pro-drug to inhibit the proteasome pathway.

**Inhibition of proteasome activities results in the induction of the CKIs.** Previous reports have shown that both p21 and p27 are substrates for ubiquitination and proteasome-dependent degradation (Blagosklonny et al., 1996; Maki and Howley, 1997; Pagano et al., 1995). On Western blot analysis of cell extracts treated with lovastatin and the pro-drug forms (but not with pravastatin), we found that antibodies to both p21 and p27 recognized specific proteins of higher molecular sizes that are likely to correspond to ubiquitinated forms of these CKIs (Fig 3A). These initial studies suggested that the proteasome pathway might have a role in the lovastatin-mediated accumulation of CKIs. To examine the contribution of the proteasome pathway in induction of the CKIs we treated MDA-MB-157 with two inhibitors of this enzyme, N-acetyl-L-leuciny-L-leucinal-L-norleucinal (LLnL), and lactacystin. Both these inhibitors resulted in a dramatic induction of p21 and p27 in a dose- and time-dependent fashion (Fig 3B & C). Since treatment of cells by lovastatin and its pro-drug form resulted in HMW laddering of p21 and p27, and since specific proteasome inhibitors such as lactacystin also resulted in dramatic induction of CKIs, we directly examined the role of the proteasome in lovastatin-mediated accumulation of the CKIs.

**Pro-drug form of lovastatin and lactacystin but not pravastatin inhibit the proteasome.** We next evaluated whether the pro-drug form of lovastatin inhibits the proteasome activity to the same degree as lactacystin (Fig 4). The proteolytic core of the 26S proteasome complex responsible for the hydrolysis of ubiquitinated proteins, consists of a 20S proteasome with distinct chymotrypsin-like, trypsin-like, and peptidylglutamyl-peptide hydrolase (PGPH) activities (Fenteany et al., 1994; Maupin-Furlow and Ferry, 1995). Both the chymotrypsin- and trypsin-like activities of this complex are inhibited by lactacystin in a dose and time dependent manner (Fenteany

et al., 1994). To determine whether the pro-drug form of lovastatin was also capable of directly inhibiting the proteasome, we measured the kinetics of inhibition of the peptidase activities by three drugs. Lactacystin (positive control), the pro-drug form of lovastatin, lovastatin mixture, and pravastatin (negative control) were added to cell extracts according to established and published procedures (Fig 4A) (Fenteany et al., 1994; Maupin-Furlow and Ferry, 1995). The inhibition of the chymotrypsin-like activities of the 20S-proteasome complex by these drugs was measured directly using a fluorescence assay containing a fluorogenic peptide substrate for the chymotrypsin-like activity of this complex (Fenteany et al., 1994; Maupin-Furlow and Ferry, 1995). These studies revealed that lactacystin was capable of inhibiting the peptidase activity of the proteasome completely at or above 1  $\mu$ M. The pro-drug also was able to inhibit the proteasome activity in a dose dependent fashion with half-maximal inhibition occurring at 40  $\mu$ M. The lovastatin mixture, which contains only 20% of the pro-drug form, also inhibited the proteasome activity but at much higher concentrations, reflecting the low percentage of the pro-drug form. Pravastatin on the other hand was incapable of inhibiting the proteasome over the concentration ranges examined (i.e. up to 6.4 mM). This analysis clearly revealed that the pro-drug form of lovastatin inhibits the proteasome activity *in vitro*. Since the concentration required to inhibit the proteasome *in vitro* is higher than that used to arrest cells, we also performed the proteasome experiments *in vivo* by treating cells with the inhibitors for 36 hours, preparing cell extracts, and measuring the peptidase activity of the proteasome (Fig 4B). These analyses revealed that lovastatin mixture, its pro-drug form, and lactacystin inhibited the activity of the proteasome at concentrations similar to those required to achieve G1 arrest *in vivo*. Differences in drug potency *in vivo* and *in vitro* are likely due to different rates of uptake and metabolism. Furthermore, mevalonate was able to reverse the inhibitory activity of these agents on the proteasome (see below). These studies (Figs 1-4) show that a specific proteasome-mediated pathway contributes to

increased expression, via stabilization, of p21 and p27 in cells treated with lovastatin mixture or the pro-drug.

**Increased protein stability of both p21 and p27 following pro-drug treatment.**

Critical to our hypothesis that lovastatin blocks proteasome activity is the stability of both p21 and p27 in response to lovastatin. Inhibition of the proteasome with the pro-drug should lead to increased stability of both proteins. The turnover rates of p21 and p27 proteins caused by the pro-drug form of lovastatin were measured by the rate of <sup>35</sup>S-methionine and cysteine incorporation into p27 and p21. We calculated the half-lives of the labeled proteins in cells treated with the pro-drug in pulse (4 hours)/chase (0-2 hours) experiments (Fig 5). At several time intervals during the pulse/chase, cells were harvested, protein extracted, and subjected to immunoprecipitation with antibodies to p21 and p27. The immunoprecipitated samples were analyzed by SDS-PAGE followed by autoradiography and densitometric analysis. This analysis showed that compared with untreated cells, pro-drug treated cells synthesized p21 more rapidly and degraded both p21 and p27 more slowly. The increased rates of incorporation (2 times more p21 was synthesized during a 4 hour pulse in pro-drug treated cells) and increased half life (0.5 versus 1.5 hours with treatment for both p21 and p27) account for the net increase of protein observed from drug treatment (Fig 5B).

**Mevalonate reversal of lovastatin and lactacystin mediated inhibition of the proteasome.** It is well established that the effects of lovastatin inhibition of HMG-CoA reductase on cholesterol synthesis are reversed by mevalonate. The lovastatin-mediated G1 arrest and CKI induction, also reversed by mevalonate, led to the conclusion that the inhibition of HMG-CoA reductase somehow causes G1 arrest. We propose that mevalonate has an important effect on the lovastatin inhibition of HMG-



CoA reductase and lactacystin inhibition of the proteasome, reversing both pathways. We show in Figure 6A that the G1 arrest mediated by both lovastatin and its pro-drug form can be reversed by mevalonate. Since the pro-drug form of lovastatin does not inhibit HMG-CoA reductase (Fig 2), it follows that mevalonate reversal of the pro-drug G1 arrest does not involve HMG-CoA reductase. As we have shown, the pro-drug form of lovastatin can inhibit the proteasome (Fig 4). We were curious if mevalonate could also reverse the lactacystin-mediated inhibition of proteasome. We directly examined this by treating cells with lactacystin in the presence or absence of mevalonate (Fig 6B). Treatment of cells with lactacystin resulted in significant apoptosis of cells. Seventy percent of cells treated with 10  $\mu$ M lactacystin for 36 hours apoptosed (Fig 6B). (10  $\mu$ M lactacystin also completely inhibited the proteasome activity as shown in Fig 4). Intriguingly, when cells were treated with lactacystin in the presence of increasing concentrations of mevalonate, the lactacystin-mediated apoptosis was completely reversed by mevalonate in a dose dependent fashion (Fig 6B). Apoptosis was measured both by accumulation of cells in sub-G1 as measured by flow cytometry (Fig 6B) and by chromosome condensation as observed by DAPI staining (Data not shown). These results show that mevalonate reverses the effects of lactacystin inhibition of the proteasome.

The reversal of lovastatin-mediated inhibition of HMG-CoA reductase by mevalonate is biochemically sound and documented extensively. However the reversal of proteasome inhibition by mevalonate is novel and represents an exciting enigma, since it suggests a novel function for mevalonate. We showed that mevalonate can reverse the apoptotic action of lactacystin and the G1 arrest mediated by the pro-drug

form of lovastatin. We also showed in figure 4B that when cells were treated with lactacystin and then assayed for proteasome activity, the activity was inhibited by 70%. However addition of mevalonate to cells reversed the lactacystin mediated inhibition of the proteasome. We also know that lactacystin does not inhibit the HMG-CoA reductase, or the cholesterol biosynthesis pathway. Treatment of cells with up to 10  $\mu$ M lactacystin for 24 hours did not result in any inhibition of the cholesterol biosynthesis as measured by the rate of incorporation of [ $^3$ H]-acetate into cholesterol (data not shown). Collectively, these results suggest that the inhibition of the proteasome by lactacystin is concomitant with apoptosis and independent of the cholesterol biosynthesis pathway. Further, the results indicate that addition of mevalonate reverses both lactacystin induced apoptosis and proteasome inhibition. To test the effect of mevalonate on proteasome activity we pretreated cells with increasing concentrations of mevalonate for 36 hours, prepared cell extracts, and measured the proteasome activity by using a fluorogenic peptide substrate as described above (Fenteany et al., 1994; Maupin-Furlow and Ferry, 1995), (Fig 6C). These studies in two different cell lines (MDA-MB-157 and MDA-MB-436 cells) revealed that when cells were treated with increasing concentrations of mevalonate, the peptidase activity of the proteasome increased 300-500 percent over the concentration range examined (Fig 6C). We believe that mevalonate reverses the action of both lactacystin and the pro-drug form of lovastatin on the proteasome by increasing the activity of the proteasome complex. Our results suggest that in addition to being an integral unit in the cholesterol biosynthesis pathway, mevalonate also has a role in proteolytic degradation.

## Discussion:

The novel hypothesis we present here is that lovastatin induces cyclin-dependent kinase inhibitors (p21 and p27) in breast cancer cells by modulation of the ubiquitin-proteasome pathway, independent of inhibition of the HMG-CoA reductase enzyme. The model for this hypothesis is presented in Figure 7. The left portion of this diagram depicts the traditional role of HMG-CoA reductase inhibitors that block mevalonate synthesis. The lack of mevalonate prevents the synthesis of farnesyl pyrophosphate and all subsequent isoprenylation of key proteins implicated in cell division. The right side of the diagram illustrates our hypothesis that the inactive inhibitor of HMG-CoA reductase (pro-drug form of lovastatin) and a specific inhibitor of the proteasome (lactacystin) cause G1 arrest or apoptosis from the accumulation of the CKIs p21 and p27. This accumulation is primarily due to the inhibition of the proteasome by both drugs. Central to our hypothesis is the unusual discovery that mevalonate, in addition to its known ability to rescue HMG-CoA reductase inhibition, unexpectedly reverses inhibition of the proteasome by lactacystin and by the pro-drug form of lovastatin. This leads to the degradation of the CKIs and resumption of cell division (Fig 7).

The rationale for the hypothesis that lovastatin, in its pro-drug form, can inhibit the proteasome became clear when it was found that the efficiency of conversion of the pro-drug to the open ring form is only 80%, leaving 20% of lovastatin in the pro-drug form which is inactive against HMG-CoA reductase. It is this 20% that inhibits the proteasome, as shown in figure 4. Since pravastatin exists entirely in the active form, inhibits HMG-CoA reductase and does not arrest cells, our data suggest that proteasome inhibition may play a more relevant role than HMG-CoA reductase inhibition when these types of drugs are used to arrest cells. Additionally we provide evidence that mevalonate has a dual function. Mevalonate clearly rescues lovastatin-

arrested cells. In addition to its known ability to rescue HMG-CoA reductase inhibition, we show that mevalonate reverses the effects of proteasome inhibition by lactacystin. We show this both by the ability of mevalonate to inhibit lactacystin-mediated apoptosis, and reversal of the proteasome inhibitory activity of the lactacystin. Mevalonate actually increases proteasome activity in cells when assayed *in vitro*. Collectively, our data suggest that the pathways of cholesterol biosynthesis and proteasome processing of cell cycle regulators clearly have an overlap.

The overlap between these two pathways is also evident when one examines the biological effects of lovastatin and lactacystin. Surprisingly there is common ground between lovastatin and lactacystin in their biological effects (Figure 7). For example, inhibitors of both HMG-CoA reductase and the proteasome have similar stimulatory effects on the differentiation of PC12 neuronal cells. Simvastatin, similar in structure and activity to lovastatin, causes neurite-like outgrowth and inhibition of cell proliferation in PC12 cells. This response was completely reversible by mevalonate. In contrast, pravastatin, which resembles only the active form of lovastatin, had no effect on these cells (Sato-Suzuki and Murota, 1996). Intriguingly, the neurite outgrowth of PC12 cells induced by inhibitors of the proteasome pathway suggests the involvement of the proteasome in cell differentiation (Saito et al., 1990; Tsubuki et al., 1993; Tsubuki et al., 1996). Lactacystin, when administered in its lactone form, results in neurogenesis, induces neurite outgrowth in a murine cell line and inhibits proliferation of other cell types by arresting them in the G0/G1 phase of the cell cycle (Fenteany et al., 1994; Omura et al., 1991). This effect of lactacystin is strongly reminiscent of the effect seen with simvastatin, described above.

While lovastatin and lactacystin have some biological effects in common, lovastatin has properties that seem unrelated to cholesterol biosynthesis. Several studies have reported that besides its cholesterol lowering ability, lovastatin also plays a role in inducing differentiation, inhibiting metastasis, and lowering cancer incidence. For example, treatment of cells by lovastatin resulted in regeneration of cultured rat skeletal muscle cells with a toxic effect on growth and differentiation, without influencing the cholesterol and phospholipid content of the cells. These studies suggest that other mechanisms besides inhibition of HMG-CoA reductase may play a role in the differentiation of muscle cells. (Veerkamp et al., 1996). In separate studies, inhibition of the HMG-CoA reductase induces differentiation of human monocytic cells associated with growth retardation and expression of monocytic differentiation markers (Weber et al., 1995). In other studies, lovastatin inhibited experimental lung metastasis of the highly metastatic B16F10 mouse melanoma in nude mice. Used *in vitro*, lovastatin pretreatment of B16F10 cells resulted in inhibition of attachment, motility, and invasion. These are key steps in the dynamic sequence of events that comprise the metastatic cascade (Jani et al., 1993). Lastly, data from a large clinical trial of lovastatin produced an unexpected finding. When patients with severe hypercholesterolemia were treated with lovastatin, a decreased incidence (14%) of cancer of all types was observed in these patients compared to the expected rates (21%) (Stein et al., 1993). Collectively these studies suggest that in addition to inhibiting HMG-CoA reductase, lovastatin may play a larger role in affecting diverse cellular pathways, unrelated to cholesterol biosynthesis, such as the proteasome pathway.

Inhibition of the proteasome leading to increased protein stabilization is not the only mechanism for up-regulating p21 levels. Lovastatin clearly regulates p21 levels by upregulating p21 mRNA, as described in several different cell lines (Gray-Bablin et al., 1997; Lee et al., 1998; Vogt et al., 1997). In one of these cell lines, the human prostate carcinoma cell line PC-3-M, p53 is null, eliminating the well-known mechanism of p21 gene expression. Lovastatin in this cell line upregulates p21 mRNA through a "lovastatin response element" in the promoter region which is coincident with the transforming growth factor Beta (TGF $\beta$ ) responsive element (Lee et al., 1998). The lovastatin effects were reversed by mevalonate. Curiously, the reporter construct was not responsive to added TGF $\beta$  suggesting that some other molecule must be activating p21 transcription through this site. Mutation of an SP1 binding site in the p21 promoter also blocks lovastatin activation of the reporter plasmid construct. The role of SP1 is very interesting since it has been shown to be degraded through the proteasome pathway as well. The authors show that lactacystin and LLnL block the rapid degradation of SP1 brought about by glucose starvation and cAMP stimulation. According to our hypothesis, SP1 could be stabilized by lovastatin via inhibition of proteasome activity. Stabilized SP1 could act directly or recruit other transcription factors to stimulate p21 transcription.

The ability of mevalonate to reverse the effects of lovastatin fits well with the idea that activity of HMG-CoA reductase is needed to provide precursors vital to cell division. However, the effect of the pro-drug form forces us to consider more complex mechanisms to explain this effect because the pro-drug does not inhibit HMG-CoA

reductase. We suggest that the key to this puzzle is that the pro-drug form of lovastatin is acting as a proteasome inhibitor, which leads to cell arrest in ways that closely mimic the effects of lactacystin (Figure 7). An entirely new role for mevalonate is to reverse the effects of both lactacystin and the pro-drug form of lovastatin. The mechanism by which mevalonate is capable of reversing the inhibitory action of the pro-drug and of lactacystin is unknown; however, it clearly involves the up-regulation of proteasome activity. There is precedent for this hypothesis. It has been reported that while HMG-CoA reductase is normally a stable enzyme with an extended half-life, downstream products such as mevalonate, sterols and their derivatives like 25-hydroxycholesterol will promote the rapid and specific degradation of this enzyme (McGee et al., 1996; Moriyama et al., 1998). Since HMG-CoA reductase is degraded through the proteasome pathway (Moriyama et al., 1998), and mevalonate increases the activity of the proteasome (this study), it follows that addition of mevalonate would promote the degradation of this enzyme as reported (McGee et al., 1996).

## **Materials and Methods:**

**Materials, cell lines and culture conditions.** Lovastatin was kindly provided by William Henckler (Merck, Sharp and Dohme research Pharmaceuticals, Rahway, NJ). Serum was purchased from Hyclone laboratories (Logan, Utah) and cell culture medium from Life Technologies, Inc. (Grand Island, NY). All other chemicals used were reagent grade. Before addition to cultures, lovastatin was converted from its inactive lactone pro-drug form to its active dihydroxy-open acid as described previously (Keyomarsi, 1996; Keyomarsi et al., 1991). The pro-drug was soluble in 60% ethanol and pravastatin was soluble in water. The culture conditions for MDA-MB-157 tumor cell lines were described previously (Keyomarsi and Pardee, 1993). All cells were cultured and treated at 37°C in a humidified incubator containing 6.5% CO<sub>2</sub>. Treatments with lovastatin, its pro-drug form, pravastatin, LLnL, or lactacystin was performed as described previously (Keyomarsi et al., 1991). Briefly, medium was removed 24-36 hrs after the initial plating, and replaced with fresh medium in the presence or absence of the aforementioned agents for 0-36 hrs. Cells were harvested at the indicated times and flow cytometry analysis was performed. For Fluorescence-Activated Cell Sorter (FACS) analysis 10<sup>6</sup> cells were centrifuged at 1,000 X g for 5 min, fixed by the gradual addition of ice cold 70% ethanol (30 min at 4°C), and washed with phosphate buffered saline. Cells were then treated with RNase (10 µg/ml) for 30 minutes at 37° C, washed once with phosphate buffered saline, and resuspended and stained in 1 ml of 69 µM propidium iodide in 38 mM sodium citrate for 30 minutes at room temperature. The cell cycle phase distribution was determined by analytical DNA flow cytometry as described previously (Keyomarsi et al., 1995).

**Western blot analysis.** Cell lysates were prepared and subjected to Western blot analysis as previously described (Rao et al., 1998). Briefly, 50 µg of protein from each



condition was electrophoresed in each lane of a 10% sodium dodecyl sulfate-polyacrylamide gel (SDS-PAGE) and transferred to Immobilon P overnight at 4° C at 35mV constant volts. The blots were blocked overnight at 4 ° C in Blotto (5% nonfat dry milk in 20mM Tris, 137 mM NaCl, 0.25% Tween, pH 7.6). After six, 10 minute washes in TBST (20mM Tris, 137mM NaCl, 0.05% Tween, pH 7.6), the blots were incubated in primary antibodies for 3 hours. Primary antibodies used were p27 monoclonal antibody (Transduction Laboratories, Lexington, KY) at a dilution of 1:100, p21 monoclonal antibody (Oncogene Research Products/Calbiochem, San Diego, CA) at a dilution of 1:100, and actin monoclonal antibody (Boehringer-Mannheim, Indianapolis, IN) at 0.63 µg/ml in Blotto. Following primary antibody incubation, the blots were washed and incubated with goat anti-mouse horseradish peroxidase conjugate at a dilution of 1:5,000 in Blotto for 1 hour and finally washed and developed with the Renaissance chemiluminescence system as directed by the manufacturers (NEN Life Sciences Products, Boston, MA).

**HPLC analysis of pro-drug, lovastatin and pravastatin:** Reverse Phase High Performance Liquid Chromatography (HPLC) was performed as previously described (Stubbs et al., 1986). Briefly, a C 18 Novopac column was equilibrated with the stationary phase of 0.1%TFA (trifluoroacetic acid). HPLC analysis was performed on a Waters 625 chromatography system, using 90% acetonitrile as the mobile phase. For HPLC analysis, the stock solution of the pro-drug was made in DMSO, pravastatin was dissolved in 0.1% TFA while lovastatin was prepared as described previously (Keyomarsi et al., 1991). The drugs were further diluted in 0.1% TFA and 10 µg of the diluted solutions were then loaded on to the HPLC column. DMSO was run on the

column as a solvent control. The separated components were eluted and subjected to mass spectrometry as described (Uchiyama et al., 1991).

**Assay for HMG-CoA reductase activity:** The HMG-CoA reductase assays in MDA-MB-157 cells were performed as previously described (Larsson et al., 1989). Briefly, 80% confluent MDA-MB-157 cells were washed 3 times in cold PBS and harvested in reaction buffer (200 mM phosphate buffer pH 7.4, 20 mM DTT, 40 mM glucose-6-phosphate, 3 mM  $\beta$ -NADPH and 2 units/ml glucose-6-phosphatase). The cells were then homogenized by sonication and the supernatant was collected following centrifugation for 15 minutes at 20,000 X g. The supernatant was incubated with the pro-drug, lovastatin, or pravastatin for 15 minutes at 37°C before the addition of the [ $^{14}$ C] HMG-CoA. The mixture was then incubated for another 1 hour at 37°C. The reaction was stopped by the addition of 20  $\mu$ l concentrated HCL and incubated for another 30 minutes at 37 °C. 40 $\mu$ l of the samples were spotted on a TLC plate with [ $^{14}$ C] mevalolactone (MVA) as running standard and developed with benzene: acetone (1:1 ratio). The efficiency of the enzymatic reaction is a measure of conversion of [ $^{14}$ C] HMG-CoA into MVA expressed as percent conversion. [ $^{14}$ C] MVA formed was quantitated with TINA2.09 program from Raytest USA (New Castle, DE) following PhosphorImager scanning of the TLC plates. The data were normalized to the microsomal protein concentration which was evaluated with the BioRad reagent, using the same buffer with the standards and for the blank.

**20S proteasome activity assay:** Seventy percent confluent MDA-MB-157 cells were washed twice in PBS and harvested in cold 5mM Hepes, pH 7.5, in the presence of 1mM dithiothreitol. The cells were then homogenized by brief sonication and subjected to centrifugation for 10 minutes at 16000Xg at 4°C. The supernatant was collected and protein concentration was determined with the BioRad reagent. For

measurement of the 20S proteasome chymotrypsin peptidase activity, 10  $\mu$ l of cellular extract (100  $\mu$ g) was diluted in a cuvette containing 2 ml of 20 mM Hepes, 0.5M EDTA, pH 8, 0.035% SDS with the indicated concentrations of lactacystin, pro-drug, lovastatin and pravastatin. (The proteasome assays of the pretreated cells were performed following treatment of MDA-MB-157 cells with the indicated drugs). The above mixture was incubated at 37°C before the addition of the fluorogenic substrate, 10  $\mu$ M succinyl-Leu-Leu-Val-Tyr-7-amido-4-methylcoumarin. Substrate hydrolysis was measured by continuous monitoring of fluorescence (emission at 440 nm, excitation at 380 nm) of the liberated 7-amino-4-methylcoumarin for 15 minutes as described (Dick et al., 1997).

**<sup>35</sup>S metabolic labeling for MDA-MB-157 cells:** MDA-MB-157 cells were grown to 70% confluency and treated with 40  $\mu$ M  $\beta$ -lactone for 36 hours. Cells were then washed with PBS and incubated in Dulbecco's modified Eagle's medium (DMEM) without methionine and cysteine and with  $\beta$ -lactone or no drug for 2 hours. EXPRESS [<sup>35</sup>S]Protein labeling Mix (0.2 mCi; NEN/Dupont) was added, and the cells were pulse labeled for 2 hours. After the pulse the cells were washed three times in PBS and methionine and cysteine were added to a final concentration of 100mg/liter. At the indicated time points following the pulse, samples of cells were washed in PBS and harvested in RIPA buffer (1% NP-40, 0.5% sodium deoxycholate, 0.1% SDS, phenyl-methylsulfonyl fluoride at 0.1 mg/ml, aprotinin at 30  $\mu$ l/ml, and 0.1 mM sodium ortho-vanadate). Following protein determination 300  $\mu$ g of cell extracts were used for p21 and p27 immunoprecipitations with polyclonal antibodies against p27 or p21 (p27-C19, and p21-C19-G, Santa Cruz Biotechnology, Santa Cruz, CA) in lysis buffer containing 50mM Tris buffer pH7.5, 250 mM NaCl, 0.1% NP-40, 25  $\mu$ g/ml leupeptin, 25  $\mu$ g/ml aprotinin, 10  $\mu$ g/ml pepstatin, 1 mM benzamidine, 10  $\mu$ g/ml soybean trypsin inhibitor, 0.5 mM PMSF, 50 mM NaF, 0.5mM sodium ortho-vanadate. The

protein/antibody mixture was incubated with protein A Sepharose for 1 hour and the immunoprecipitates were then washed four times with lysis buffer. The immunoprecipitates were separated by SDS-PAGE (13%), gels were treated with Fluoro-Hance (Research Products International, Mount Prospect, IL) and used for autofluorography.

## **Acknowledgments**

We gratefully acknowledge Dr. Katherine Henrickson and Mr. Christopher G. Danes for the critical reading of this manuscript, Dr. Julie Gray-Bablin for helpful discussions during the course of this work, and the use of Wadsworth Center's Immunology, Biochemistry, Mass Spectrometry, Tissue Culture, and Photography/Graphics core facilities. S.R. is a fellow of the Cancer Research Foundation of America. This research was supported in part by Grant DAMD-17-94-J-4081 from the U.S. Army Medical Research Acquisition Activity and by Grant No. R29-CA666062 from the National Cancer Institute (both to K.K.)

## References:

Blagosklonny, M. V., Wu, G. S., Mura, S., and Eldeiry, W. S. (1996). Proteasome dependent regulation of p21 expression. *Biochem. Biophys. Res. Comm.* 227, 564-569.

Bradford, D. L., Silva, C. J., and Simoni, R. D. (1992). Squalene synthase-deficient mutant of Chinese hamster ovary cells. *J. Biol. Chem.* 267, 18308-18314.

Casey, P. J., Solis, P. A., Der, C. J., and Buss, J. E. (1989). p21ras is modified by a farnesyl isoprenoid. *Proc. Natl. Acad. Sci. USA* 86, 8323-8327.

Ciechanover, A. (1994). The ubiquitin-proteasome proteolytic pathway. *Cell* 79, 13-21.

Clurman, B. E., Sheaff, R. J., Thress, K., Groudine, M., and Roberts, J. M. (1996). Turnover of cyclin E by the ubiquitin-proteasome pathway is regulated by cdk2 binding and cyclin phosphorylation. *Genes & Dev.* 10, 1979-1990.

Corsini, A., Maggi, F. M., and Catapano, A. L. (1995). Pharmacology of competitive inhibitors of the HMG-CoA reductase. *Pharmacol. Res.* 31, 9-27.

Dick, L. R., Cruikshank, A., Destree, T., Grenier, L., McCormack, T. A., Melandri, F. D., Nunes, S. L., Palombella, V. J., Parent, L. A., Plamondon, L., and Stein, R. L. (1997). Mechanistic studies on the inactivation of the proteasome by Lactacystin in cultured cells. *J. Biol. Chem.* 272, 182-188.

Diehl, J. A., Zindy, F., and Sherr, C. J. (1997). Inhibition of cyclin D1 phosphorylation on threonine-286 prevents its rapid degradation via the ubiquitin-proteasome pathway. *Genes & Dev.* 11, 957-972.

Endo, A., Kuroda, M., and Tansawa, K. (1976). Competitive inhibition of 3-hydroxy-3-methylglutaryl coenzyme A reductase by ML-236A and ML-236B, fungal metabolites having hypocholesterolemic activity. *FEBS Lett.* 72, 323-326.

Feldman, R. M. R., Correll, C. C., Kaplan, K. B., and Deshaies, R. J. (1997). A complex of CDC4P, SKPIP, and CDC53P/Cullin catalyzes ubiquitination of the phosphorylated CDK inhibitor SIC1P. *Cell* 91, 221-230.

Fenteany, G., Standaert, R. F., Lane, W. S., Choi, S., Corey, E. J., and Schreiber, S. L. (1995). Inhibition of proteasome activities and subunit-specific amino-terminal threonine modification by lactacystin. *Science* 268, 726-731.

Fenteany, G., Standaert, R. F., Reichard, G. A., Corey, E. J., and Schreiber, S. L. (1994). A  $\beta$ -lactone related to lactacystin induces neurite outgrowth in a neuroblastoma cell line and inhibits cell cycle progression in an osteosarcoma cell line. *Proc. Natl. Acad. Sci.* 91, 3358-3362.

Glotzer, M., Murray, A. W., and Kirschner, M. W. (1991). Cyclin is degraded by the ubiquitin pathway. *Nature* 349, 132-138.

Gray-Bablin, J., Rao, S., and Keyomarsi, K. (1997). Lovastatin induction of cyclin-dependent kinase inhibitors in human breast cells occurs in a cell cycle independent fashion. *Cancer Res.* 57, 604-609.

Haas, A. L., and Siepmann, T. J. (1997). Pathways of ubiquitin conjugation. *FASEB J.* **11**, 1257-1268.

Hall, S. C., Smith, D. M., Masiarz, F. R., Soo, V. W., Tran, H. M., Epstein, L. B., and Burlingame, A. L. (1993). Mass spectrometric and Edman sequencing of lipocortin I isolated by two-dimensional SDS/PAGE of human melanoma lysates. *Proc. Natl. Acad. Sci.* **90**, 1927-1931.

Halpin, R. A., Ulm, E. H., Till, A. E., Karl, P. H., Vyas, K. P., Hunninghake, D. B., and Duggan, D. E. (1993). Biotransformation of Lovastatin: Species differences in in vivo metabolite profiles of mouse, rat, dog, and human. *Drug Met. Dis.* **21**, 1003-1011.

Haupt, Y., Maya, R., Kazaz, A., and Oren, M. (1997). mdm2 promotes the rapid degradation of p53. *Nature* **387**, 296-299.

Henchoz, S., Chi, Y., Catarin, B., Herskowitz, I., Deshaies, R. J., and Peter, M. (1997). Phosphorylation- and ubiquitin-dependent degradation of the cyclin-dependent kinase inhibitor FAR1P in budding yeast. *Genes & Dev.* **11**, 3046-3060.

Hengst, L., and Reed, S. I. (1996). Translational control of p27Kip1 accumulation during the cell cycle. *Science* **271**, 1861-1864.

Hershko, A., and Ciechanover, A. (1992). The ubiquitin system for protein degradation. *Ann. Rev. Bioch.* **61**, 761-807.



Hochstrasser, M. (1992). Ubiquitin and intracellular protein degradation. *Curr. Opin. Cell Biol.* 4, 1024-1031.

Hochstrasser, M. (1995). Ubiquitin, proteasomes, and the regulation of intracellular protein degradation. *Curr. Opin. Cell Biol.* 7, 215-223.

Hochstrasser, M. (1996). Ubiquitin-dependent protein degradation. *Ann. Rev. Genet.* 30, 405-439.

Ichihara, A., and Tanaka, K. (1995). Role of proteasome in cell growth. *Mol. Bio. Reports* 21, 49-52.

Jani, J. P., Specht, S., Stemmler, N., Blanock, K., Singh, S. V., Gupta, V., and Katoh, A. (1993). Metastasis of B16F10 mouse melanoma inhibited by Lovastatin, an inhibitor of cholesterol biosynthesis. *Inv. Metas.* 13, 314-324.

Jentsch, S. (1992). The ubiquitin-conjugation system. *Ann. Rev. Genet.* 26, 179-207.

Keyomarsi, K. (1996). Synchronization of mammalian cells by Lovastatin. *Methods in Cell Science* 18, 109-114.

Keyomarsi, K., Conte, D., Toyofuku, W., and Fox, M. P. (1995). Deregulation of cyclin E in breast cancer. *Oncogene* 11, 941-950.

Keyomarsi, K., and Pardee, A. B. (1993). Redundant cyclin overexpression and gene amplification in breast cancer cells. *Proc. Natl. Acad. Sci. USA* 90, 1112-1116.

Keyomarsi, K., Sandoval, L., Band, V., and Pardee, A. B. (1991). Synchronization of tumor and normal cells from G1 to multiple cell cycles by lovastatin. *Cancer Res.* 51, 3602-3609.

Kubbatat, M. H. G., Jones, S. N., and Vousden, K. H. (1997). Regulation of p53 stability by mdm2. *Nature* 387, 299-303.

Lanker, S., Valdivieso, M. H., and Wittenberg, C. (1996). Rapid degradation of the G1 cyclin Cln2 induced by CDK-dependent phosphorylation. *Science* 271, 1597-1601.

Larsson, O., Barrios, C., Latham, C., Ruiz, J., Zetterberg, A., Zickert, P., and Wedge, J. (1989). Abolition of mevinolin-induced growth inhibition in human fibroblasts following transformation by Simian Virus 40. *Cancer Res.* 49, 5605-5610.

Lee, S. J., Ha, M. J., Lee, J., Nguyen, P. M., Choi, Y. H., Pirnia, F., Kang, W.-K., Wang, X.-F., Kim, S.-J., and Trepel, J. B. (1998). Inhibition of the 3-hydroxy-3-methylglutaryl-coenzyme A reductase pathway induces p53-independent transcriptional regulation of p21 in human prostatic carcinoma cells. *J. Biol. Chem.* 273, 10618-10623.

Lupas, A., Koster, A. J., and Baumeister, W. (1993). Structural features of the 26S and 20S proteasomes. *Enzy. & Prot.* 47, 252-273.

Mahaffey, D. T., Yoo, Y., and Rechsteiner, M. (1995). Ubiquitination of full-length cyclin. *FEBS Lett.* 370, 109-112.

Maki, C. G., and Howley, P. M. (1997). Ubiquitination of p53 and p21 is differentially affected by ionizing and UV radiation. *Mol. Cell. Bio.* 17, 355-363.

Maltese, W. A. (1990). Posttranslational Modification of Proteins by Isoprenoids in Mammalian Cells. *FASEB J.* 4, 3319-3328.

Maltese, W. A., and Sheridan, K. M. (1987). Isoprenylated proteins in cultured cells: subcellular distribution and changes related to altered morphology and growth arrest induced by mevalonate deprivation. *J. Cell. Physiol.* 133, 471-481.

Maupin-Furlow, J. A., and Ferry, J. G. (1995). A proteasome from the methanogenic archaeon *Methanosarcina thermophila*. *J. Biol. Chem.* 270, 28617-28622.

McGee, T. P., Cheng, H. H., Kumagai, H., Omura, S., and Simoni, R. D. (1996). Degradation of 3-hydroxy-3-methylglutaryl reductase in endoplasmic reticulum membranes is accelerated as a result of increased susceptibility to proteolysis. *J. Biol. Chem.* 271.

Moriyama, T., Sather, S. K., McGee, T. P., and Simoni, R. D. (1998). Degradation of HMG-CoA reductase in vitro. Cleavage in the membrane domain by a membrane-bound cysteine protease. *J. Biol. Chem.* 273, 22037-22043.

Murray, A. (1995). Cyclin ubiquitination: The destructive end of mitosis. *Cell* 81, 149-152.

Omura, S., Fujimoto, T., Otoguro, K., Matsuzaki, K., Moriguchi, R., Tanaka, H., and Sasaki, Y. (1991). Lactacystin, a novel microbial metabolite, induces neuritogenesis of neuroblastoma cells. *J. Antibiotics* 44, 113-116.

Pagano, M. (1997). Cell cycle regulation by the ubiquitin pathway. *FASEB J.* 11, 1067-1075.

Pagano, M., Tam, S. W., Theodoras, A. M., Beer-Romero, P., Del Sal, G., Chau, V., Yew, R. P., Draetta, G. F., and Rolfe, M. (1995). Role of the ubiquitin-proteasome pathway in regulating abundance of the cyclin-dependent kinase inhibitor p27. *Science* 269, 682-685.

Peters, J. M., Cejka, Z., Harris, J. R., Kleinschmidt, J. A., and Baumeister, W. (1993). Structural features of the 26S proteasome complex. *J. Mol. Biol.* 234, 932-937.

Raiteri, M., Arnaboldi, L., McGeady, P., Gelb, M. H., Verri, D., Tagliabue, C., Quarato, P., Ferraboschi, P., Santaniello, E., Paoletti, R., Fumagalli, R., and Corsini, A. (1997). Pharmacological control of the mevalonate pathway: effect on arterial smooth muscle cell proliferation. *J. Pharmac. Exp. Therap.* 281, 1144-1153.

Rao, S., Lowe, M., Herliczek, T., and Keyomarsi, K. (1998). Lovastatin mediated G1 arrest in normal and tumor breast cells through inhibition of CDK2 activity and redistribution of p21 and p27, independent of p53. *Oncogene In press.*

Rettersol, K., Stuggard, M., Gorbitz, C., and Ose, L. (1996). Results of intensive long term treatment of familial hypercholesterolemia. *Am. J. Card.* 78.

Rock, K. L., Gramm, C., Rothstein, L., Clark, K., Stein, R., Dick, L., Hwang, D., and Goldberg, A. L. (1994). Inhibitors of the proteasome block degradation of most cell proteins and the generation of peptides presented on MHC class I molecules. *Cell* 78, 761-771.

Saito, Y., Tsubuki, S., Ito, H., and Kawashima, S. (1990). The structure function relationship between peptide aldehyde derivatives on initiation of neurite outgrowth in PC12 cells. *Neurosci. Lett.* 120, 1-4.

Sato-Suzuki, I., and Murota, S.. (1996). Simvastatin inhibits the division and induces neurite-like outgrowth in PC12 cells. *Neuro. Let.* 220, 21-24.

Skowyra, D., Craig, K. L., Tyers, M., Elledge, S. J., and Harper, J. W. (1997). F-box proteins are receptors that recruit phosphorylated substrates to the SCF ubiquitin-ligase complex. *Cell* 91, 209-219.

Stein, E. A., Lazkarzewski, P., Steiner, P., and IV, L. S. g. I. t. (1993). Lovastatin 5-year safety and efficacy study. *Arch. Intern. Med.* 153, 1079-1087.

Stubbs, R. J., Schwartz, M., and Bayne, W. F. (1986). Determination of mevinolin and mevinolic acid in plasma and bile by reversed-phase high-performance liquid chromatography. *J. Chromat.* 383, 438-443.

Tanahashi, N., Tsurumi, C., Tamura, T., and Tanaka, K. (1993). Molecular structure of 20S and 26S proteasomes. *Enzy. & Prot.* 47, 241-251.

Tsubuki, S., Kawasaki, H., Saito, Y., Miyashita, N., Inomata, M., and Kawashima, S. (1993). Purification and characterization of a Z-Leu-Leu-Leu-MCA degrading protease expected to regulate neurite formation: A novel catalytic activity in proteasome. *Biochem. Biophys. Res. Commun.* 196, 1195-1201.

Tsubuki, S., Saito, Y., Tomioka, M., Ito, H., and Kawashima, S. (1996). Differential inhibition of calpain and proteasome activities by peptidyl aldehydes of di-leucine and tri-leucine. *J. Biochem.* 119, 572-576.

Uchiyama, N., Kagami, Y., Saito, Y., Abe, S., Ohtawa, M., and Hata, S. (1991). Metabolic fate of 2,2-dimethylbutyryl moiety of simvastatin in rats: Identification of metabolites by gas chromatography/mass spectrometry. *Eu. J. Drug Met. and Pharm.* 16, 189-196.

Varshavsky, A. (1997). The ubiquitin system. *Trends Bioch. Sci.* 22, 383-387.

Veerkamp, J. H., Smit, J. W. A., Benders, A. A. G. M., and Oosterhof, A. (1996). Effects of HMG-CoA reductase inhibitors on growth and differentiation of cultured rat skeletal muscle cells. *Bioch. Biophys. Acta* 1315, 217-222.

Vogt, A., Sun, J., Qian, Y., Hamilton, A. D., and Sebt, S. M. (1997). The geranylgeranyltransferase-I inhibitor GGTI-298 arrests human tumor cells in G0/G1 and induces p21 in a p53-independent manner. *J. Biol. Chem.* 272, 27224-27229.

Weber, C., Erl, W., and Weber, P. C. (1995). Lovastatin induces differentiation of mono Mac 6 cells. *Cell Bioch. Funct.* 13, 273-277.

Wedje, J., Calberg, M., Hjertman, M., and Larsson, O. (1993). Isoprenoid regulation of cell growth: Identification of mevalonate labeled compounds including DNA synthesis in human breast cancer cells depleted of serum and mevalonate. *J. Cell Physiol.* 155, 539-548.

Won, K.-A., and Reed, S. I. (1996). Activation of cyclin E/cdk2 is coupled to site-specific autophosphorylation and ubiquitin-dependent degradation of cyclin E. *EMBO J* 15, 4182-4193.

## Figure Legends:

**Figure 1: Induction of CKIs by the  $\beta$ -lactone form of lovastatin.** **A:** Chromatographic separation of Lovastatin mixture and closed ring form. Lovastatin mixture (top) was prepared and subjected to HPLC analysis as described (Keyomarsi et al., 1991; Stubbs et al., 1986). The closed ring form of lovastatin (bottom) was prepared by dissolving the compound in 100% ethanol. **B:** Fractions corresponding to each HPLC peak were collected and subjected to molecular weight determination by electrospray ionization quadrupole mass spectrometry analysis as described (Hall et al., 1993). In addition, the lovastatin mixture and closed ring forms were also subjected to mass spec. analysis to determine the components of each reagent. **C:** MDA-MB-157 tumor cells were treated with the indicated concentrations of lovastatin, mixture (open and closed rings), lovastatin, closed  $\beta$ -lactone ring, or pravastatin for 36 hours. Following treatments, cells were harvested and cell lysates were prepared and subjected to Western blot analysis (left panel): 50 $\mu$ g of protein extracts from each condition were analyzed by Western analysis with anti-p21, anti-p27, or anti-actin specific antisera and blots developed with the ECL reagent. Flow cytometry analysis (right panel): percentage of cells in different phases of the cell cycle for each treatment was determined from flow cytometric measurements of DNA content.

**Figure 2: Inactivation of HMG-CoA reductase enzyme by lovastatin.** Microsomes were prepared from subconfluent cultures of MDA-MB-157. 100  $\mu$ g protein extract was incubated in the presence of the indicated concentrations of lovastatin, pro-drug, or pravastatin at 37 °C for 15 minutes.  $^{14}$ C-HMG-CoA was added to each sample and



after a 1 hour incubation the reaction was stopped by the addition of HCl, and samples were allowed to lactonize. The samples were then resolved by TLC and analyzed by phosphorimaging. The activity of HMG-CoA reductase is a measure of the percent conversion of  $^{14}\text{C}$ -HMG-CoA into mevalolactone, the end product of the HMG-CoA reductase. Symbols are (●) lovastatin mixture, (○)  $\beta$ -lactone, and (■) pravastatin

**Figure 3. Induction of p21 and p27 by proteasome inhibitors.** MDA-MB-157 tumor cells were treated with (A) 40  $\mu\text{M}$  of either lovastatin mixture (open and closed rings), lovastatin closed  $\beta$ -lactone ring (pro-drug), or pravastatin for 36 hours, (B) 10  $\mu\text{M}$  LLnL for 0-36 hours, or (C) indicated concentrations of lactacystin for 24 hours. Following treatments, cells were harvested and cell lysates were prepared and subjected to Western blot analysis: 50 $\mu\text{g}$  of protein extracts from each condition were analyzed by Western analysis with anti-p21 or anti-p27 (or anti-actin, data not shown) specific antisera and blots developed with the ECL reagent. Brackets in panel A point to the high molecular weight laddering of p21 and p27 which are diagnostic for poly-ubiquitination of these proteins.

**Figure 4: Inhibition of the proteasome activity by the pro-drug form of lovastatin and lactacystin:** Cell extracts were prepared from either MDA-MB-157 cells (A) without drug treatment or (B) treated with either lovastatin (lov) (40 $\mu\text{M}$ ),  $\beta$ -lactone ( $\beta$ -lac) (40  $\mu\text{M}$ ), or lactacystin (lact) (1  $\mu\text{M}$ ) in the presence or absence of mevalonate (mev) (5 mM) for 36 hours and assayed for proteasome enzyme activity. The extracts in panel A

were incubated in the presence of the indicated concentrations of the drugs for 20 minutes at 37°C at which point the fluorogenic peptide substrate (100  $\mu$ M final concentration) for the chymotrypsin like activity of the proteasome (i.e. Suc-LLVY-AMC) was added to extracts. The fluorescence assays (excitation/emission 380/440 nm) were conducted at 37°C for 750 seconds. Each experiment was performed at least three times. The pre-treated extracts in panel B were not further incubated in the presence of the inhibitors and were directly assayed for the proteasome activity.

Symbols are (■) lactacystin, (○)  $\beta$ -lactone, (●) lovastatin mixture, and (□) pravastatin.


**Figure 5: Increased stability of p21 and p27 by the pro-drug form of lovastatin.** MDA-MB-157 cells were cultured in the presence or absence of 40  $\mu$ M pro-drug for 36 hours at which point the cells were incubated for 4 hours with  $^{35}$ S-methionine and  $^{35}$ S-cysteine (pulse) and subsequently incubated in the presence of an excess of nonradioactive methionine and cysteine for the additional times indicated (chase). Cells were lysed, extracts were adjusted for equal amounts of protein, and p21 and p27 were precipitated from nondenatured protein extracts with polyclonal antibodies. The immunoprecipitates were separated by SDS-PAGE and the radioactive p21 and p27 were detected by autofluorography. Panel B shows differences in half-lives of p21 and p27 in MDA-MB-157 cells treated with pro-drug. All data were quantitated on the basis of PhosphorImager scans.

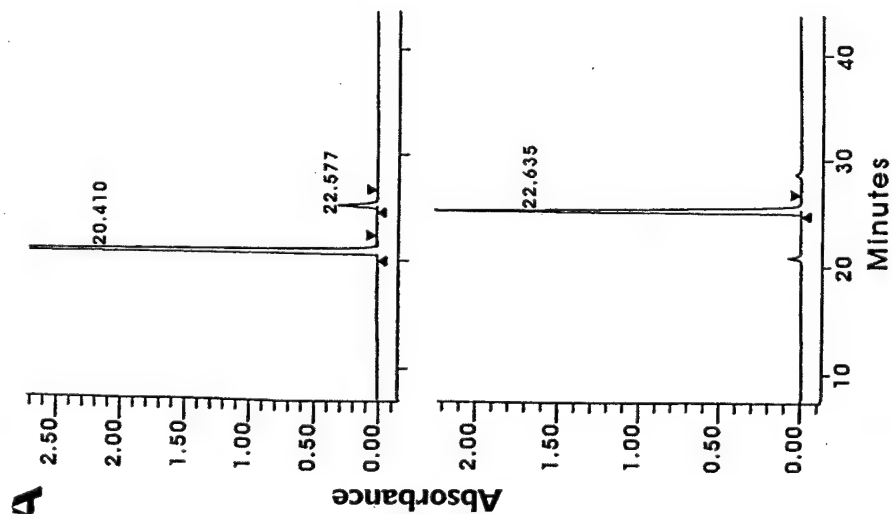
**Figure 6: Mevalonate reversal of lovastatin, lovastatin pro-drug, and lactacystin.** A MDA-MB-157 cells were treated with the indicated concentration of lovastatin (lov) or

the pro-drug in the presence or absence of 4 mM mevalonate (Mev) for 36 hours. Percentages of cells in different phases of the cell cycle following each treatment were obtained from flow cytometric measurements of DNA content from three separate experiments and the averages of the values are indicated. As shown, both lovastatin and its pro-drug inhibited DNA synthesis (i.e. decreased S phase) and caused the accumulation of cells in G1 phase. Addition of mevalonate reversed the G1 arrest mediated by both agents. **B.** MDA-MB-157 cells were treated with 10  $\mu$ M lactacystin (lact) in the presence or absence of 10 mM or 50 mM mevalonate for 36 hours. At the end of treatment cells were subjected to flow cytometric measurement of DNA content. Percent apoptosis reflects the accumulation of cells with sub-G1 DNA content. Each treatment was repeated at least 3 times and the averages of the values are indicated. **C.** Induction of the proteasome activity by mevalonate. MDA-MB-436 (closed symbols) and MDA-MB-157 (open symbols) were treated with the indicated concentrations of mevalonate for 36 hours. Following treatment, crude cell extracts were prepared and assayed for proteasome enzyme activity by measuring the chymotrypsin-like activity of the proteasome (described for Figure 4B). Values are expressed as fold increase over no treatment controls.

**Figure 7 : Cell cycle regulation by inhibitors of HMG-CoA Reductase and the**

**Proteasome:** Symbols:  positively regulates,

 negatively regulates, ? mechanism not known



**B**

Compound	MW
Peak 20.410	423.4
Peak 22.577	405.7
Peak 22.635	405.5
Lovastatin, mixture	423 (80%) 405 (20%)
Lovastatin, closed ring form	405 (99%)

Figure 1

Figure 1A

C

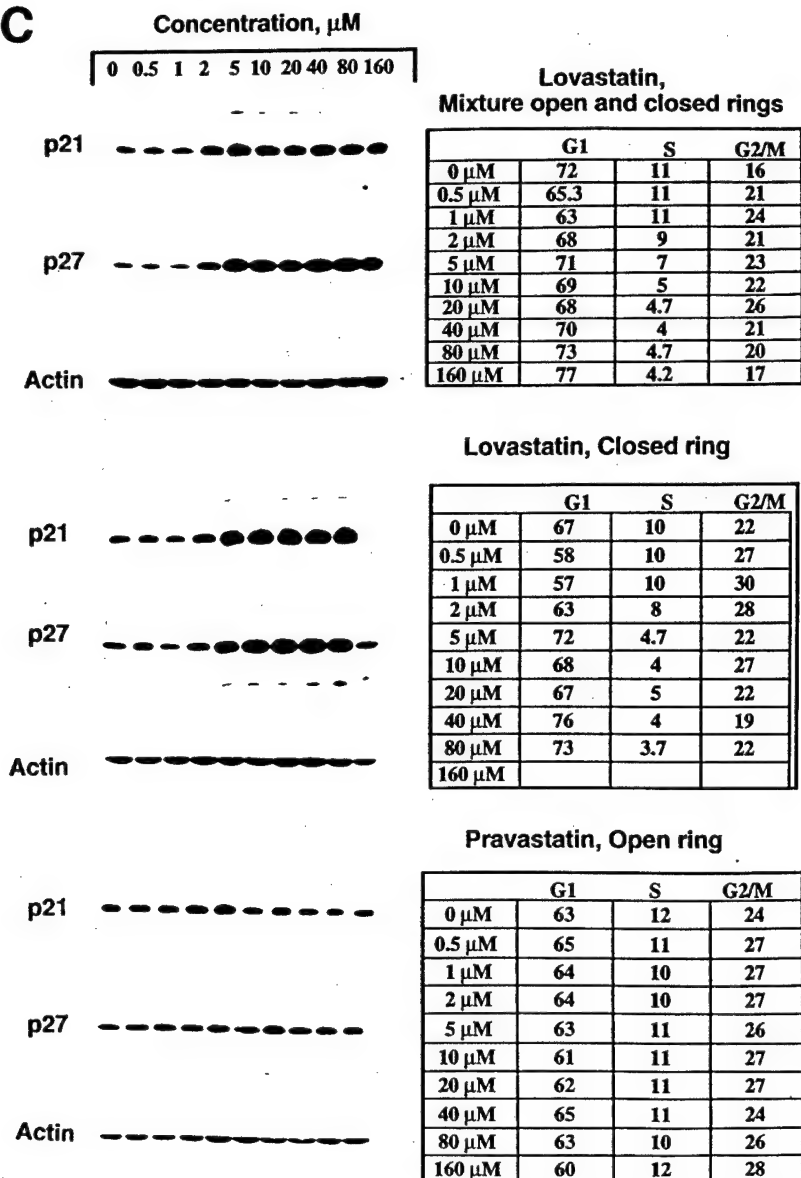


Figure 2

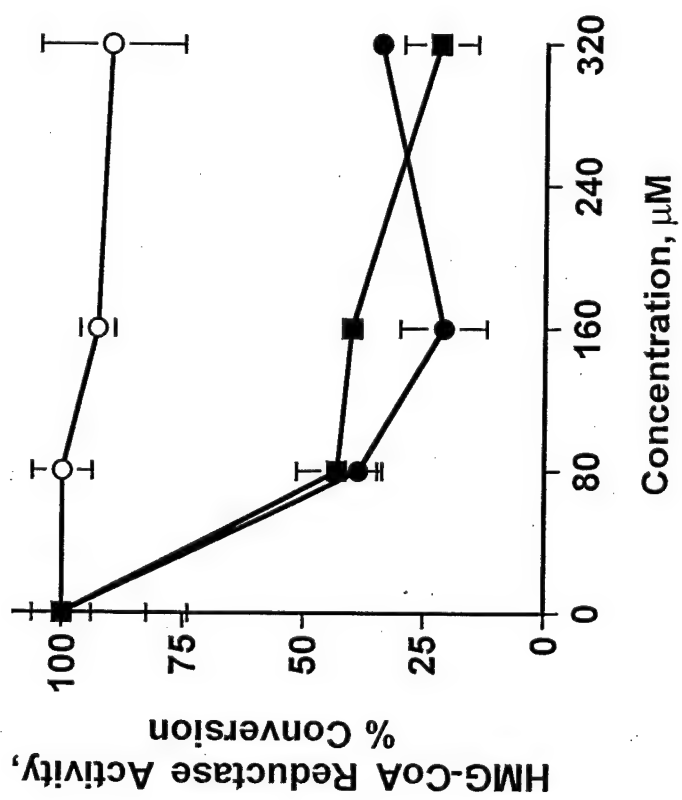
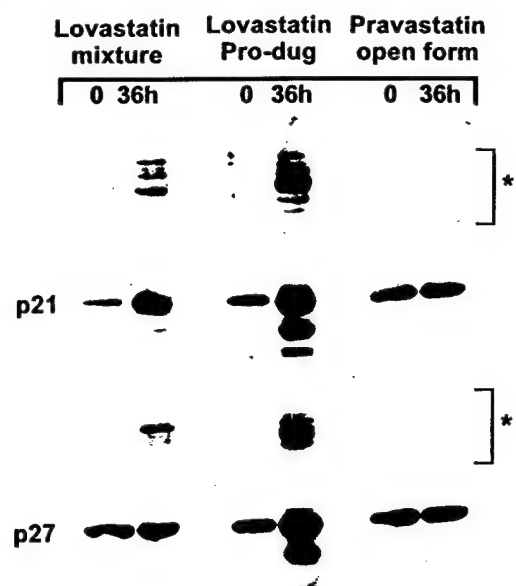
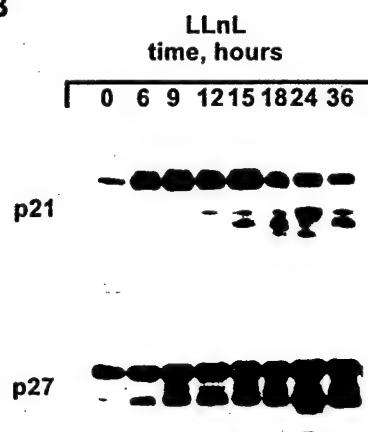


Figure 3

A



B



C

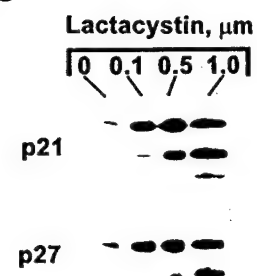


Figure 4

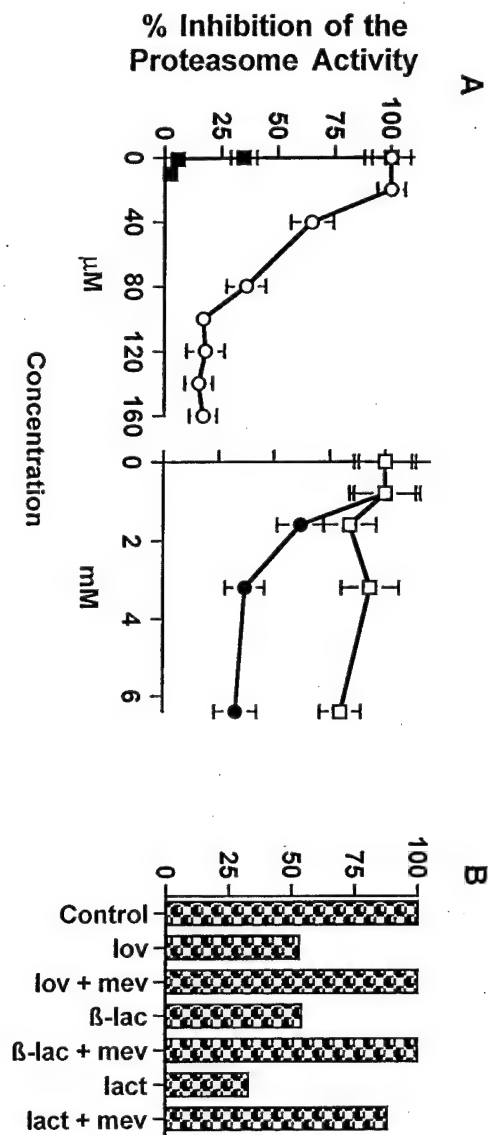




Figure 5

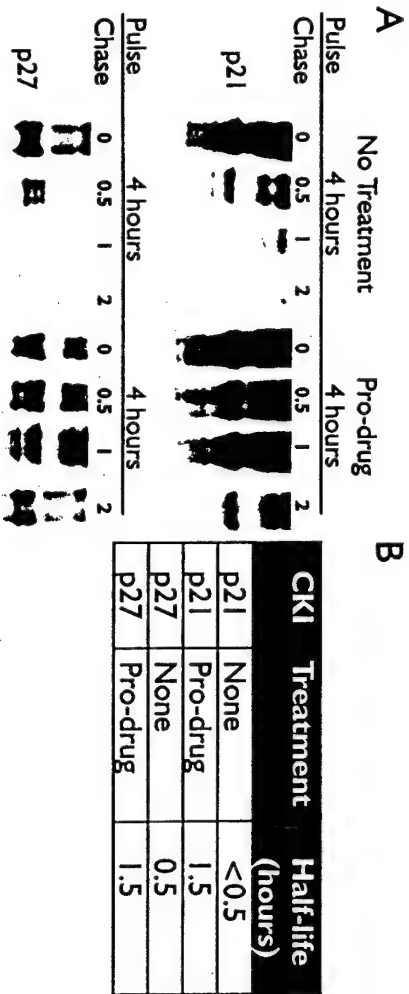


Figure 6

**A**

Treatment	% G1	% S	% G2
None	56	12	31
Mev, 4 mM	56	12	32
Lov, 40 $\mu$ M	61	4	35
Lov + Mev	51	13	34
$\beta$ -lactone, 40 $\mu$ M	62	3	34
$\beta$ -lactone + Mev	53	12	34

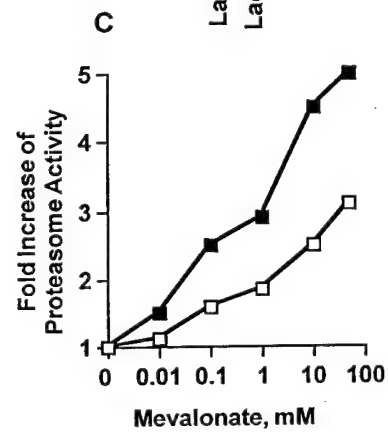
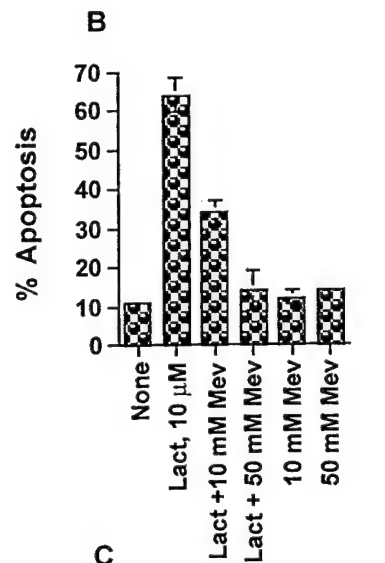
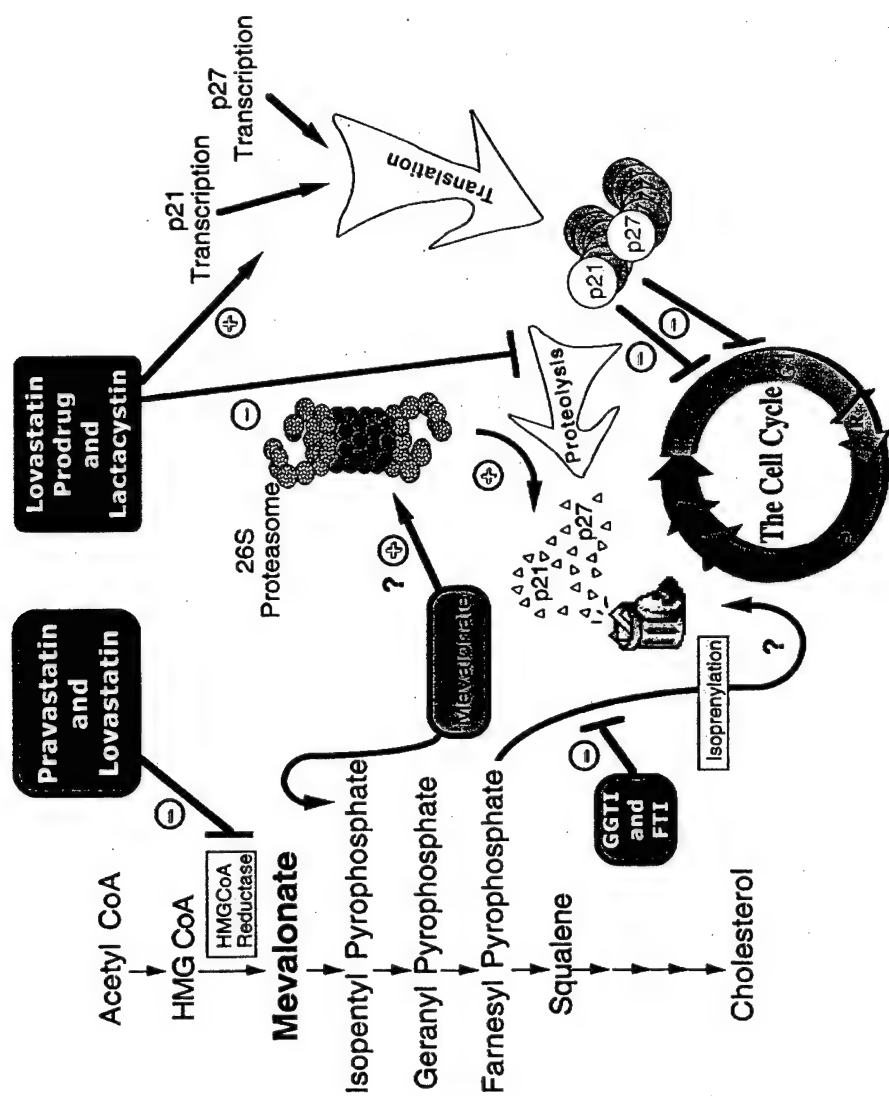


Figure 7



# **UCN-01 Mediated G1 Arrest in Normal But Not Tumor Breast Cells is pRb Dependent and p53 Independent**

Xiaomei Chen<sup>1</sup>, Michael Lowe<sup>1</sup>, and Khandan Keyomarsi<sup>1,2\*</sup>

<sup>1</sup> Division of Molecular Medicine, Wadsworth Center, Albany New York 12201-0509.

<sup>2</sup> Department of Biomedical Sciences, State University of New York, Albany, NY 12222.

\* To whom correspondence should be addressed:

Wadsworth Center  
Empire State Plaza  
P.O. Box 509  
Albany, NY 12201-0509

Phone: (518) 486-5799  
FAX: (518) 486-5798  
E-mail: keyomars@wadsworth.org

Running title: UCN-01 Induced G1 Arrest is via pRb

Key Words: UCN-01, cell cycle, p53, pRb, E6, E7

## Summary

In this study we investigated the growth inhibitory affects of UCN-01 in several normal and tumor-derived human breast epithelial cells. We found that while normal mammary epithelial cells were very sensitive to UCN-01 with an  $IC_{50}$  of 10 nM, tumor cells displayed little to no inhibition of growth with any measurable  $IC_{50}$  at low UCN-01 concentrations (i.e. 0-80nM). The UCN-01 treated normal cells arrested in G1 phase and displayed decreased expression of most key cell cycle regulators examined, resulting in inhibition of CDK2 activity due to increased binding of p27 to CDK2. Tumor cells on the other hand displayed no change in any cell cycle distribution or expression of cell cycle regulators. Examination of E6 and E7 derived strains of normal cells revealed that pRb and not p53 function is essential for UCN-01 mediated G1 arrest. Lastly, treatment of normal and tumor cells with high doses of UCN-01 (i.e. 300 nM) revealed a necessary role for a functional G1 checkpoint in mediating growth arrest. Normal cells, which have a functional G1 checkpoint, always arrest in G1 even at very high concentrations of UCN-01. Tumor cells on the other hand have a defective G1 checkpoint and only arrest in S phase with high concentrations of UCN-01. The effect of UCN-01 on the cell cycle is thus quite different from staurosporine, a structural analogue of UCN-01, which arrests normal cells in both G1 and G2, while tumor cells arrest only in the G2 phase of the cell cycle. Our results show the different sensitivity to UCN-01 of normal compared to tumor cells is dependent on a functional pRb and a regulated G1 checkpoint.

## Introduction

Protein kinases are essential for cellular signal transduction leading to differentiation, gene expression, and tumor progression. Clinical and experimental studies have already established the importance of protein kinase expression in the proliferation of human breast cancer (1-3), suggesting that drugs that interrupt signaling pathways mediated by protein kinases could be useful cancer therapeutic agents. UCN-01 (7-hydroxystaurosporine), a staurosporine analogue initially developed as a selective protein kinase C (PKC) inhibitor, was isolated from the culture broth of *Streptomyces* sp. in 1987 (4). Subsequent studies have shown that this compound inhibits PKC *in vitro*. However, it also inhibits a variety of other kinases at nanomolar concentrations, including PKC (IC<sub>50</sub>:4.1nM), PKA (IC<sub>50</sub>:42nM), CDK1 (IC<sub>50</sub>:31nM), CDK2 (IC<sub>50</sub>:30nM), CDK4 (IC<sub>50</sub>:32nM), MAPK (IC<sub>50</sub>:910nM), p60<sup>v</sup>-Src and protein tyrosine kinase (IC<sub>50</sub>:45nM) (5-8). Studies with cultured cells revealed that UCN-01 exhibited potent anti-tumor activity against several human cancer cell lines such as human epidermoid carcinoma A431, fibrosarcoma HT1080, acute myeloid leukemia HL-60, human lung carcinoma A549, and breast carcinoma MDA-MB-468 cell lines (5,8-10). UCN-01 also exhibited significant anti-tumor activities in several experimental animal models *in vivo* (4,5,11). In addition, UCN-01 has been shown to enhance anti-tumor activities of chemotherapeutic agents such as cisplatin, 5-fluorouracil, mitomycin C, etc. *in vitro* and *in vivo* (12-16). Studies identifying the cellular pathways affected by UCN-01 resulting in G1 arrest suggest that although UCN-01 possesses potent PKC-inhibitory activity, inhibition of PKC activity is not essential for its growth inhibitory activity (17). Recent studies on the role of cell cycle regulators in UCN-01 mediated G1 arrest indicate that in human epidermoid carcinoma A431 cells, UCN-01 induced G1 arrest was accompanied by decreased cyclin-dependent kinase 2 (CDK2) activity

and induction of CDK inhibitors p21 and p27 (18). However, the precise mechanism of action of UCN-01 in either normal or tumor cells remains unresolved.

The roles of p53 and pRb, in UCN-01 mediated G1 arrest are also still pending. p53 and the retinoblastoma protein (pRb) are two major tumor suppressors that are frequently inactivated in human cancer (19-29). Alterations in p53 are linked to poor prognosis, tumor progression, and decreased sensitivity to chemotherapeutic agents. As an important G1 checkpoint regulator, p53 is involved in controlling the G1 to S phase transition in response to DNA damage. p53 also blocks cell cycle progression or induces apoptosis through transcriptional activation of downstream genes including the CDK inhibitor p21. Similar to p53, pRb also functions as a negative regulator of cell cycle. Phosphorylation of pRb is necessary for the progression through G1 and is regulated primarily by cyclin D/CDK4 /CDK6 complexes. The hypophosphorylated pRb serves as a tumor suppressor by interacting with and inhibiting cellular proteins such as E2F-DP heterodimeric transcription factors which activate many genes required for DNA replication pivotal for G1/S transition (30-33).

The activities of CDKs are regulated by positive regulators such as cyclins and CAK (CDK-activating kinase), and by negative regulators such as cyclin-dependent-kinase inhibitors (CKIs) (34-36). There are two families of structurally distinct CDK inhibitors, one is the INK family of proteins which include p16, p15, p18, and p19, the other is CIP/KIP family of proteins including p21, p27, and p57 (37-40). The CDK inhibitor p21 is a p53-regulated gene (41,42), but can also be induced through a p53 independent pathway (43,44). The INK family of CDK inhibitors target the CDK4 and CDK6 and prevent their interaction with cyclin D. The CIP/KIP family of CDK inhibitors bind to cyclin/CDK complexes and inhibit their activity. More recently, it has been reported that the CIP family of CDK inhibitors also function as adaptor molecules, which promote

the association of CDK4 with D-type cyclins and increase CDK4 kinase activity (45-49). Therefore, the CIP/KIP family of CDK inhibitors have both an adaptor/activating function as well as a kinase inhibitory function depending on which cyclin/CDK they are in complex with.

Even though UCN-01 is currently in phase 1 clinical trials in both the United States and Japan, there are several questions on the growth inhibitory effect of this agent in normal and tumor cells. In this study we examined the growth inhibitory activity and other cell cycle perturbations mediated by UCN-01 in several normal and tumor-derived breast epithelial cells. Our results reveal three novel findings on the sensitivity and mechanism of action of UCN-01 in normal and tumor cells. First, we document a significant difference in sensitivity to UCN-01 between normal and tumor cells. UCN-01 is capable of inducing a G1 arrest in normal cells at very low concentrations (i.e. 10 nM), while in tumor cells concentrations up to 80 nM did not result in a significant growth inhibition. Furthermore, we show that the UCN-01 mediated G1 arrest only occurs in normal cells and is concomitant with inhibition of CDK2 activity, decreased phosphorylation of pRb, and increased binding of p27 to CDK2. Secondly, we show that UCN-01 mediated G1 arrest is p53 independent and pRb dependent using the E6 and E7 transformed strains of the normal cells. Lastly, we show that at very high concentrations, there is a major difference in the mechanism by which UCN-01 mediates growth inhibition in normal versus tumor cells. Treatment of normal cells with UCN-01, at all concentrations examined (i.e. up to 300 nM), results only in G1 arrest, unlike staurosporine which arrests normal cells in both G1 and G2. Treatment of tumor cells, on the other hand, with high concentrations of UCN-01 results only in an S phase arrest, unlike staurosporine which arrest tumor cells only in G2. We show that this difference in UCN-01 mediated perturbation of normal versus tumor cells is also pRb dependent. Collectively our studies suggest that the mechanism of



differential sensitivity of UCN-01 in normal versus tumor cells is dependent on a regulated G1 checkpoint involving a functional pRb pathway.

## **Experimental Procedures:**

**Materials, Cell lines, and culture conditions:** UCN-01 was provided by the National Cancer Institute. Serum was purchased from Hyclone Laboratories (Logan, Utah) and cell culture medium from Life Technologies, Inc. (Grand Island, NY). All other chemicals used were reagent grade. The culture conditions for 76N, 81N, and 70N normal cell strains, MCF-10A immortalized cell line, and MCF-7, ZR75T, MDA-MB-157, Hs578T, T47D, and MDA-MB-231 breast cancer cell lines were described previously (50,51). 76N-E6 and 76N-E7 cell lines (gifts from Dr. V Band, Tufts Medical Institute Boston, MA) were immortalized and cultured as described previously (52,53). All cells were cultured and treated at 37°C in a humidified incubator containing 6.5% CO<sub>2</sub> and maintained free of mycoplasma as determined by Hoechst staining (54).

**MTT assay:** The MTT (3-[4,5-dimethylthiazol-2yl]-2,5-diphenyltetrazolium bromide) assay was performed as described (55). Exponentially growing cells were counted by a Coulter Counter (Halieah, Florida) and plated at a density of 25,000 cells/ml in the wells of 96 well tissue culture plates (200 µl culture fluid per well) and allowed to recover for 24 hours prior to drug treatment. Cells were incubated with the indicated concentration of UCN-01 or staurosporine for 48 hours and subjected to the MTT survival assay. Each data point represents the average of six determinations, and the MTT assay for each experimental condition was performed at least 3 times.

**Cell Synchronization and flow cytometry:** Normal mammary epithelial (81N) cells were synchronized at the G1/S boundary by a modification of the double thymidine block procedure as described (56). Briefly, 48 h after the initial plating of cells, the medium was replaced with fresh medium containing 2mM thymidine for 24 h. This

medium was then removed, the cells were washed three times, and subsequently incubated in fresh medium lacking thymidine for 12 h. Next, cells were again incubated in medium containing 2mM thymidine, as above, washed with fresh medium, and incubated in thymidine free medium in the presence or absence of 300 nM UCN-01. Cells were harvested at the indicated times, cell density was measured using a Coulter Counter and flow cytometry analysis was performed. For flow cytometry studies,  $10^6$  cells were centrifuged at 1000 X g for 5 min, fixed with ice-cold 70% ethanol (30min at 4° C), and washed with phosphate buffered saline (PBS). Cells were suspended in 5 ml of PBS containing 10 µg/ml RNase, incubated at 37° C for 30 min, washed once with phosphate buffered saline, and resuspended in 1 ml of 69 µM propidium iodide in 38 mM sodium citrate. Cells were then incubated at room temperature in the dark for 30 min. and filtered through a 75 µm Nitex mesh. DNA content was measured on a FACScan flow cytometer system (Becton Dickinson, San Jose, CA), and data were analyzed using CELLFIT software system (Becton Dickinson).

**Blotting, Immunoprecipitation, and H1 Kinase Analysis:** Cell lysates from UCN-01 treated cells were prepared and subjected to Western blot analysis as previously described (45). Briefly, 50 µg of protein from each condition was electrophoresed in each lane of either a 7% sodium dodecyl sulfate-polyacrylamide gel (SDS-PAGE) (pRb), 10% SDS-PAGE (p53, cyclin A, cyclin D1, cyclin D3), 13% SDS-PAGE (p21, p27, CDK2, CDK4), or a 15% SDS-PAGE (p16), and transferred to Immobilon P overnight at 4° C at 35mV constant volts. The blots were blocked overnight at 4 ° C in Blotto (5% nonfat dry milk in 20mM Tris, 137 mM NaCl, 0.25% Tween, pH 7.6). After six, 10 minute washes in TBST (20mM Tris, 137mM NaCl, 0.05% Tween, pH 7.6), the blots were incubated in primary antibodies for 3 hours. Primary antibodies used were pRb monoclonal antibody (PharMingen, San Diego, CA), at a dilution of 1:100, monoclonal

antibody to p16 (a gift from Jim DeCaprio, Dana Farber Cancer Institute) at a dilution of 1:20, CDK2, CDK4, and p27, monoclonal antibodies (Transduction Laboratories, Lexington, KY) each at a dilution of 1:100, p21 and p53 monoclonal antibodies (Oncogene Research Products/Calbiochem, San Diego, CA) at a dilution of 1:100 cyclin D1 monoclonal antibody (Santa Cruz Biochemicals, Santa Cruz, CA) at a dilution of 1:100, and actin monoclonal antibody (Boehringer-Mannheim, Indianapolis, IN) at 0.63 µg/ml in Blotto. Following primary antibody incubation, the blots were washed and incubated with goat anti-mouse horseradish peroxidase conjugate at a dilution of 1:5,000 in Blotto for 1 hour and finally washed and developed with the Renaissance chemiluminescence system as directed by the manufacturers (NEN Life Sciences Products, Boston, MA).

For immunoprecipitations followed by Western blot analysis 300 µg of cell extracts were used per immunoprecipitation with polyclonal antibody to CDK2 (45) or CDK4 (Santa Cruz Biochemicals, Santa Cruz, CA) in lysis buffer containing 50mM Tris buffer pH 7.5, 250 mM NaCl, 0.1% NP-40, 25 µg/ml leupeptin, 25 µg/ml aprotinin, 10 µg/ml pepstatin, 1 mM benzamidine, 10 µg/ml soybean trypsin inhibitor, 0.5 mM PMSF, 50 mM NaF, 0.5mM sodium ortho-vanadate. The protein/antibody mixture was incubated with protein A Sepharose for 1 hour and the immunoprecipitates were then washed twice with lysis buffer and four times with kinase buffer (50mM Tris HCL pH 7.5, 250 mM NaCl, 10 mM MgCl<sub>2</sub>, 1 mM DTT and 0.1 mg/ml BSA). The immunoprecipitates were then electrophoresed on 13% gels, transferred to Immobolin P, blocked and incubated with the indicated antibodies at dilutions described above. For Histone H1 kinase assay the immunoprecipitates were incubated with kinase assay buffer containing 60 µM cold ATP and 5 µCi of [<sup>32</sup>P] ATP in a final volume of 50 µl at 37°C for 30 minutes. The products of the reaction were then analyzed on a 13% SDS-PAGE gel. The gel was then stained, destained, dried and exposed to X-ray film. For

quantitation, the protein bands corresponding to histone H1 were excised and the radioactivity of each band was measured by Cerenkov counting.

## RESULTS

**UCN-01 selectively arrests normal, but not tumor, cells in G1.** We initially investigated whether UCN-01 has a different growth inhibitory effect in normal versus tumor cells. For this purpose we examined the effects of UCN-01 in several normal and tumor-derived breast epithelial cells (Fig 1). The normal cells examined were 76N and 81N (both mortal). We also examined MCF-10A, a near diploid immortalized cell line as well as 4 breast cancer cell lines with different p53 and pRb status (45). Following treatment of cells with 0-80 nM UCN-01 for 48 hours, growth inhibition was analyzed by the MTT assay (Fig 1A), and the effect of UCN-01 on cell cycle distribution was examined by flow cytometry (Fig 1B). The data clearly shows that normal breast epithelial cell strains 76N and 81N were highly sensitive to UCN-01, revealing a 60-70% growth inhibition following treatment with only 20nM UCN-01 and an  $IC_{50}$  of 10-12 nM. Breast cancer cell lines T47D and MDA-MB-157 cells showed little to no response to UCN-01 over the concentration range examined. MCF-10A, MCF-7 and MDA-MB-436, showed an intermediate response to UCN-01 with a 20-25% growth inhibition at 40nM, and less than 50% growth inhibition at 80nM of UCN-01. These results demonstrate that at low concentrations (i.e. 0-80 nM) normal cell strains are much more sensitive to UCN-01 than tumor cells. Flow cytometry analysis revealed that treatment of normal cells (76N and 81N) with UCN-01 resulted in a significant accumulation of cells in the G1 phase of the cell cycle (i.e an increase of 15% in G1 phase) in a dose dependent fashion (Fig 1B). The G1 accumulation in normal cells was concurrent with an S phase decrement (Fig 1B), while G2+M phase had no significant change (data not shown). The partial growth inhibition of UCN-01 in MCF-10A and MCF-7 cell lines was due to a slight (less than 5%) accumulation in G1 (data not shown). Lastly, UCN-01 was ineffective in inducing any accumulation in the G1 phase of the cell cycle in MDA-MB-157 or MDA-MB-436 cell lines. In fact treatment of

MDA-MB-436 cells with 80 nM UCN-01 resulted in a slight increase in S phase (Fig 1B and see below). The data from figure 1 suggests that UCN-01 selectively mediates growth inhibition in normal but not tumor cells by arresting the cells in the G1 phase of the cell cycle.

**UCN-01 mediated G1 arrest in normal cells results in inactive cyclin/CDK2 complexes due to increased p27 binding to CDK2.** To determine which key cell cycle regulators were required for UCN-01 mediated G1 arrest in normal cell strains, we examined the expression of several positive and negative cell cycle proteins in both 76N and 81N mortal cell strains. Both normal cell strains were treated with the indicated concentrations of UCN-01 for 48 hours at which point cells were harvested and subjected to Western blot analysis with antibodies to p27, p21, p16, pRb, p53, CDK2, CDK4, cyclin D1, and cyclin D3 (Fig 2A). These analysis revealed that the total levels p53 and pRb tumor suppressor proteins decreased significantly in the normal cell strains following UCN-01 treatment. In untreated cells pRb is present in both its phosphorylated (upper band) and unphosphorylated (lower band) forms. However the only form of pRb remaining at 40-80 nM UCN-01 is its hypo-phosphorylated form. The generation of hypo-phosphorylated pRb occurred concomitantly with growth inhibition, G1 arrest, decreased expression of cyclin D1, cyclin D3, CDK2 and CDK4 in a dose dependent manner following UCN-01 treatment (Fig 2A)

The simultaneous decrease in p53 and p21 (Fig 2A) in normal cells suggest that in these cells p21 expression may be strongly influenced by p53. The levels of p27 were unchanged following UCN-01 treatment. This analysis raised the question whether p21 and p27 play a role in UCN-01 mediated G1 arrest. Does the decrease in the CDK4 and CDK2 levels in response to UCN-01 contribute to this arrest? A likely explanation for the UCN-01 mediated G1 arrest is that UCN-01 treatment results in

the inhibition of CDK2 activity necessary for cells to overcome the G1 restriction point. In order to examine the kinase activity associated with CDK2 in normal cells, we measured the phosphorylation of histone H1 in immunoprecipitates prepared from UCN-01 treated cells using an antibody to CDK2 (Fig 2 D). Treatment of normal cells with UCN-01 caused a rapid decrease of CDK2 activity. At 40 nM UCN-01 (the concentration causing G1 arrest) and pRb hypo-phosphorylation) the level of CDK2 activity reaches its nadir.

To determine if the decreased activity of CDK2 is due to its association with CKIs, a two step experiment consisting of an immunoprecipitation with anti-CDK2 antibody followed by Western blot analysis with p21 or p27 was performed (Fig 2B). The decreased CDK2 activity observed (Fig 2D) was coupled with increased binding of p27 to CDK2 in the normal cells. The binding of p21 to CDK2 however, decreased in these cells (Fig 2B). These observations raise the question, why is there increased binding of p27 to CDK2 in normal cells (Fig 2B) when the levels of p27 don't change?

Recently several laboratories have proposed that p21 and p27 can function as adaptor molecules, which promote the association of CDK4 with D-type cyclins and increase CDK4 kinase activity (45-49). Since UCN-01 causes the arrest of cells, apparently by increasing binding of p27 to CDK2 complexes (Fig 2B), it can be hypothesized that this increased binding may be due to the switching of p27 from CDK4 to CDK2, mediated by UCN-01. To test this hypothesis we examined the association of p21 and p27 to CDK4 following UCN-01 treatment (Fig 2C). Our results clearly demonstrate that in untreated normal cells p21 and p27 bind to CDK4, and upon treatment with UCN-01, both p21 and p27 are released from CDK4 in a dose dependent fashion (Fig 2C) which corresponds to the binding (i.e. switching partners) of p27 to CDK2 (Fig 2B). Our results suggest that UCN-01 mediated G1



arrest in normal epithelial cells is through decreased expression of CDK4 and CDK2. As CDK4 decreases p27 is released to bind to CDK2, resulting in a decreased CDK2 kinase activity and decreased phosphorylation of pRb.

**UCN-01 has no effect on cell cycle regulators in tumor cells.** While UCN-01 had a profound affect in inducing G1 arrest and lowering the expression of key cell cycle regulators in normal cells, tumor cells showed no significant change in any of the cell cycle regulators examined (Fig 3). Furthermore, although the expression of some of these regulators was different between the 3 different tumor cell lines examined, within each tumor cell line the levels remained unchanged. For example, the levels of cyclin D1, CDK2 and CDK4 were the same within and between each cell line, following UCN-01 treatment. Cyclin D3 is overexpressed in MCF-7 cell line, moderately expressed in MDA-MB-157 and not expressed in MDA-MB-436 cells. MCF-7 cells was the only cell line examined which was wild-type for p53 and pRb and no significant change in the levels of these tumor suppressors was observed following UCN-01 treatment. Although pRb is expressed in MDA-MB-157 cells, it is functionally inactive as previously reported (57). Lastly, the levels of p21 and p27 are elevated in MCF-7 compared to the other two cell lines, while p16 was absent in MCF-7 and overexpressed in MDA-MB-157 and MDA-MB-436 (Fig 3). We also examined the CDK2 kinase activity in these tumor cell lines and as expected the activity of CDK2 was unchanged following UCN-01 treatment in all tumor cell lines examined (data not shown). These results suggest that tumor cells have lost the checkpoint control affected by UCN-01 resulting in no growth inhibition or cell cycle perturbation following treatment.

**UCN-01 mediated G1 arrest is through a p53 Independent and pRb Dependent Pathway.** To directly determine if alterations in p53 or pRb mediate G1 arrest in

normal but not tumor cells, we examined the effects of UCN-01 in E6 and E7 strains of 76N cells. 76NE6 and 76NE7 are immortalized cell strains derived from normal mammary epithelial cell strain 76N by infection with human papilloma virus (HPV) 16E6 or 16E7 (52,53). The E6/p53 and E7/pRb<sub>1</sub> interaction promote degradation/inactivation of p53 and pRb respectively, resulting in the loss of the normal phenotype (58-60). We initially examined the pattern of growth inhibition of UCN-01 in 76NE6 and 76NE7 as compared to the parental 76N cells (Fig 4A). This analysis revealed that 76NE6 were as sensitive to the growth inhibitory activity of UCN-01 as 76N parental cell strain with a super-imposable dose response curve and an IC<sub>50</sub> of 10nM. 76NE7 cells were much more resistant to UCN-01; however, their growth was also retarded with an IC<sub>50</sub> of 75 nM (Fig 4A). Flow cytometry analysis revealed that the UCN-01 mediated growth inhibition in 76NE6 and 76NE7 cells were quite different. Treatment of 76NE6 cells resulted in accumulation of cells in the G1 phase of the cell cycle with a concomitant decrease in S phase cells (Fig 4A) identical to the pattern observed in 76N cells following drug treatment (Fig 1B). However, treatment of 76NE7, pRb deficient, cells resulted in accumulation of cells in S phase at 80nM UCN-01 with a concomitant decrease in the G1 phase, opposite to the pattern observed with 76NE6, p53 deficient cells (Fig 4B). This data suggests that UCN-01 induced G1 arrest is dependent on a functional Rb, but not a functional p53.

Next we examined the expression of key cell cycle regulatory proteins in 76NE6 and 76NE7 cells following UCN-01 treatment (Fig 5A). 76NE6 cells are devoid of p53, but express pRb at very high levels. Treatment of these cells with UCN-01 resulted in accumulation of the hypo-phosphorylated form of Rb, a decrease in CDK4 levels, and an increase in p21 and p27 levels. The levels of CDK2 and cyclin D1 remained unchanged during the course of treatment and p16 levels were undetectable. 76NE7 cells, on the other hand express p16, apparently due to pRb mutation (61,62).

Treatment of 76NE7 cells with UCN-01 resulted in no detectable changes in any of the cell cycle regulators examined (Fig 5A). Next we measured the binding of p21 and p27 to CDK2 and CDK4 in 76NE6 and 76NE7 cells (Fig 5B,C). This analysis revealed that in 76NE6 cells the binding of p21 and p27 to CDK2 increased, while in 76NE7 cells the binding of these CKIs to CDK2 or CDK4 remained unchanged. Furthermore the increased binding of both CKIs to 76NE6 cells was concomitant with decreased binding of p21 and p27 to CDK4 suggesting a switching of partners of these CKIs from CDK4 to CDK2 mediated by UCN-01 (Fig 5B,C). Lastly, measurement of CDK2 activity in 76NE6 and 76NE7 cells revealed that treatment of 76NE6 cells with UCN-01 resulted in a dose dependent decline in the kinase activity with maximum inhibition achieved at 40 nM. The increased expression and binding of p21 and p27 to CDK2 observed (Fig 5B) contributes to the inhibition of CDK2 kinase activity in 76NE6 cells. The CDK2 activity in 76NE7 cells, on the other hand, was completely unabated by UCN-01 treatment. These results strongly suggest that the UCN-01 mediated growth inhibition, G1 arrest, and decreased CDK2 activity are p53 independent, but pRb dependent.

**High concentrations of UCN-01 induces S phase arrest in tumor and 76NE7 but not normal and 76NE6 cells.** While examining the cell cycle effects of UCN-01 in tumor (Fig 1) and 76NE7 (fig 4B) cells we noticed that treatment with 80 nM UCN-01 resulted in a slight increase in S phase and no G1 accumulation. These results raised the question if UCN-01 treatment of cells without a regulated G1 checkpoint and/or functional pRb could lead to only an S phase arrest. To explore this possibility we examined cell cycle phase distribution of 76NE6 and 76NE7 cells at low (i.e. 80 nM) and high (i.e 300 nM) concentration of UCN-01. At 300 nM the growth of both cell types is completely inhibited (data not shown). We observed a clear difference between the ability of 76NE6 cells and 76NE7 cells to arrest in G1 or S phase (Fig 6). Treatment of

76NE6 cells, which have an intact pRb, with any concentration of UCN-01 resulted only in a G1 arrest. However, treatment of 76NE7 cells, which have no detectable pRb, results in only an S phase arrest at higher concentrations of UCN-01 (i.e.  $\geq 80$  nM) (Fig 6). These results suggest that the disruption of the pRb pathway abrogates the ability of cells to arrest in G1 in response to UCN-01 treatment, instead they arrest in the S phase of the cell cycle.

To determine if synchronization of normal cells would sensitize their ability to arrest in S versus G1 phase, we synchronized 81N normal cells in the G1/S boundary by double-thymidine block prior to UCN-01 treatment (Fig 7). Under these conditions up to 30% of the cells (i.e. 3 fold higher than the asynchronous controls) accumulate in S phase following release from this block, and the cells undergo synchronous traverse through the cell cycle for the duration of the experiment (Fig 7). Following the double thymidine block, cells were treated with 300 nM UCN-01 for 3 to 12 hours. We used a high (i.e. 300 nM) concentration of UCN-01, since this concentration was sufficient to arrest 76NE7 cells in the S phase of the cell cycle (Fig 6). At every time interval examined, treatment of 81N with UCN-01 resulted in the accumulation of cells in the G1 but not S phase of the cell cycle (Fig 7). Hence, the UCN-01 mediated G1 accumulation occurred in both asynchronous and synchronized cells. Our results suggest that normal cells, with a functional pRb and G1 checkpoint, are incapable of arresting in any other phase but G1 upon treatment with UCN-01, no matter what their cell cycle distribution is prior to treatment.

The results obtained with UCN-01 treated normal cells are quite different than those with staurosporine treated cells. It has been well documented that staurosporine, a close structural analogue of UCN-01, can arrest normal cells in both G1 and G2 phases of the cell cycle, and tumor cells in only the G2 phase of the cell cycle. Our

results show that UCN-01, also known as 7-hydroxy staurosporine, arrests normal cells in G1 and tumor cells in S phase when used in high concentrations. To compare the effects of staurosporine and UCN-01 in normal versus tumor cells we treated 2 normal cell strains and 2 tumor cell lines with equally cytotoxic concentrations of UCN-01 and staurosporine (Fig 8). UCN-01 and staurosporine produced quite different effects. These results show that as predicted normal cells respond to high concentrations of staurosporine by arresting in both G1 and G2. However, treatment of these cells with high concentrations of UCN-01 resulted to only a G1 arrest. Furthermore, tumor cells, which have a defect in the pRb pathway, respond to high concentrations of staurosporine by arresting predominately in the G2 phase of the cell cycle. On the other hand, the same tumor cells respond to UCN-01 mediated growth inhibition by arresting in the S phase of the cell cycle (Fig 8). These results clearly indicate that normal and tumor cells respond to these very close structural analogues quite differently. Furthermore, the ability of cells to arrest in either G1 or S phase by UCN-01 is dictated by a functional pRb, while the ability of cells to arrest in G2 by staurosporine is independent of pRb.

## Discussion:

In this manuscript we investigated the growth inhibitory effects and cell cycle pathways affected by UCN-01 in several normal and tumor-derived breast epithelial cells. This data revealed three novel findings: First, we found that normal cells are significantly more sensitive to UCN-01 than tumor cells. Treatment of normal cells with concentration as low as 10 nM resulted in 50 % growth inhibition. Tumor cells were much more resistant to growth inhibitory effects of UCN-01 and concentrations as high as 80 nM resulted in minor to no growth inhibition. The normal cells used in this study were normal cell strains which were established from reduction mammaplasty samples of non-tumor bearing women (63). These cells have not lost their growth factor requirements and they undergo senescence after several passages. They are normal, diploid, mortal cells with regulated checkpoint control. As shown in figures 1 and 2 these cells are very sensitive to UCN-01. On the other hand MCF-10A cell line, a near diploid immortalized cell line, with reduced growth factor requirements were much more resistant to the growth inhibitory activity of UCN-01. In fact the growth inhibitory activity of UCN-01 in MCF-10A was similar to that of MCF-7 and MDA-MB-436, two cancer cell lines used in this study (Fig 1A). These observations suggest that the pathways altered by the immortalization process makes MCF-10A cells resistant to the effects of low concentrations of UCN-01.

The growth inhibitory effects of UCN-01 in normal cells are due to a G1 arrest. We show that such an arrest was concomitant with decreased pRb phosphorylation and CDK2 activity, coincident with increased binding of p27 to CDK2 and switching of p27 from CDK4 to CDK2. There were no significant cell cycle perturbations observed in tumor cells by UCN-01. Several studies have reported that UCN-01 inhibits cell cycle progression from G1 to S phase in various mammalian transformed cell lines

(5,11,18). However, it is not clear from these studies why some cells respond to UCN-01 by arresting in the G1 phase of the cell cycle while others accumulated in S phase. In this study we clearly show that normal cells with a regulated G1 checkpoint respond to UCN-01 by arresting in G1 while tumor cells, depending on their pRb status arrest either in G1 or S. For example, both MCF-7 cells and MCF-10A cells which have an intact pRb respond to the growth inhibitory activity of UCN-01 by arresting in the G1 phase of the cell cycle (data not shown). However MDA-MB-436, T47D, and MDA-MB-157 cell lines which are pRb negative, arrest in the S phase of the cycle (Fig 8 and data not shown).

Secondly, our studies suggest that the pRb pathway is involved in UCN-01 inhibition of growth in normal but not tumor cells. Using the 76NE6 and 76NE7 model system where the HPV E6 and E7 proteins bind to and degrade p53 and Rb respectively, we found that UCN-01 inhibited the growth, and perturbed key cell cycle regulatory proteins in 76NE6 similarly to that of the parental 76N normal cell strain (Fig 2 & 5). However, UCN-01 was incapable of mediating G1 arrest or perturbing the cell cycle regulators in 76NE7 cells (Figs 4-6). These results clearly suggest that pRb plays a crucial role in UCN-01 mediated G1 arrest. Both pRb and p53 have been previously implicated in UCN-01 mediated growth inhibition in different cell lines. For example, treatment of a human epidermoid carcinoma A431 cell line which is mutated for p53 but wild-type for pRb with UCN-01 is associated with dephosphorylation of pRb and G1 arrest (18). Similarly treatment of MDA-MB-468 breast cancer cell line, which is mutant for p53 (64) and null for pRb (24), with UCN-01 resulted in accumulation of cells in S phase resulting in block of progression through S phase (11). In other studies treatment of leukemic cells with 300 nM UCN-01 resulted in S phase arrest (8). The latter studies also suggested that the inhibition of PKC alone is not sufficient for the growth inhibitory activity of UCN-01, rather inactivation of CDKs correlates and

could mediate the actions of UCN-01. Our cell cycle studies in normal breast cells clearly confirm this conclusion (Figs 1-2). Collectively, the aforementioned studies show that UCN-01 arrests different tumor cells in G1 or S, which is also consistent with our studies. The novel conclusion of our studies is that the UCN-01 mediated G1 arrest is dependent on a functional pRb and when cells contain a mutant or non-functional pRb, they arrest in the S phase of cell cycle in response to UCN-01.

Lastly, we show that normal and tumor cells respond differently to high concentrations of UCN-01 as compared to staurosporine. Treatment of normal cells with either high (300 nM) or low concentrations of UCN-01 results in only a G1 arrest. Furthermore, synchronization of normal cells in the G1/S boundary prior to their treatment with UCN-01 did not alter their response to G1 arrest mediated by UCN-01 (Figs 7 and 8). On the other hand, treatment of tumor cells with high concentrations of UCN-01 completely inhibits their growth by arresting them in the S phase of the cell cycle (Fig 8). The effect of UCN-01 on normal and tumor cells is very different than its structural analogue, staurosporine, which arrests normal cells in G1 and G2 and tumor cells only in G2 (Fig 8). The G2 (staurosporine) versus S (UCN-01) phase arrest seen in the same tumor cells treated with equally toxic concentrations of these two drugs (Fig 8) is very surprising, since these two agents are structural analogues and differ only in the presence of a 7-OH group on UCN-01. Although this structural difference is subtle the two agents have different specificity toward CDKs. In a series of experiments [reviewed in (65)] aimed at examining the specificity of UCN-01 and staurosporine toward different proteins kinases, it was discovered that even though the IC50s of these two structural analogues against purified PKC were similar (i.e. 7 nM for UCN-01, and 5 nM for staurosporine), their IC50s toward CDKs were quite different. UCN-01 displayed IC50s of 30-32nM against purified CDK1, CDK2 and CDK4. On the other hand, staurosporine displayed IC50s of 3-9 nM against CDK1



and CDK2, and  $<10,000$  nM against CDK4. These studies suggest that the mechanism by which UCN-01 and staurosporine mediate their growth inhibitory effects may be different, and that CDKs and not PKC could dictate such difference.

The common link between UCN-01 and staurosporine is that at low concentrations, both agents arrest normal cells in G1 and such an arrest is lost in tumor cells. The mechanistic basis of staurosporine induced G1 arrest in normal cells and its loss in tumor cells was recently reported to be through pRb (66). Using mouse embryonic fibroblasts (MEFs) from transgenic mice lacking p53, p21, pRb, or p16, the authors clearly show that although p53 function was not essential for staurosporine induced G1 arrest, pRb was since MEFs from pRb knockout mice were incapable of arresting in G1 (66). These and other studies performed on bladder carcinoma cell line 5637 (67) provided strong support for the importance of pRb in inducing G1 arrest in cells by staurosporine. The studies we have presented here also provide strong evidence for the role of pRb in UCN-01 mediated G1 arrest in normal cells and loss G1 arrest in tumor cells lacking pRb. Thus the ability of both UCN-01 and staurosporine to induce G1 arrest seems to be through pRb, independent of p53. The difference between these two agents is 2 fold: First, these two agents are different in their ability to induce either G2 arrest, with staurosporine, or S phase arrest, with UCN-01. Secondly, staurosporine induces G2 arrest in both normal and tumor cells, while UCN-01 mediates S phase arrest only in tumor cells. The mechanism by which UCN-01 induces S phase arrest in tumor but not normal cells although unclear at this point, does not involve either p53 or pRb since treatment of tumor cells lacking both p53 and pRb resulted in S phase arrest.

In summary, our results show that UCN-01 can induce G1 arrest in normal cells at very low concentrations while tumor cells are completely resistant to UCN-01

mediated G1 arrest. This G1 arrest is independent on p53, and dependent on pRb. We also show that tumor cells respond to UCN-01 induced growth inhibition by arresting in S phase independent of either p53 or pRb. Understanding the mechanism by which tumor cells arrest in S phase in response to UCN-01 could provide insight into the regulation of the S phase checkpoint in normal and tumor cells.

## **Acknowledgments**

We thank Dr. Edward Sausville for UCN-01, Dr. Vimla Band for 76NE6 and 76NE7 cell lines, Dr. Donald C. Porter, Dr. Katherine Henrickson, Mr. Christopher G. Danes, and Mr. Richard Harwell for the critical reading of this manuscript. We also gratefully acknowledge the use of Wadsworth Center's Immunology, Tissue Culture, and Photography/Graphics core facilities. X.C. is a fellow of the Cancer Research Foundation of America. This research was supported in part by Grant DAMD-17-94-J-4081 from the U.S. Army Medical Research Acquisition Activity and by Grant No. R29-CA666062 from the National Cancer Institute (both to K.K.)

## References

1. Boorne, A., Donnelly, N., and Schrey, M. (1998) *Breast Can. Res. & Treat.* **48**, 117-124
2. Ciardiello, F., and Tortora, G. (1998) *Clin. Can. Res.* **4**, 821-828
3. Platet, N., Prevostel, C., Derocq, D., Joubert, D., Rochefort, H., and Garcia, M. (1998) *Int. J. of Can.* **75**, 750-756
4. Takahashi, I., Kobayashi, E., Asano, K., Yoshida, M., and Nakano, H. (1987) *J. Antibiot.* **40**, 1782-4
5. Kawakami, K., Futami, H., Takahara, J., and Yamaguchi, K. (1996) *Biochem. Biophys. Res. Comm.* **219**, 778-783
6. Tamaoki, T., and Nakano, H. (1990) *Biotechnology* **8**, 732-735
7. Takahashi, I., Asano, K., Kawamoto, I., Tamaoki, T., and Nakano, H. (1989) *J. of Antibiot.* **42**, 564-70
8. Wang, Q., Worland, P., Clark, J., Carlson, B., and Sausville, E. (1995) *Cell Grow. & Diff.* **6**, 927-936
9. Hill, D., Tillery, K., Rose, L., and Posey, C. (1994) *Can. Chemoth. & Pharmacol.* **35**, 89-92
10. Shao, R., Shimizu, T., and Pommier, Y. (1997) *Exp. Cell Res.* **234**, 388-397
11. Seynaeve, C., Stetler-Stevenson, M., Sebers, S., Kaur, G., Sausville, E., and Worland, P. (1993) *Can. Res.* **53**, 2081-6
12. Bunch, R., and Eastman, A. (1996) *Clin. Can. Res.* **2**, 791-797
13. Bunch, R., and Eastman, A. (1997) *Cell Grow. & Diff.* **8**, 779-788
14. Pollack, I. F., Kaweck, S., and Lazo, J. S. (1996) *J. Neuro.* **84**, 1024-1032
15. Tsuchida, E., and Urano, M. (1997) *Int. J. Rad. Onc., Bio., Phys.* **39**, 1153-1161
16. Wang, Q., Fan, S., Eastman, A., Worland, P., Sausville, E., and Oconnor, P. (1996) *J. Nat. Can. Ins.* **88**, 956-965

17. Courage, C., Budworth, J., and Gescher, A. (1995) *Brit. J. of Can* **71**(4), 697-704
18. Akiyama, T., Yoshida, T., Tsujita, T., Shimizu, M., Mizukami, T., Okabe, M., and Akinaga, S. (1997) *Can. Res.* **57**, 1495-1501
19. Picksley, S., and Lane, D. (1994) *Curr. Opin. Cell Biol.* **6**, 853-58
20. Friend, S. (1994) *Science* **265**, 334-35
21. Berns, A. (1994) *Curr. Biol* **4**, 137-139
22. Horowitz, J. M., Park, S., Bogenmann, E., Cheng, J., Yandell, D. W., Kaye, F. J., Minna, J. D., Dryja, T. P., and Weinberg, R. A. (1990) *Proc. Natl. Acad. Sci.* **87**, 2775-2779
23. Harbour, J. W., Lai, S. L., Whang-Peng, J., Gazdar, A. F., Minna, J. D., and Kaye, F. J. (1988) *Science* **241**, 353-7
24. Lee, E. Y.-H. P., To, H., Shew, J.-Y., Bookstein, R., Scully, P., and Lee, W.-H. (1988) *Science* **241**, 218-221
25. T'Ang, A., Varley, J. M., Chakraborty, S., Murphree, A. L., and Fung, Y.-K. T. (1988) *Science* **242**, 263-266
26. Sasano, H., Comerford, J., Silverberg, S. G., and Garrett, C. T. (1990) *Cancer* **66**, 2150-4
27. Furukawa, Y., DeCaprio, J. A., Belvin, M., and Griffin, J. D. (1991) *Oncogene* **6**, 1343-6
28. Ookawa, K., Shiseki, M., Takahashi, R., Yoshida, Y., Terada, M., and Yokota, J. (1993) *Oncogene* **8**, 2175-81
29. Ginsberg, A. M., Raffeld, M., and Cossman, J. (1991) *Blood* **77**, 833-40
30. Weinberg, R. A. (1995) *Cell* **81**, 323-330
31. Bartek, J., Bartkova, J., and Lukas, J. (1996) *Curr. Opin. Cell Biol.* **8**, 805-814
32. Bartek, J., Bartkova, J., and Lukas, J. (1997) *Exp. Cell Res.* **237**, 1-6
33. Ikeda, M. A., Jakoi, L., and Nevins, J. R. (1996) *Proc. Natl. Acad. Sci. USA* **93**, 3215-3220

34. Arellano, M., and Moreno, S. (1997) *Int. J. Biochem. & Cell Bio.* **29**, 559-573
35. Gartel, A., Serfas, M., and Tyner, A. (1996) *Proceed. Soc. Exp. Bio. & Med.* **213**, 138-149
36. Nigg, E. (1995) *Bioessays* **17**, 471-480
37. Elledge, S. J., and Harper, J. W. (1994) *Curr. Opin Cell Biol.* **6**, 847-852
38. Harper, J. W. (1997) *Cancer Surv.* **29**, 91-108
39. Harper, J. W., and Elledge, S. J. (1996) *Curr. Opin. Gene. & Dev.* **6**, 56-64
40. Sherr, C. J., and Roberts, J. M. (1995) *Genes & Dev.* **9**, 1149-1163
41. Harper, J. W., Adami, G. R., Wei, N., Keyomarsi, K., and Elledge, S. J. (1993) *Cell* **75**, 805-816
42. El-Deiry, W. S., Tokino, T., Velculescu, V. E., Levy, D. B., Parsons, R., Trent, J. M., Lin, D., Mercer, W. E., Kinzler, K. W., and Vogelstein, B. (1993) *Cell* **75**, 817-825
43. Sheikh, M. S., X., L., Chen, J., Shao, Z., Ordonez, J. V., and Fontana, J. A. (1994) *Oncogene* **9**, 3407-3415
44. Michieli, P., Chedid, M., Lin, D., Pierce, J. H., Mercer, W. E., and Givol, D. (1994) *Cancer Res.* **54**, 3391-3395
45. Rao, S., Lowe, M., Herliczek, T., and Keyomarsi, K. (1998) *Oncogene* **17**, 2393-2402
46. Poon, R. Y. C., Toyoshima, H., and Hunter, T. (1995) *Mol. Biol. Cell* **6**, 1197-1213
47. Prall, O. W. J., Sarcevic, B., Musgrove, E. A., Watts, C. K. W., and Sutherland, R. L. (1997) *J. Biol. Chem.* **272**, 10882-10894
48. Planas-Silva, M. D., and Weinberg, R. A. (1997) *Mol. Cell. Biol.* **17**, 4059-4069
49. LaBaer, J., Garrett, M. D., Stevenson, L. F., Slingerland, J., Sandhu, C., Chou, H. S., Fattaey, A., and Harlow, E. (1997) *Genes & Dev.* **11**, 847-862
50. Keyomarsi, K., and Pardee, A. B. (1993) *Proc. Natl. Acad. Sci. USA* **90**, 1112-1116

51. Keyomarsi, K., Conte, D., Toyofuku, W., and Fox, M. P. (1995) *Oncogene* **11**, 941-950
52. Band, V., DeCaprio, J. A., Delmolino, L., Kulesa, V., and Sager, R. (1991) *J. Virology* **65**, 6671-6676
53. Band, V., Zajchowski, D., Kulesa, V., and Sager, R. (1990) *Proc. Natl. Acad. Sci. USA* **87**, 463-467
54. Hessling, J. J., Miller, S. E., and Levy, N. L. (1980) *J. Immunol. Meth.* **38**, 315-324
55. Carmichael, J., Mitchell, J. B., DeGraff, W. G., Gamson, J., Gazder, A. F., Johnson, B. E., Glatstein, E., and Minna, J. D. (1988) *Br. J. Cancer* **57**, 540-547
56. Rao, P. N., and Johnson, R. T. (1970) *Nature* **225**, 159-164
57. Gray-Bablin, J., Zalvide, J., Fox, M. P., Knickerbocker, C. J., DeCaprio, J. A., and Keyomarsi, K. (1996) *Proc. Natl. Acad. Sci.* **93**, 15215-15220
58. Band, V., Dala, S., Delmolino, L., and Andropphy, E. J. (1993) *EMBO J.* **12**, 1847-1852
59. Dyson, N., Guida, P., Munger, K., and Harlow, E. (1992) *J. Virol.* **66**, 6893-902
60. Werness, B. A., Levine, A. J., and Howley, P. M. (1990) *Science* **248**, 76-9
61. Reznikoff, C. A., Yeager, T. R., Belair, C. D., Savelieva, E., Puthenveetil, J. A., and Stadler, W. M. (1996) *Can. Res.* **56**, 2886-2890
62. Khleif, S. N., Degregori, J., Yee, C. L., Otterson, G. A., Kaye, F. J., Nevins, J. R., and Howley, P. M. (1996) *Proc. Natl. Acad. Sci. USA* **93**, 4350-4354
63. Band, V., and Sager, R. (1989) *Proc. Natl. Acad. Sci. USA* **86**, 1249-1253
64. Nigro, J. M., Baker, S. J., Preisinger, A. C., Jessup, J. M., Hostetter, R., Cleary, K., Bigner, S. H., Davidson, N., Baylin, S., Devilee, P., Glover, T., Collins, F. S., Weston, A., Modali, R., Harris, C. C., and Vogelstein, B. (1989) *Nature* **342**, 705-708
65. Meijer, L. (1996) *Trends Cell Bio.* **6**, 393-397

66. Orr, M. S., Reinhold, W., Yu, L., Schreiber-Agus, N., and O'Connor, P. M. (1998) *J. Biol. Chem.* **273**, 3803-3807
67. Schnier, J. B., Nishi, K., Goodrich, D. W., and Bradbury, E. M. (1996) *Proc. Natl. Acad. Sci.* **93**, 5941-5946



## Figures and legends

### **Figure 1. Normal cells are significantly more sensitive to UCN-01 than tumor cells.**

(A) Seven different human breast epithelial cell lines comprised of normal cell strains (76N, 81N), immortalized cell line (MCF10A) and breast tumor cell lines (MCF-7, MDA-MB-157, MDA-MB-436, and T47D) were treated with UCN-01 at 0, 10 20, 40, and 80nM for 48h. Growth inhibition by UCN-01 was measured by the MTT assay. The experiment was repeated 3 times and error bars are indicated for each condition and each cell line. In most cases the error bars were smaller than the symbol size and cannot be seen. (B) Percent change in cell cycle distribution of cells in G1 and S phase following UCN-01 treatment of normal (76N and 81N) and tumor (MDA-MB-157 and MDA-MB-436) cells. The bar graph reflects the percent change of G1 and S phases of UCN-01 treated cells relative to the untreated controls, for each cell line.

### **Figure 2. Cell cycle perturbation induced by UCN-01 in normal cell strains.**

Normal cell strains (76N and 81N) were treated with the indicated concentrations of UCN-01 for 48 hours. Following treatment cells were harvested, cell lysates prepared and subjected to (A) Western blot analysis, (B) CDK2 immune-complex formation, (C) CDK4 immune-complex formation, and (D) Histone H1 kinase analysis. For Western blot analysis 50  $\mu$ g of protein extract from each condition was analyzed by Western blot analysis with the indicated antibodies or actin used for equal loading. The blots were developed by chemiluminescence reagents. The same blots were sequentially hybridized with different antibodies (see Materials and Methods). The blots were stripped between the antibodies in 100 mM 2-mercaptoethanol, 62.5 mM Tris-HCl (pH 6.8), and 2% SDS for 10 min at 55°C. For immunoprecipitation followed by Western blot analysis, equal amounts of protein (300  $\mu$ g) from cell lysate prepared from each cell line were immunoprecipitated with anti-CDK2 (polyclonal) (B) or anti-CDK4

(polyclonal) (C) coupled to protein A beads and the immunoprecipitates were subjected to Western blot analysis with the indicated antibodies. For kinase activity, equal amounts of protein (300  $\mu$ g) from cell lysates were prepared from each cell line immunoprecipitated with anti-CDK2 antibody (polyclonal) coupled to protein A beads using histone H1 as substrate. For each cell line we show the resulting autoradiogram of the histone H1 SDS-PAGE and the quantitation of the histone H1 associated kinase activities by Cerenkov counting. The numbers on the left ordinate refer to cpm obtained from H1 kinase assay for 76N cells (solid bars), and the numbers on the right ordinate refer to the cpm obtained from H1 kinase assay for 81N cells (shaded bars).

**Figure 3. No change in the expression of cell cycle regulators by UCN-01 in tumor cells.** MCF-7, MDA-MB-157, and MDA-MB-436 tumor cell lines were treated with the indicated concentrations of UCN-01 for 48 hours. Following treatment cells were harvested, cell lysates prepared and subjected to Western blot analysis as described for figure 2.

**Figure 4. UCN-01 mediated G1 arrest is pRb dependent and p53 independent. (A)** 76N, 76NE6, and 76NE7 cells were treated with the indicated concentrations of UCN-01 for 48 hours and subjected to growth inhibition analysis as measured by MTT assay and repeated 3 times. Error bars are indicated for each condition and each cell line. In all cases the error bars were smaller than the symbol size and cannot be seen. **(B)** Percent change in cell cycle distribution of cells in G1 and S phase following UCN-01 treatment. The bar graph reflects the percent change of G1 and S phases of UCN-01 treated cells relative to the untreated controls, for each cell line.

**Figure 5. Cell cycle perturbation induced by UCN-01 in 76NE6 and 76NE7 cells.** 76NE6 and 76NE7 cells were treated with the indicated concentrations of UCN-01 for 48 hours. Following treatment cells were harvested, cell lysates prepared and subjected to (A) Western blot analysis, (B) CDK2 immune-complex formation, (C) CDK4 immune-complex formation, and (D) Histone H1 kinase analysis as described for Figure 2. In panel D the numbers on the left ordinate refer to cpm obtained from H1 kinase assay for 76NE6 cells (solid bars), and the numbers on the right ordinate refer to the cpm obtained from H1 kinase assay for 76NE7 cells (shaded bars).

**Figure 6. 76NE7 cells arrest in S phase with high concentrations of UCN-01.** 76NE6 and 76NE7 were treated with 0, 80 and 300 nM UCN-01 for 48 hours at which point samples were isolated and cell cycle distribution was analyzed by flow cytometry as described. Black, %G1; white, %S; shading, % G2/M

**Figure 7. Synchronization of normal cells in the G1/S phase does not abrogate their ability to arrest in G1 by UCN-01.** Asynchronously growing 81N cells (top panel) were synchronized at the G1/S boundary by double-thymidine block (see Materials and Methods). Synchronized cells were treated with either 0 or 300 nM UCN-01. At the indicated times following UCN-01 treatment cells were harvested for analysis by flow cytometry.

**Figure 8. UCN-01 and staurosporine act at different cell cycle checkpoints.** Normal breast epithelial (70N and 81N) cell strains and tumor (MDA-MB-157 and MDA-MB-436) cell lines were treated with no drug or equally cytotoxic concentrations of UCN-01 (i.e 300 nM) or staurosporine (i.e. 64nM) for 48 hours. Following treatment cells were harvested for analysis by flow cytometry.

**This Page Intentionally  
Left Blank**

A

Fig 1

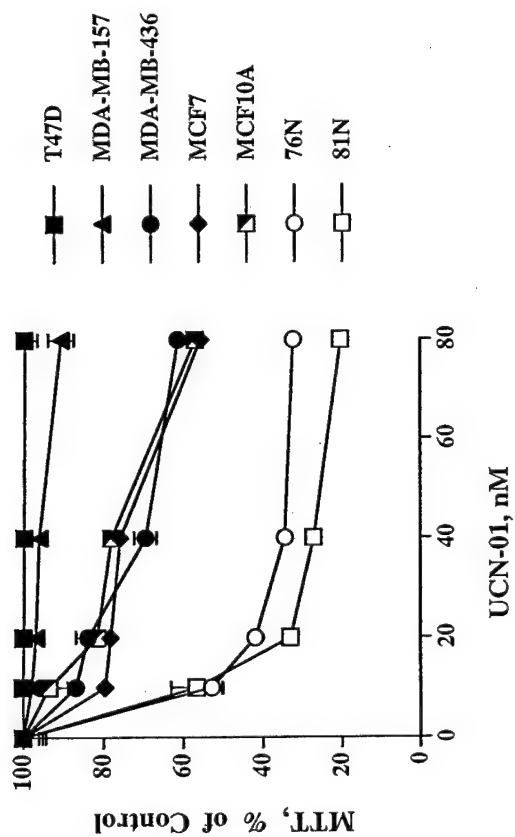


Figure 1

B

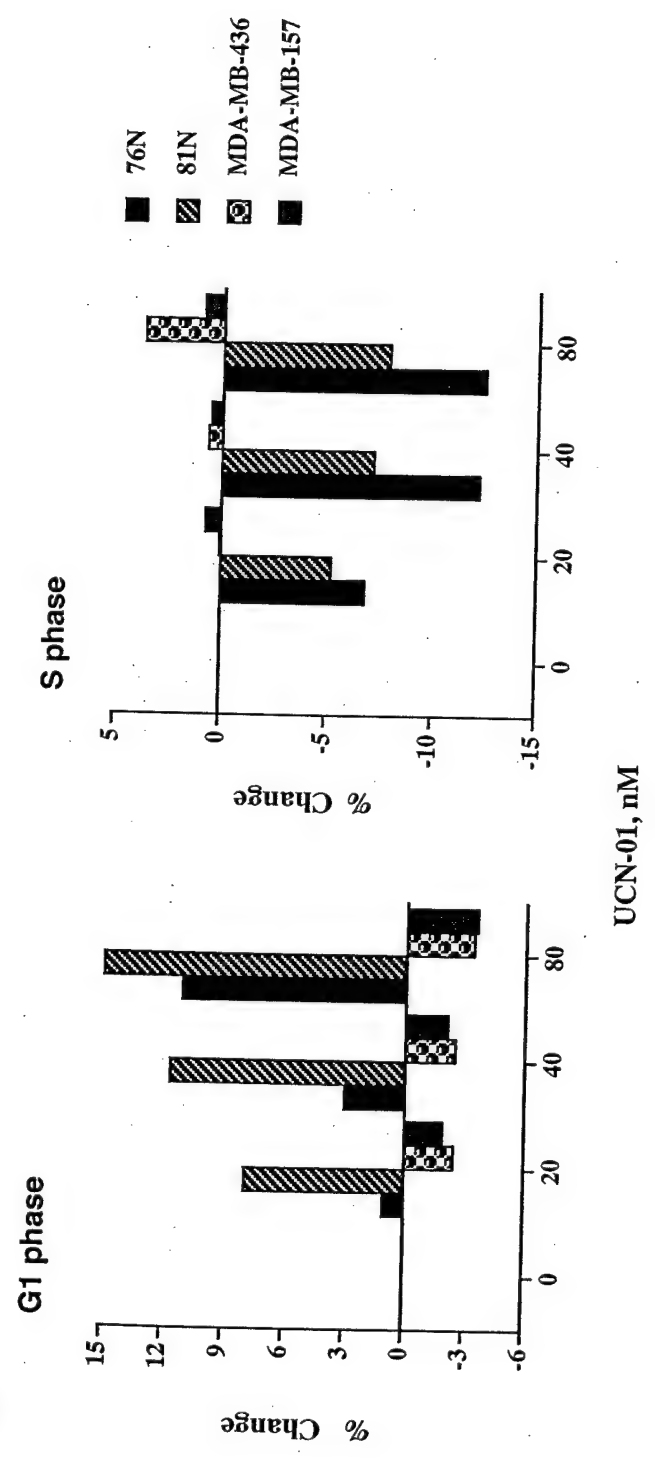


Figure 2

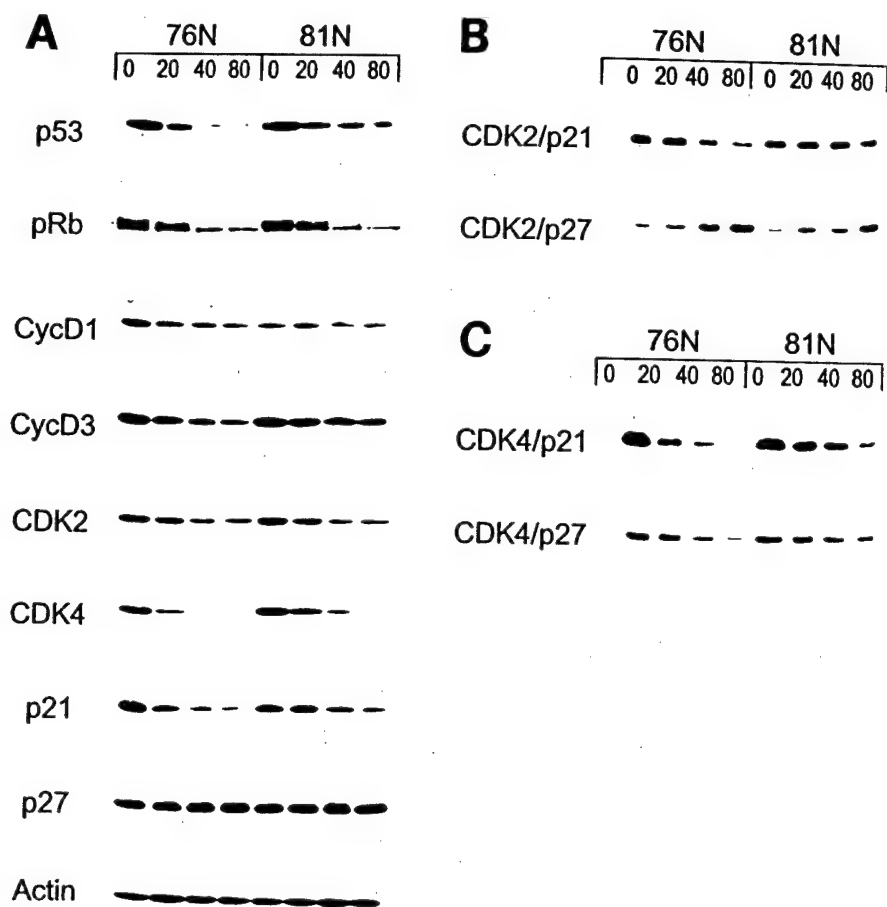


Figure 2 (Cont)

D

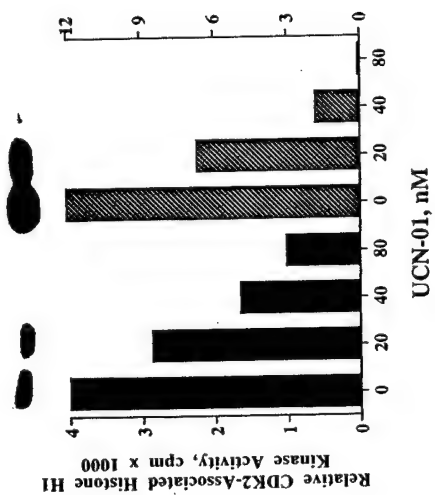




Figure 3

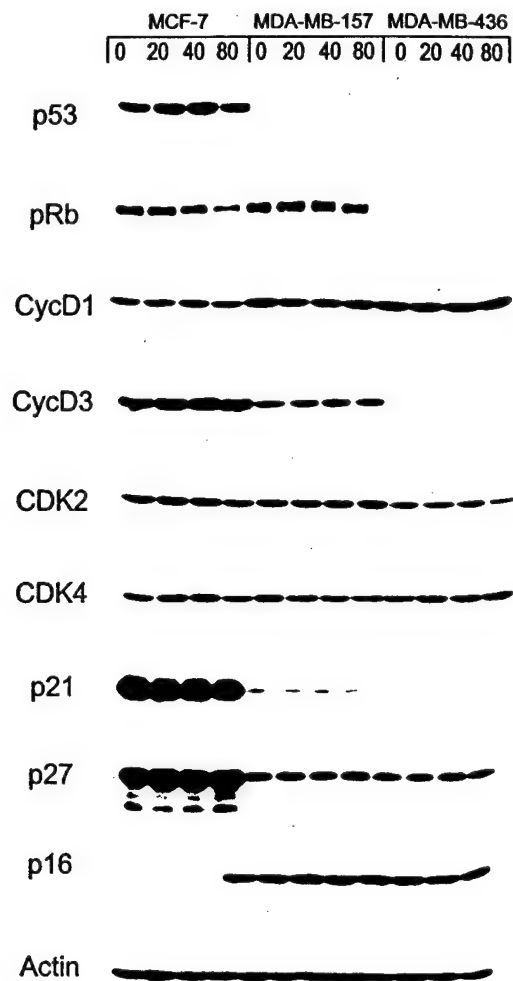


Figure 4 A

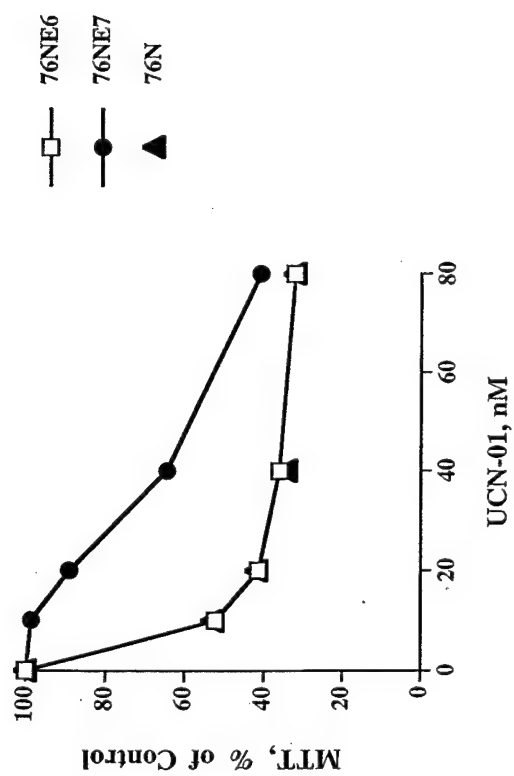


Figure 4 (Cont)

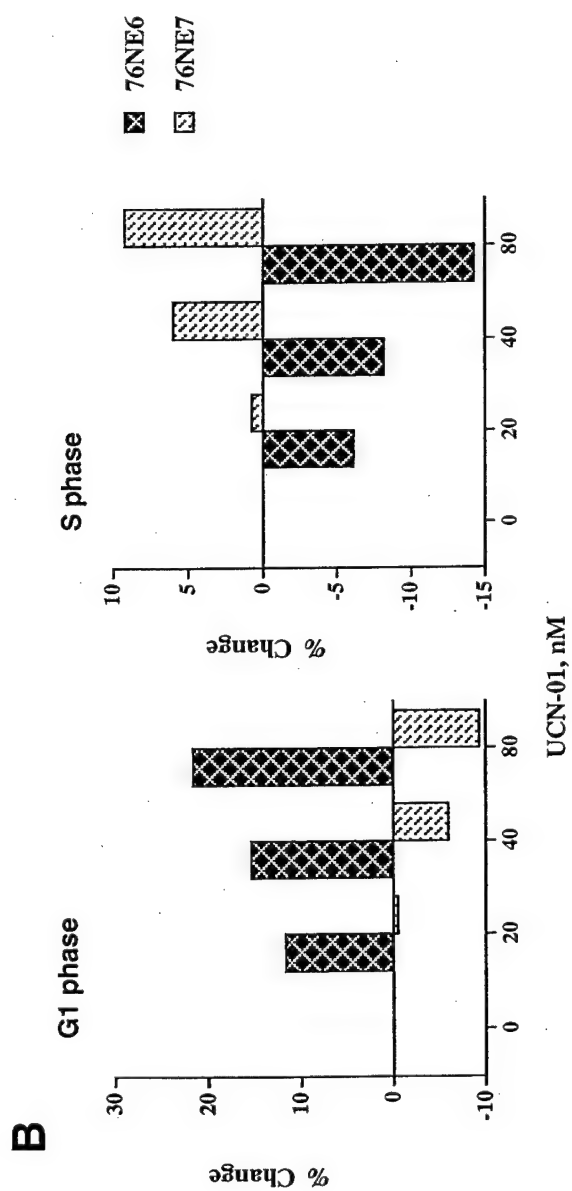


Figure 5

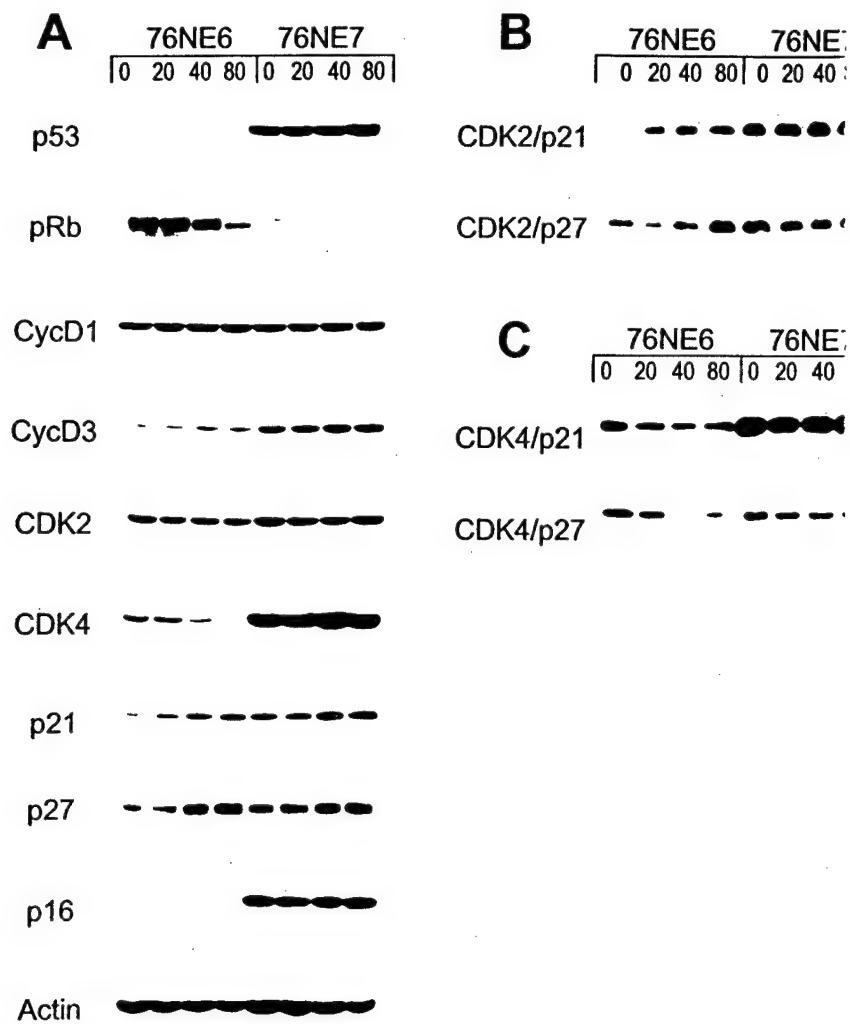


Figure 5 (Cont)

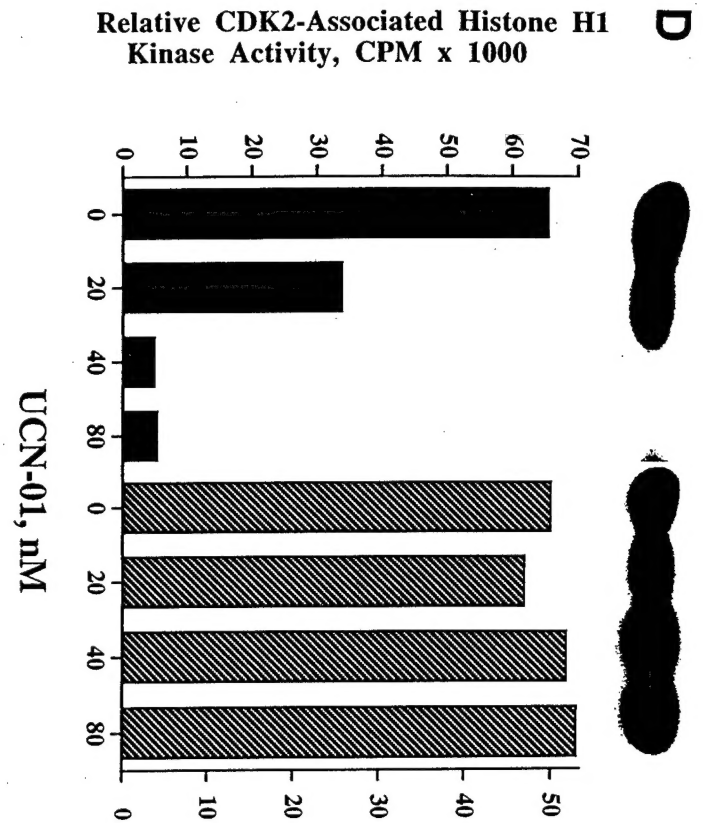


Figure 6

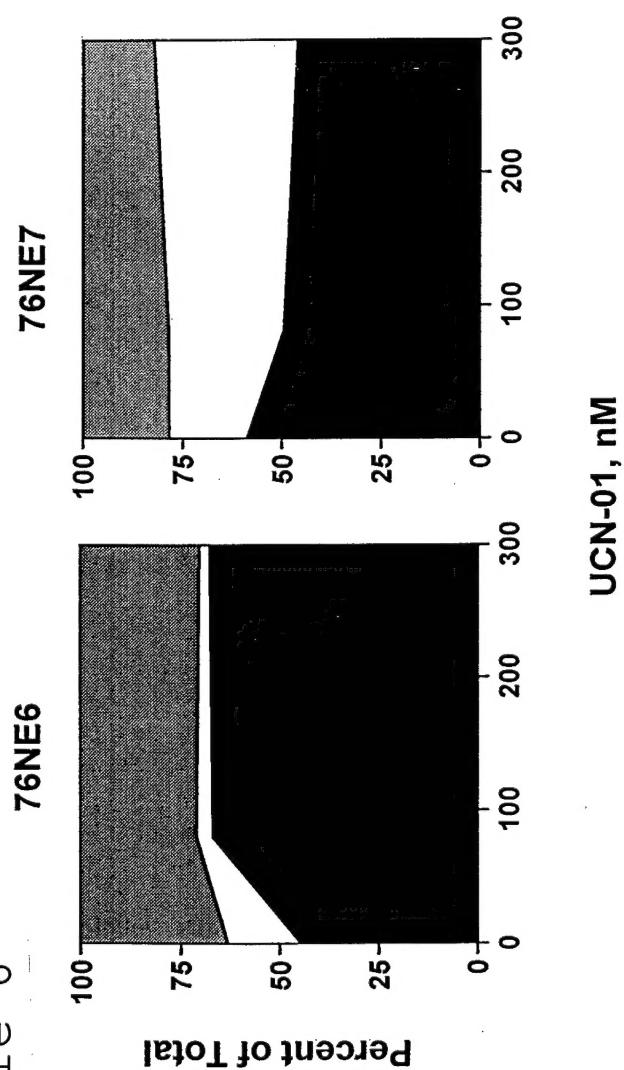


Figure 7

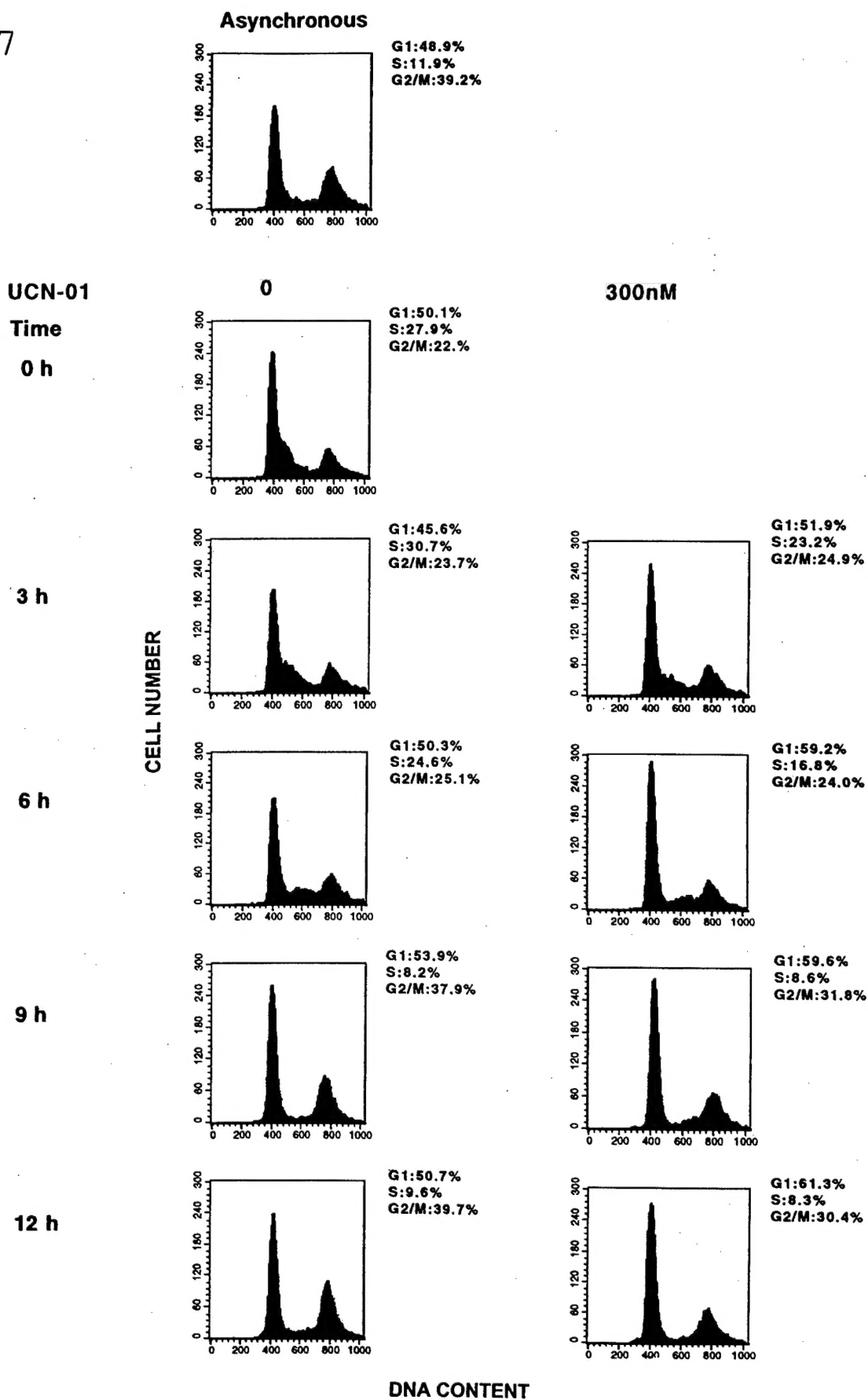


Figure 8

